Åbo Akademi University

Per Dahlsten

# Specific Surface Charging of Latex, Clay and Mineral Oxide Particles in Aqueous, Non-Aqueous and Mixed Solvent Systems

A study of particle interactions in suspensions

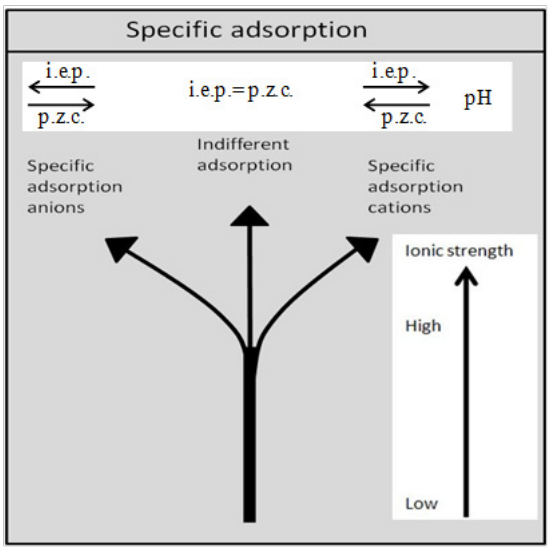


# Per Dahlsten

Per Dahlsten was born in Gävle, Sweden, 1974. He came to Finland in 1999 and graduated with a Master of Science (Tech.) from Åbo Akademi University in 2003. This thesis represents his work to become a Doctor of Science (Tech.) at Åbo Akademi University.

Åbo Akademi University Press
Tavastgatan 13, FI-20500 Åbo, Finland
Tel. +358 (0)2 215 3478
E-mail: forlaget@abo.fi

Sales and distribution:
Åbo Akademi University Library
Domkyrkogatan 2–4, FI-20500 Åbo, Finland
Tel. +358 (0)2 -215 4190
E-mail: publikationer@abo.fi

# Specific Surface Charging of Latex, Clay and Mineral Oxide Particles in Aqueous, Non-aqueous and Mixed Solvent Systems

**Per Dahlsten**


**2012**

**Laboratory of Physical Chemistry, Department of Chemical Engineering**
**Åbo Akademi University**

***From:***
Laboratory of Physical Chemistry
Åbo Akademi University
Turku, Finland

***Supervised by:***
Professor Emeritus Jarl B. Rosenholm
Laboratory of Physical Chemistry
Åbo Akademi University

***Reviewed by:***
Professor Emeritus Brian Vincent
School of Chemistry
University of Bristol
Bristol, UK

and

Professor Björn Lindman
Physical Chemistry, Centre for Chemistry and Chemical Engineering
Lund University, Lund, Sweden

***Opponent:***
Professor Björn Lindman
Physical Chemistry, Centre for Chemistry and Chemical Engineering
Lund University, Lund, Sweden

***Kustos:***
Professor Jouko Peltonen
Laboratory of Physical Chemistry
Åbo Akademi University

ISBN 978-952-12-2818-6
Painosalama Oy – Turku, Finland 2012

## Contents

# Referat

En djupare förståelse för växelverkan mellan partiklar i suspensioner är av betydelse för utvecklingen av en mängd olika industriella produkter och processer. Till exempel kan nämnas pigmentbaserade färger och bestrykning av papper. Genom att öka kontrollbarheten kan dessa lättare optimeras för att uppnå förbättrade produktegenskaper och/eller sänkta produktionskostnader. Av stor betydelse är även en förbättrad möjlighet att minska produktens miljöpåverkan.

I avhandlingen studerades jonstyrkans och jonspecificitetens inverkan i olika akvatiska suspensioner innehållande olika elektrolyter. De partiklar som avhandlingen omfattade var metalloxider, leror samt latex. Jonstyrkan studerades från låga ($c < 10^{-3}$M) till och med höga ($c > 10^{-1}$M) elektrolytkoncentrationer. Vid koncentrationer under 0.1 M var partikelladdningen styrd av pH och jonstyrkan. Vid högre elektrolytkoncentrationer påverkade även jonspecificiteten partikelladdningen. Jonspecificiteten arrangerades i fenomenologiska serier funna i litteraturen samt med Born modellen definierad i termodynamiken. Överraskande höga absoluta zeta-potential värden erhölls vid höga elektrolytkoncentrationer vilket visar att den elektrostatiska repulsionen har betydelse även vid dessa förhållanden.

Vidare studerades titanoxidsuspensioners egenskaper i akvatiska, icke-akvatiska och blandade lösningssystem under varierande koncentration av oxal- och fosfatsyra. Vid lågt vatteninnehåll studerades även suspensioner med svavelsyra. Konduktiviteten i suspensioner med lågt vatteninnehåll ökade med tillsatt oxal- eller fosforsyra vilket är en omvänd effekt jämfört med svavelsyra eller akvatiska suspensioner. Den omvända effekten skiftade gradvis tillbaka med ökad vatteninnehåll. En analys av suspensionernas adsorption i höga etanolkoncentrationer gjordes med konduktiviteten, pH och zeta-potentialen. Viskositet studerades och applicerades framgångsrikt i viskositet/ytladdningsmodeller utvecklade för akvatiska suspensioner.

# List of original publications

**I. Electrokinetics at high ionic strengths: Alumina**, Marek Kosmulski, Per Dahlsten, Piotr Prócniak, Jarl B. Rosenholm, Surf. Colloids Surf. A, Volume 301, Issues 1-3, 5 July 2007, Pages 425-431.

**II. High ionic strength electrokinetics of clay minerals,** Marek Kosmulski, Per Dahlsten, Colloids and Surfaces A: Physicochemical and Engineering Aspects, Volume 291, Issues 1-3, 15 December 2006, Pages 212-218.

**III. High ionic strength electrokinetics of melamine–formaldehyde latex,** Marek Kosmulski, Per Dahlsten, Piotr Próchniak, Jarl B. Rosenholm, Journal of Colloid and Interface Science, Volume 301, Issue 2, 15 September 2006, Pages 538-541.

**IV. Electrokinetic behavior of melamine–formaldehyde latex particles at moderate electrolyte concentration,** Per Dahlsten, Piotr Próchniak, Marek Kosmulski, Jarl B. Rosenholm, Journal of Colloid and Interface Science, Volume 339, Issue 2, 15 November 2009, Pages 409-415.

**V. Surface-induced electrolytic dissociation of oxalic and phosphoric acid in mixed alcohol–water solvents,** Per Dahlsten, Marek Kosmulski, Jarl B. Rosenholm, Colloids and Surfaces A: Physicochemical and Engineering Aspects, Volume 376, Issues 1-3, 20 February 2011, Pages 42-46.

**VI. Surface Charge and Conductance in Dispersions of Titania in Nonaqueous and Mixed Solvents,** Marek Kosmulski, Per Dahlsten, Piotr Prócniak, Jarl B. Rosenholm, Progr. Colloid Polym. Sci., (2011), 138.

**VII. Interaction between oxalic acid and titania in aqueous ethanol dispersions,** Per Dahlsten, Jarl B. Rosenholm, Journal of Colloid and Interface Science. In press (DOI 10, 1016/j.jeis.2012.10.010).

**VIII. Visco-coulombic characterization of aqueous and alcoholic titania suspensions,** P. Dahlsten, P. Próchniak, M. Kosmulski, J.B. Rosenholm, Colloids and Surfaces A: Physicochemical and Engineering Aspects, Volume 376, Issues 1-3, 20 February 2011, Pages 76-84.

# List of supporting publications

**1. Influence of long-term aqueous exposure on surface properties of plasma-sprayed oxides $Cr_2O_3$ and $Cr_2O_3$–25 wt% $TiO_2$,** Mika Harju, Mikael Järn, Per Dahlsten, Juha-Pekka Nikkanen, Jarl B. Rosenholm, Tapio Mäntylä, *Journal of* Colloid and Interface Science, Volume 326, Issue 2, 15 October 2008, Pages 403-410.

**2. Influence of long-term aqueous exposure on surface properties of plasma sprayed oxides $Al_2O_3$, $TiO_2$ and their mixture $Al_2O_3$–13$TiO_2$,** Mika Harju, Mikael Järn, Per Dahlsten, Jarl B. Rosenholm, Tapio Mäntylä, Applied Surface Science, Volume 254, Issue 22, 15 September 2008, Pages 7272-7279.

**3. Electrokinetic studies in the presence of alkali trichloroacetates, trifluoroacetates, and trifluoromethanesulfonates,** Marek Kosmulski, Per Dahlsten, Jarl B. Rosenholm, Journal of Colloid and Interface Science, Volume 313, Issue 1, 1 September 2007, Pages 202-206.

# Contributions of the author

The author is responsible for the experimental work in the original articles with the following exceptions:

In paper I the surface charge density measurements were made at Department of Electrochemistry, Lublin University Technology, Lublin, Poland. In paper I, II and the electroacoustic measurements where mainly preformed by Piotr Próchniak.

In paper III thermal stability measurements and synthesis were performed at Department of Electrochemistry, Lublin University Technology, Lublin, Poland.

The SEM image in paper IV was conducted by Dr Mikael Järn.

# List of symbols and abbreviations

| | | |
|---|---|---|
| A | Area | [$m^2$] |
| a | Particle radius | [m] |
| c | Electrolyte concentration | [$mol/dm^3$] |
| $c_c$ | Critical coagulation concentration | [$mol/dm^3$] |
| F | Faraday's constant | [C/mol] |
| H | Hamaker constant | [J] |
| I | Ionic strength | [$mol/m^3$] |
| k | Boltzmann constant | [J/K] |
| $l_0$ | Minimum particle separation distance | [m] |
| $l_f$ | Minimum aggregate separation distance | [m] |
| N | Coordination number | |
| $N_A$ | Avogadro's constant | [$mol^{-1}$] |
| R | Ideal gas constant | [J/Kmol] |
| r | Ionic radius | [m] |
| T | Absolute temperature | [K] |
| U | Internal energy | [J] |
| $U_A$ | Attractive internal energy | [J] |
| $U_R$ | Repulsive internal energy | [J] |
| z | Ionic valency (formal charge) | |
| $\Lambda_m$ | Molar conductivity | [$Sm^2/mol$] |
| $\Lambda_m^0$ | Limiting molar conductivity | [$Sm^2/mol$] |
| $\psi$ | Surface potential | [V] |
| $\Gamma$ | Normalized concentration | [$mol/m^2$] |
| $\Omega$ | Normalized conductivity | [$S/m^3$] |
| $\sigma$ | Surface charge | [$C/m^2$] |
| $\varepsilon_0$ | Permittivity of vacuum | [$C^2/Nm^2$] |
| $\varepsilon_r$ | Relative permittivity | |
| $\zeta$ | Zeta-potential | [V] |
| $\eta$ | Dynamic viscosity | [Pas] |
| $\kappa$ | Reciprocal length of double layer | [$m^{-1}$] |

| | | |
|---|---|---|
| $\kappa^{-1}$ | Debye length (thickness of double layer) | [m] |
| $\kappa_{dis}$ | Electrical conductivity of the dispersion | [S/m] |
| $\kappa_{red}$ | Reduced electrical conductivity | [S/m] |
| $\kappa_{sol}$ | Electrical conductivity of the solution | [S/m] |
| $\tau_Y$ | Yield stress | [Pa] |
| $\tau_B$ | Bingham yield stress | [Pa] |
| $\upsilon$ | Nr of cat/anions per formula unit of salt | |
| $\phi$ | Volume fraction | |
| DLS | Dynamic light scattering | |
| DLVO | Derjaguin-Landau and Verwey-Overbeek theory | |
| EDL | Electrical double layer | |
| HIS | High ionic strength | |
| HSAB | Hard-Soft Acid-Base principle | |
| i.e.c. | Isoelectric concentration | |
| i.e.p. | Isoelectric point | |
| LIS | Low ionic strength | |
| MF | Melamine-formaldehyde | |
| MIS | Moderate ionic strength | |
| p.z.c. | Point of zero charge | |
| SIED | Surface-Induced Electrolytic Dissociation | |

# 1. Introduction

The colloidal properties of a suspension are strongly dependent on the interactions between species in solution and on particle surface. In a colloidally stable suspension the particles repel each other preventing collisions. The opposite occurs in a non-stable suspension where the particles aggregate after impact. The colloidal stability/instability of suspensions is important in many different industrial processes/products as well as in phenomena found in nature. In the industry both non-stable (e.g. cleaning of dirt and debris from raw materials) and highly stable (e.g. coatings, paints and inks) colloidal suspensions are utilized. The stability strongly influences the sedimentation and flow of the suspension. Physically the sedimentation is determined by gravity and its ability to prevail over forces caused by random Brownian motion and flow. Aggregation magnifies the influence of gravity and this leads to faster sedimentation. In addition, aggregated beds will be less dense than beds formed by primary particles. On the contrary, a higher colloidal stability enables a higher loading of particles.

The stability of aqueous suspensions is governed by charges at the surface of the particle. A non-charged particle tends to aggregate since it lacks a repulsive barrier. The sign of the surface charge is strongly dependent on the pH. In general, high pH leads to negative and low pH to positive surface charges. However, this is also strongly affected by the nature of surface groups. The surface charge can be modified by adsorption of species from the solution. The charges may further influence the rheology of the suspension. In some cases the viscosity can be changed by several orders of magnitude.

The charges in solution (ionic species) will form an electrical double layer around charge particles and the particles will at a given distance from the surface possess a surface potential. The DLVO-theory was developed in mid-$20^{th}$ century by Derjaguin-Landau and Verwey-Overbeek and is based on a balance between attractive and repulsive forces in the sphere surrounding the particles. It takes into account the influence of electrolyte concentration and valency. The theory has been proved superior in describing the colloidal stability in aqueous suspensions. In non-

polar suspensions the applicability of the theory is rather limited. There is a range of polar organic as well as mixed aqueous suspensions where the colloidal properties are not fully investigated. Moreover, a strictly electrostatic model sometimes has a limited predictability and this is especially pronounced at higher ionic strength where ion specificity may be of significance. The ion selectivity is commonly interpreted by different phenomenological series. Those cover both anions and cations of different valency and are usefully implemented in a wide range of scientific fields. However, it should be emphasized that they can be ambiguous since they are not fully consistent. Another method to interpret ion selectivity is by means of thermodynamics. In contrast to the phenomenological series such an approach will be of a quantitative value.

# 2. Outline of the research

The research in this thesis can be divided into two main parts. Firstly, it will consider the influence of ionic strength and selectivity of 1:1 electrolytic aqueous suspensions from high to relatively low electrolytic strength (articles I-IV). This part aims to enhance the knowledge of why and under what conditions ions adsorb in a particular way. Eventually the adsorption will be sub-divided into specific anionic and cationic or indifferent nature. In the second part the anionic adsorption is considered. The influence of the solvent will be investigated in alcoholic, mixed aqueous/alcoholic and aqueous suspensions (articles V-VIII). The latter papers will also include correlations between the charges and the physical properties of the suspensions. The aim of the thesis is to enhance the knowledge of the influence of the solute-surface interactions on the charge properties of the suspension. Since the charging behavior strongly affects the physical properties of the suspensions an increased understanding will improve the ability to control suspension properties which may be utilized in a broad range of industrial processes.

In articles I-III the ionic selectivity of suspensions at high 1:1 electrolyte concentration is investigated. These concern suspensions of alumina, clay particles as well as melamine-formaldehyde lattices. ζ-potentials of the suspensions are measured as a function of pH using a number of selected 1:1 salts at different ionic strengths. The measurements are mostly performed at high ionic strength i.e. $c_{salt}$ > 0.1 M. The selectivity is investigated by the position of the iso electric point, i.e.p. and the absolute value of the ζ-potential. Two electroacoustic and one electrophoretic technique are used to derive the ζ-potentials. Each method is concerned with the mobility of the particles but the approaches are different and by performing complementing measurements the validity of the methods for determining ζ-potential are evaluated. In article IV the ionic influence of moderately (0.001-0.1M) concentrated 1:1 electrolyte melamine-formaldehyde latex suspensions was investigated. Ions are arranged in series according to different models. The models of concern are the phenomenological Hard-Soft Acid-Base, Hofmeister series and the Born equation defined in thermodynamic terms.

Article V considers the influence of oxalic, phosphoric and sulfuric acid on aqueous, alcoholic (ethanol and methanol) and mixed alcohol-water Titania suspensions. To a large extent the measurements are made as a function of acid concentration. Focus is placed on the conductance of the suspension and in particular on the recently discovered surface-induced electrolytic dissociation (SIED) effect. In article VI the complexity of the systems studied in paper V is considered and related to a quantitative adsorption model that considers the SIED effect. In article VII the assumption that conductivity represents proton concentration (paper V and VI) and the proposed model are evaluated. The ζ-potential is related to conductivity, proton concentration and surface charge density. In the final article (VIII) titania suspensions are investigated and the viscosity is correlated to the ζ-potentials. The applicability of different visco-Coulombic models based on the DLVO-theory and mainly developed for aqueous system is tested for alcoholic suspensions. The purpose of using the models is to further establish the factors that govern the colloidal and viscous properties of the suspensions.

# 3. Interactions in suspensions

In suspensions there is a balance between the interparticle attractive forces and the repulsive forces associated with the overlap of the electrical double layer surrounding the particle. A suspension will remain kinetically stable if the repulsive forces prevail over the attractive forces. The DLVO-theory[1,2] (Derjaguin-Landau and Verwey-Overbeek) summarizes the forces and is able to predict stability/instability of colloidal particles. The theory is crucial in colloidal science and can for instance predict the influence of ionic strength and particle charge as evidenced by the Schulze-Hardy rule[3,4]. A brief presentation of interaction forces and the DLVO-theory is made below, including other interactions present in the suspension.

### 3.1 Attractive forces (van der Waals forces)

The attractive van der Waals forces arise from oriented dipole interactions between atoms and/or molecules. This appears when a negatively charged dipole orients in the direction of a positively charged dipole. The nature of the dipoles can be both permanent and induced and the different phenomena may be separated into three classes. Those are induced dipole-induced dipole (London or dispersive), dipole-induced dipole (Debye) and dipole-dipole (Keesom) interactions[5,6]. At relatively short separation distances the attractive internal energy $U_A$ for all types of molecular forces is proportional to the inverse sixth power of separation. At larger separation distances London dispersive forces experience a retardation effect and the attractive energy is then proportional to the inverse seventh power of the distance between atoms/molecules. This effect is described in the Casmir-Polder interaction[7].

For colloids the individual contributions are compounded. In such conditions there is no net dipole moment or polarizations. This means that vector forces such as Keesom and Debye tend to cancel and the only force that needs to be considered is London[8].

The most common way to analyze the contribution of attractive van der Waals forces is by the Hamaker approach[9]. This is a microscopic approach that predicts, in an

approximate manner, the attractive energy by adding individual interaction contributions between atoms/molecules.

The van der Waals forces may further be described by a macroscopic approach[10]. The method is based on the correlation of electric fluctuation between two macroscopic phases. It is more accurate and the retardation effect is directly incorporated. The drawback is that it can only be applied to a limited number of systems where the dielectric dispersion data have been quantified[8].

### 3.2 The electrical double layer

A particle immersed in a polar solvent usually forms a cloud of ions distributed around it. The particle itself is electrically neutral but when it is immersed it becomes charged. At a charged surface ions of opposite sign (counterions) accumulate; over a certain distance from the surface an excess of counter-ions and a deficit of co-ions (ions with charge equal to the surface) form a diffuse layer. The phenomenon is known as the electrical double layer (EDL). It is overall electrically neutral and hence the EDL is formed from a redistribution of ions. The dominant mechanisms governing the redistribution of ions are listed below[11,12].

1) The unequal adsorption/desorption of oppositely charged ions from the solvent.
2) The dissociation of ionogenic groups present at the solid surface. e.g. carboxylic groups where the charge will be dependent on the pH.
3) The unequal dissolution of ions which the solid is composed from.
4) The adsorption/orientation of dipoles at the solid surface. This will not affect the net charge but may affect the nature of double layer.
5) Isomorphic substitution, i.e. replacement of an ion (cation) of high z for another cation with low z in a mineral where the element size is similar and the crystal structure does not change, (e.g. in clays). The reduced charge is compensated for by counterion adsorption.

The EDL model was developed by Helmholtz in the 19th century. A diffuse EDL model was later developed by Gouy and Chapman and further modified by Stern. The EDL in its simplest form is built up of an inner and an outer region. The inner region is called a Helmholtz or Stern layer and the outer a diffuse or Gouy layer and they are separated by the Outer Helmholtz plane (OHP) also called as a Stern plan. The Helmholtz layer consists of stationary counterions and the diffuse layer of mobile counter and co-ions. The ζ-potential is measured at the first mobile layer called a slipping plane.

The specifically adsorbed ions may be partly dehydrated in the direction of the surface[13]. In contrast, indifferent ions are restricted to experience only Coulombic forces and they will therefore only diffuse across the OHP. However, they are based on the same premises which are listed below[11].

1) Ions are point charges.
2) The ionic adsorption is only dependent on electrostatics.
3) The average electrical potential incorporated in the Poisson's law equals the potential of mean force in the Boltzmann equation.
4) The solvent is primitive and the distribution is only affected by the bulk value of the permittivity, ε.

### 3.3 Repulsive Coulombic forces

When the particles in a suspension are separated by sufficiently large distances they do not physically affect each other since the system is electrically neutral[11]. When the double layers of two particles of equal charge overlap a repulsive barrier builds up between them and its strength increases with a decreasing distance. In the overlap of the double layers the surface potential determines the magnitude of the repulsion and the thickness of the double layer settles at what distances the repulsive forces occur[11]. The repulsive interactions can be analyzed by examining the osmotic pressure[14]. This is because of the local increase in ion concentration in the overlap region and this increase is proportional to the pressure[14]. However, there is no simple

way to express the repulsive energy and a normal practice is to use an approximated expression valid for limited conditions[11,14,15].

### 3.4 Total energy of interactions

The total internal energy is the sum of the repulsive and the attractive contribution (eq. 3.1).

$$U_T = U_A + U_R \tag{3.1}$$

Index T refers to total and A and R to attractive and repulsive internal energy, respectively. The equation is fundamental for the DLVO-theory from which the total potential energy is given as a function of the separation distance between particles. This is important and was early used to explain the theory of the stability of lyophobic colloids[16]. In figure 3.1 the dashed lines correspond to the attractive and repulsive potential energy and the full-drawn line to the total potential energy. The state of the suspension is dependent on whether the thermal energy (kT) of the particles is sufficient to surmount the energy barrier ($U_{max}$) and hence enter the primary minimum, and also the existence and depth of a secondary minimum[11]. If $U_{max}$ is much larger than kT relatively few particles will make contact and the suspension will remain colloidally stable. Sometimes the particles possess a secondary minimum and this causes particle flocs in the suspension. However, flocculated particles in the secondary minimum are much easier to re-disperse compared to coagulated particles in connected at the primary minimum and thus they can readily be re-dispersed by shaking[11].

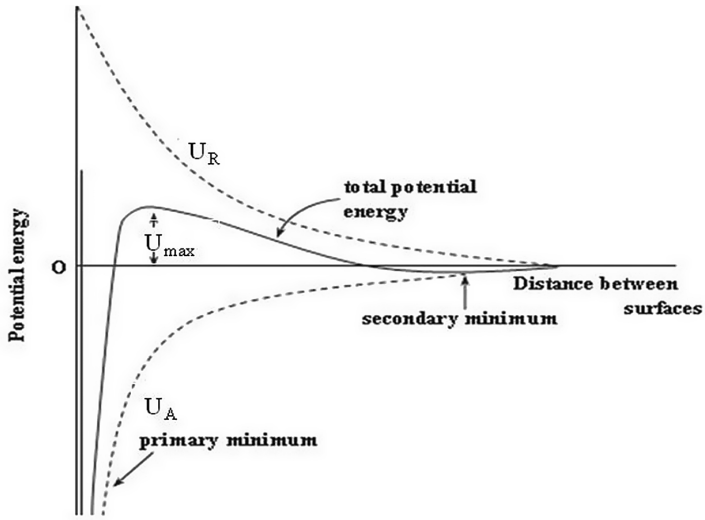


Figure 3.1: The potentially attractive, repulsive and total surface energy plotted as a function of distance between surfaces.

A decreased electrolyte concentration will increase the height of $U_{max}$ and this will also reduce the secondary minimum since the range of $U_R$ will be considerable greater than the range of $U_A$.

### 3.5 Coagulation/aggregation in suspensions

Thermodynamically an aqueous suspension is not completely colloidally stable since all suspensions exhibit to some extent coagulation[15]. The rate of coagulation depends on the number of collisions between the particles in the suspension and the probability that their thermal energies overcome the repulsive barrier which will cause aggregation [15]. A quantitative method to assess the stability is to measure the stability ratio, $W=k_0/k$[8]. This is expressed as the ratio between fast diffusion controlled coagulation, $k_0$, and slow repulsion barrier controlled aggregation, k. The model for fast flocculation, developed by Smoluchowski, assumes that no interaction occurs between particles before they collide and when they do the end result is always a permanent aggregate[8]. An expression for slow aggregation which assumes that collisions occur in the presence of an energy barrier was developed by Fuchs[15].

There are also other means of interpreting coagulation. The Schulze-Hardy rule may be used to determine the critical coagulation concentration, $c_c$, of a lyophobic sol[14]. The $c_c$ is the concentration of an indifferent electrolyte at which the suspension starts to coagulate. From a phenomenological point of view, the transition where a suspension experiences a slow to a fast coagulation is continuous. However, in reality this is usually fairly sharp[11]. The transition is determined by the counterion and the surface potential of the solid and it rapidly decreases with increased valency[14]. In table 3.1 the influence of valence is demonstrated for some salts in hydrophobic sols of $Al_2O_3$.

Table 3.1: The critical coagulation concentration ($c_c$) for $Al_2O_3$ hydrophobic sols at mono- and multi-valency[15] .

| $Al_2O_3$ $c_c$ in mmol/dm$^3$ | | | | | |
|---|---|---|---|---|---|
| NaCl | 43.5 | $K_2SO_4$ | 0.30 | $K_3[Fe(CN)_6]$ | 0.08 |
| KCl | 46.0 | $K_2Cr_2O_7$ | 0.63 | | |
| $KNO_3$ | 60.0 | $K_2$Oxalate | 0.69 | | |
| Average | 49.8 (1) | | 0.54 (0.011) | | 0.08 (0.0016) |

The $c_c$ is nearly proportional to the inverse of the six power of the valency of the counterion. Thus the average $c_c$ for the 1;2;3 charged anions relate as 1;0.011;0.0016 while $1/z^6$ dependency predicts 1;0.016;0.0014. In low dielectric medium assuming that $\psi_0 \approx \zeta$ $c_c$ may be expressed as follows:

$$c_c = k\left(\frac{\varepsilon_r^3 \zeta^4}{H_{212}^2}\right) \tag{3.2}$$

where k is a constant dependent on valency and temperature and $H_{212}$ the Hamaker constant.

The colloidal stability in non aqueous suspensions can usually not be interpreted by the DLVO-theory since the Debye length parameter expressing the extension of the ion cloud around the particle (eq. 5.2) is not known[17]. However, a model for

electrostatic stability in non-aqueous media has been developed by Morrison[17]. The model considers the repulsion only as a simple Coulombic repulsion and not the repulsive forces caused by overlapping of double layers. An expression for the stability ratio of dispersed medium of neglecting ionic strength was thereafter found by assuming an infinite Debye length. By selecting $10^5$ as a minimum value of W above which the suspension is stable many non-aqueous suspensions seem to obey the following expression, where $a$ is the particle radius and $\zeta$ is the minimum zeta potential required for stability:

$$\zeta^2 \approx \psi_0^2 > \frac{1000}{\epsilon_r a} \leftrightarrow \frac{\epsilon_r a \zeta^2}{1000} > 1 \tag{3.3}$$

where $\zeta$ is given in mV and a in μm.

### 3.6 Ions in solutions

Ionic or polar solutes are easily dissolved in aqueous solutions due to the high polarity and high dielectric constant of water[18]. In aqueous solutions ions are solvated by a number of water molecules. The number of molecules surrounding a cation (with coordination number, N) will increase with its polar strength that for an ion may be defined as the $z/r_{ion}^2$ ratio (or ion charge density)[18]. The solvation may be described in terms of a first and a second solvation layer. For small sized and strongly polarized monovalent ions a first layer will be formed by a tetrahedron of water molecules. For larger monovalent cations the first layer is occupied by 6-8 water molecules and the exact number will further be influenced by the concentration, temperature and the nature of the cation[18]. The number of water molecules in the first solvation layers for multivalent cations is 4-8. The cation can be coordinated by the aqua, hydroxo and oxo ligands. The coordination is well established in thermodynamic equilibrium constants and enables calculation of distribution of species as a function of pH and the solution concentration. Additionally it is possible to assign the cations coordination with a complexing constant[19]. However, a more complex situation occurs in the presence of a

condensation reaction. A method developed to approach the problem without involving thermodynamic data is the Particle Charge Model (PCM)[20]. It uses the electro negativities i.e. the negative chemical potential of the electrons, to explain the direction of electron transfer between atoms[20]. Except for the applicability for condensation reactions the model may be used for complexation reactions and hydrolysis of cations in solutions and further for acid-base properties for elements and cations in solutions. However, the model uses many approximations and does not take into account the concentration and structural issues and therefore it will only provide qualitative information[20]. The solubility of ionic species in non-aqueous solutions is much lower than in water since the polarity of the solvent is less. For multi protic acids this means that they to a large extent appear in its molecular form. Their $pK_a$'s are shifted to higher values and often only the single protonated ionic acid needs to be considered[21,22,23].

### 3.7 Adsorption of solutes to the solid/liquid interface

There are different theories on adsorption mechanisms developed for the solid/liquid interface. A similar type of solid absorbent may adsorb solutes differently depending on the nature of the bond between the surface and the absorbent[24]. As mentioned earlier the adsorption can be of indifferent or specific nature. When discussed in terms of solvation of the particle a first immobilized layer can be referred to as chemisorbed and the highly structured layer surrounding the particle as physisorbed[25]. For non-hydrolyzable and non-structural cations such as $Li^+$ and $Na^+$ adsorption tends to be "non-specific" (indifferent) as long as the electrolyte concentration is not too high[24]. These ions are thus referred to as physisorbed since they will not adsorb directly at the surface but in the structured solvation layer[24]. Non-specific bonding may further be present for ion complexes in suspensions for certain surfaces and pH conditions[24]. Easily hydrated cations (typically divalent cations or transition metals) experience a strong affinity toward a metal oxide surface. The adsorption of these species may be specific (e.g. against electrostatic forces) and is strongly dependent on pH. A typical adsorption process will occur within a narrow pH range of 1-2 units[24]. The adsorption process will onset at a pH

lower than it would be if the cation would hydrolyze or precipitate in a "pure" solution[24].

### 3.8 The influence of pH and ionic strength on the effective surface potential

It is well known that the ζ-potential of metal oxides, clays and latices in aqueous solutions of low or moderate electrolyte concentration is strongly dependent on pH. If an acid (in an indifferent system) is added to an aqueous suspension there will be a decrease in pH and a protonation of the surface which eventually will lead to a positive ζ-potential. Alternatively, if base is added it will lead to a deprotonation and a negative ζ-potential. Obviously, at some pH in between the surface is neutral and the ζ-potential zero. The pH at which the ζ-potential is zero is referred to as the isoelectric point (i.e.p.) of the suspension. There are large variations in pH of the i.e.p. depending on the nature of the solid. For silica the i.e.p. is found at low pH and for magnesium oxides at high pH[26]. For latices an i.e.p. is commonly not found and the particles remain negative independent of pH[26]. However as shown in publication (IV) the melamine-formaldehyde latex contains –NH and $–NH_2$ groups which can obtain positive charges. Moreover, large differences are found between crystal structures and due to the synthesis method[26]. The influence of an indifferent monovalent electrolyte on the ζ-potential as a function of pH is illustrated in figure 3.2. An increased electrolyte concentration will decrease the ζ-potential. This is due to the so called "ion screening" effect resulting in a reduced ζ-potential at the slipping plane. This is further strongly dependent on the solvent and a measure on the extent of screening can be related to the $\varepsilon_r$ value[27]. The charge reversal of ζ may be successive and thus there will be a pH region in which the repulsive electrostatic forces are small. Moreover, for an indifferent electrolyte the i.e.p. is independent of moderate electrolyte concentration. In such a case the i.e.p. (3.2.b) corresponds to the point of zero charge (p.z.c.) (3.2.a). The latter represents the point at which the surface charge density ($\sigma_0$) obtained by acid-base titrations is zero[28]. In cases where specific adsorption occurs the p.z.c. may differ from i.e.p. and the magnitude of the shift is further dependent on electrolyte concentration[28]. However, it is sometimes possible to find a common intersection point (c.i.p.) defined by the intersection of ζ-

pH curves at different electrolyte concentrations as a function of pH above (specific cation ads.) or below (specific anionic ads.) the $\zeta = 0$ axis.

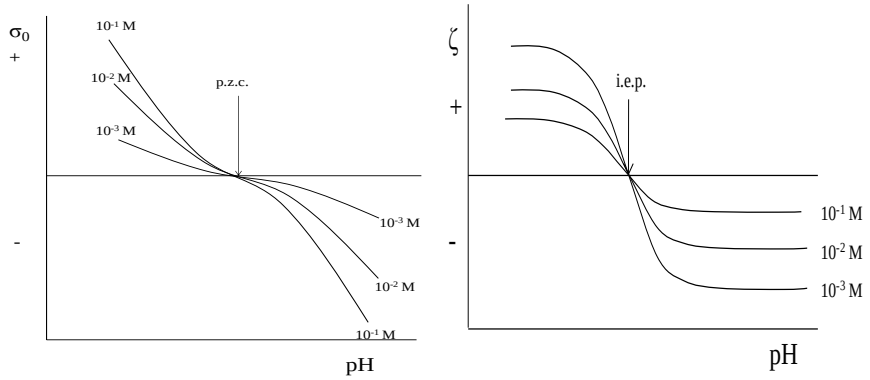


Figure 3.2: a) Surface charge as a function of pH and b) ζ-potential as a function of pH at indifferent monovalent electrolyte concentration.

In section 3.2 it was mentioned that specifically adsorbed ions penetrate the Helmholtz layer due to the fact that those ions experience an affinity toward the surface other than purely Coulombic[29]. This behavior is typically seen for multivalent ions and for molecules with a strong affinity toward the surface, e.g. $PO_4^{3-}$. In agreement with the Schulze-Hardy rule the absolute ζ-potentials of multivalent electrolytes will be depressed much faster upon an increase in electrolyte concentration. As mentioned the ions acting specifically will shift the i.e.p. of the suspension. The shift is dependent on whether the specificity is cationic or anionic. The former type of ion will shift the i.e.p. toward higher pH and the latter type toward lower pH values[11].

### 3.9 Ion selectivity

The DLVO-theory does not consider the influence of ions more than to their valency. This is for many suspensions satisfactory but may also be a limitation especially at high ionic strength. When the secondary influence of ions is studied the result is commonly presented as ionic series. A well known series is the lyotropic Hofmeister

series (1888)[30] that originally arranged ions according to their ability to precipitate white protein from hen eggs. Recently it has been utilized to demonstrate various properties of proteins and also aspects of colloidal stability[31,32,33]. Typical sequences of cations and anions are seen below.

Anions: $CO_3^{2-} > SO_4^{2-} > S_2O_3^{2-} > H_2PO_4^- > F^- > Cl^- > Br^- > NO_3^- > I^- > ClO_4^- > CSN^-$

Cations: $N(CH_3)_4^+ > NH_4^+ > NH_4^+ > Cs^+ > Rb_4^+ > K^+ > Na^+ > H^+ > Ca^{2+} > Mg^{2+} > Al^{3+}$

The phenomenological series has been discussed in different terms since the dominating underlying mechanism varies[34,35]. Thus the series is not absolute and small differences in the sequence of ions exist. In general, the ionic arrangement can be related to specific ion-solid, ion-solvent and ion-ion interactions. When considering the ability of the ions to stabilize proteins, the more stabilizing ions are seen to the left.

The behavior of hydrophobic surfaces may contradict the DLVO-theory, since increasing the electrolyte concentration may increase the solubility. This effect is referred to as “salting in” and the mechanism has been suggested to be due to preferential binding of ions with a relatively low charge density which eventually will increase the net charge of the surface[36]. The opposite, “salting out”, occurs as the concentration further increases and/or for ions possessing a high charge density. The effect has been found to be entropic and may be explained by the greater tendency ions with a higher charge density possess to form hydration complexes[34].

The ionic effects in “bulk” water have also been described in terms of water structure makers or kosmotropes and water structure breaker or chaotropes[35]. These relate to thermodynamic properties such as hydration energy, surface tension, Jones-Dole B coefficient[37] and ionic radius. The ionic interactions can be classified in the ion-solvent category if they are treated individually or in the ion-ion interaction category if treated in pairs. An approach to quantitatively describe the ion-solvent interactions is provided by the Born equation[38]

$$\Delta G_{I-S} = -\frac{N_A(z_i e_0)^2}{2r_{ion}}\left(1-\frac{1}{\varepsilon_r}\right) \tag{3.4}$$

where the free energy of ion-solvent interaction equals the sum of the work of discharging an equivalent sphere in vacuum and the work of charging the equivalent sphere in solvent. The equation is expressed per moles of ions where $N_A$ is the Avogadro's constant, $r_{ion}$ is the radius of the ion, $\varepsilon_r$ is the relative dielectric constant and $z_i e_0$ the charge (valency).

The ion-ion interactions or ion-pair interactions may be explained by the tendency of opposite ions with similar charge density and sizes to form inner sphere ion pairs[37]. In other words, chaotrope prefer chaotrope and kosmotrope prefer kosmotrope ions and this can be seen in a well known relationship between the standard heat of solution of crystalline alkali halide at infinite dilution and the absolute heats of hydration of the corresponding gaseous anion and cation[39].

Another model that categorizes ions according to their properties is the Hard-Soft Acid-Base principle (HSAB) developed by Pearson[40,41,42]. According to the model hard Lewis acids show greater affinity toward hard Lewis bases and soft Lewis bases shown grater affinity toward soft Lewis bases. The HSAB principle is qualitative and a sub-division is made in three classes as seen in Table 3.2 listing the classification criteria.

Table 3.2: Criteria and categorization of ions accordingly to HSAB-principle[43,111].

| | Small ionic/atomic radius<br>High oxidation state<br>Low polarizability<br>High electronegativity | | | | | | | Large ionic/atomic radius<br>Low oxidation state<br>High polarizability<br>Low electronegativity | | | |
|---|---|---|---|---|---|---|---|---|---|---|---|
| | **Hard** | | | | **Borderline** | | | **Soft** | | | |
| **Acids** | $H^+$ | $Li^+$ | $Na^+$ | $K^+$ | $Fe^{2+}$ | $Co^{2+}$ | $Ni^{2+}$ | $Cu^+$ | $Ag^+$ | $Au^+$ | $Tl^+$ |
| | $Be^{2+}$ | $Mg^{2+}$ | $Ca^{2+}$ | $Cr^{2+}$ | $Cu^{2+}$ | $Zn^{2+}$ | $Pb^{2+}$ | $Hg^+$ | $Cd^{2+}$ | $Pt^{2+}$ | $Hg^{2+}$ |
| | $Cr^{3+}$ | $Al^{3+}$ | $SO_3$ | $BF_3$ | $SO_2$ | $BBr_3$ | | $BH_3$ | | | |
| **Bases** | $F^-$ | $OH^-$ | $H_2O$ | $NH_3$ | $\underline{N}O_2^-$ | $SO_3^{2-}$ | $Br^-$ | $H^-$ | $C_2H_5^-$ | CO | $I^-$ |
| | $CO_3^{2-}$ | $NO_3^-$ | $O^{2-}$ | $SO_4^{2-}$ | $N_3^-$ | $N_2$ | $C_6H_5N$ | $\underline{S}CN$ | $(C_2H_5)_3P$ | $C_6H_6$ | $(C_2H_5)_2S$ |
| | $PO_4^{3-}$ | $ClO_4^-$ | | | $SC\underline{N}^-$ | | | $\underline{C}N^-$ | | | |

Underlined element referred to the the site of attachment for the categorization

Measurements of suspensions at high ionic strength are more difficult to perform and this is related to the physical properties of the suspension. In particular, particles at high ionic strength tend to sediment quickly due to the lack of a repulsive barrier that prevents aggregation. The settling of the suspensions was insuperable to handle until the introduction of the electroacoustic technique. However, later refinements in electrophoretic techniques have enabled measurements at high ionic strength as well.

An early electroacoustic study at high ionic strength was carried out by Kosmulski and Rosenholm[44] who investigated the effect of selected ions in anatase and zirconia suspensions as a function of pH and electrolyte concentration. A clear influence of the ions on the isoelectric point was found and the ions could be arranged in $Cs^+<K^+<Na^+<Li^+$ sequence for cations and $CH_3COO^-<Cl^-<NO_3^-<ClO_4^-<Br^-<I^-$ sequence for anions. They further investigated the specificity of divalent cations in aqueous rutile suspensions in electrolyte concentrations up to 0.1 M[45]. For a given electrolyte in a suspension a c.i.p. were found when the suspensions were measured as a function of pH and electrolyte concentration. The location of the c.i.p. was found at higher pH values for larger cations. The more strongly affected suspensions did not undergo a sign reversal even at high pH at considerable electrolyte concentration. A study of alumina suspensions at high ionic strength was carried out by Scales et al[46]. Measurements were performed with different cations and anions as a function of pH. They were able to arrange the cations in the sequence $Li^+<Na^+<K^+<Cs^+$ related to the change in ζ-potential towards higher pH values. However, they were not able to find any trends for the anions in potassium systems. In an additional approach with alumina suspensions at high electrolyte concentrations, Kosmulski et al. demonstrated an anionic specificity in the series of $NO_3^-<ClO_4^-<Cl^-<Br^-<I^-$[47] using sodium as a cation. The shift in i.e.p. at high ionic strength was argued to dominantly depend on ion-ion and solvent-ion interactions. The influence of selected monovalent cations in aqueous silica suspensions has been investigated by Franks et al.[48]. Measurements were made at moderate and high electrolyte concentrations and gave no shift in i.e.p. and insignificant differences in absolute ζ-potential values for moderate electrolyte concentration. Higher concentrations induced a shift of the i.e.p. toward higher values and the magnitude of the increase was dependent on degree of hydration of the ion and well-hydrated ions more extensively shifted the i.e.p.

The specificity is often insignificant at electrolyte concentrations less than 0.1 M. However, in a recent study by Das et al.[49] six monovalent anions with $Na^+$ and two divalent cations where used in alumina suspensions and specificity was found when the ζ- potentials were measured as a function of pH in as low concentrations as $5*10^{-4}$ M[49]. They were further able to arrange the ions into a sequence chiefly following Hofmeister series by studying the amount of p-hydroxybenzoate on the α-alumina in the presence of different ions. In addition, an increased valency of the cation increased the adsorption. The result at low electrolyte concentration was presumed to be dependent on polarizability of the ion in addition to the ion-solvent and ion-ion interactions. The specificity at low electrolyte concentration has further been investigated theoretically and the findings support the selectivity[50,51].

### 3.10 Adsorption models for the solid/liquid interface

There are very few surface specific quantities which are experimentally accessible and this prevents a direct quantitative analysis of the structural details[52]. Therefore, it is a necessity to use a model for quantitative analysis which eventually may enhance the understanding of the particles behavior in suspension[52]. Adsorption of a solute at the particle interface can be evaluated by a single-sited or multi-sited adsorption model. The most widely used single-sited models used are the empirical Langmuir and Freundlich isotherms. Langmuir isotherm was originally derived for adsorption of gases on flat surfaces[53]. An expression for the isotherm is given by equation 3.5

$$\Gamma^s = \Gamma_m \frac{K_L c}{1 + K_L c} \tag{3.5}$$

where $\Gamma_m$ is the maximum surface excess, c is the equilibrium solute concentration and $K_L$ is the Langmuir adsorption equilibrium constant. The model assumes that all sites are equal and that there are no interactions between adjacent absorbents on the surface[52]. Further, the adsorption of the absorbent covers only a monolayer. Freundlich isotherm may be expressed by equation 3.6

$$\Gamma = kc^{\left(\frac{1}{n}\right)} \tag{3.6}$$

where n is an adjustable valued parameter possessing values n>1. In this model the surface excess will not be directly proportional to the concentration and adsorption is not limited to a single layer[54]. Another often utilized multilayer adsorption model is the BET isotherm. From the shape of a surface excess-equilibrium concentration diagram the point of monolayer formation can be derived.

The solid-liquid interface of metal oxides may consist of several different types of chemical groups[55,56]. However, in a single-site adsorption model this is not accounted for. An often utilized multi-site model is the MUltiSIte Complexation model (MUSIC) for metal oxides developed by Hiemstra et al.[57,58] which is based on the following assumptions. In a stable ionic structure the charge of the anion is generally compensated by several partial cationic contributions to charge neutralization. The model uses Pauling's principle of local neutralization of charge, where the sum of the cationic strength is expressed in bonds and will neutralize the anionic contribution. This is seen in the formal bond valence (ν) which is the quotient of the charge divided by the coordination number (z/N). Further, the sites for proton adsorption are located at the surface oxygen where they may associate with one or two protons. The surface may be heterogeneous and therefore more than one type of oxygen may be present. Moreover, different crystal planes are exposed at the surface and this will generally induce different surface oxygen. The protonation of metal oxide surface groups is represented by the following reactions:

$M_n\text{-}O^{(n*\nu-2)} + H_s^+ \leftrightarrow M_n\text{-}OH^{(n*\nu-1)}$; $K_{n,1}$

$M_n\text{-}OH^{(n*\nu-1)} + H_s^+ \leftrightarrow M_n\text{-}OH_2^{(n*\nu)}$; $K_{n,2}$

where n is the number of metal cations coordinated with surface hydroxyls O(H) and the amount of surface protons is related to that of the bulk through Boltzmann equation:

$$H_s^+ = H_b^+ e^{-\frac{F\psi_0}{RT}} \tag{3.7}$$

where F is Faraday´s constant.

# 4. Suspension properties

## 4.1 Rheology

Rheology can be defined as the study of flow and deformation of matter under the influence of a mechanical (shearing) force (IUPAC). The rheological behavior of matter is of increasingly technological importance for e.g. paints and coatings[15]. A first general separation of the rheological behavior can be made into Newtonian viscous fluids and (Hookean) elastic solids[15]. In colloids of satisfying particle content the mechanical behavior is often an intermediate between the two and such materials are termed viscoelastic[15]. The rheological properties of suspensions can be affected by a number of factors[11,15]:

1) Viscosity of the liquid.
2) Particle concentration.
3) Particle size and shape.
4) Size distribution.
5) Flexibility and deformability of the particle.
6) Particle-particle and particle-solvent interactions.
7) Thermodynamic conditions of the suspension.

### *4.1.1 Viscosity*

The flow properties of liquids can be characterized by the viscosity, η, and this can be described as the resistance of a liquid to flow or the internal friction[11]. Further, it can be defined into dynamic and kinematic components. In the latter case the viscosity equals the quotient of dynamic viscosity divided by the liquid density. The measurement of dynamic viscosity involves a liquid confined between a fixed and a movable plate of area A. A constant force, F, is applied to the movable plate which will accelerate to a constant velocity v acting in the direction x. The force per unit

area will denote a shear stress, $\tau$, and it will cause a deformation or strain, $\gamma = \tan \alpha$ (See Fig. 4.1).

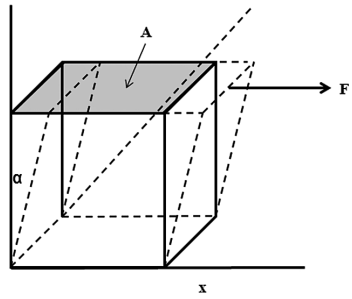


Figure 4.1: The strain after applying a force F.

Viscosity is stress (applied force per unit area)/strain rate and therefore:

$$\eta = \frac{\tau}{\dot{\gamma}} \left[\frac{\mathrm{Ns}}{\mathrm{m}^2} = \mathrm{Pas}\right] \tag{4.1}$$

### 4.2 Flow behavior of suspensions

For a liquid that experiences a Newtonian behavior the applied shear stress is directly proportional to the shear rate. However, as mentioned a suspension commonly exhibits a non-Newtonian behavior. There are several types of non-Newtonian flow behaviors; the most common ones, including Newtonian, are illustrated in Fig. 4.2.

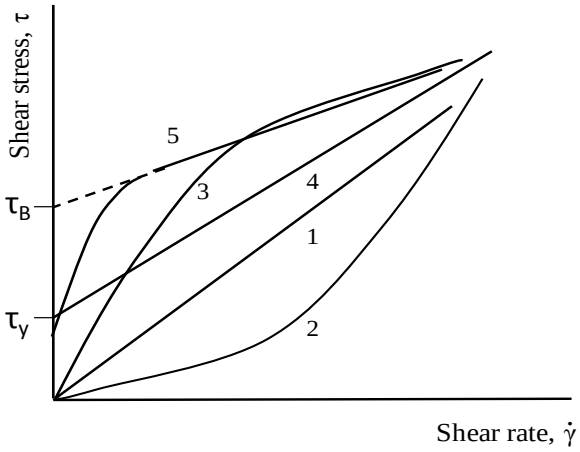


Figure 4.2: Common flow behaviors for suspensions[14].

Newtonian behavior is illustrated by curve (1). Curve (2) is shear thickening or dilatant flow where the viscosity of the suspension increases with increased shear rate. This typically appears when flow is limited by particles in the suspension. The opposite, shear thinning or pseudo plastic flow, is illustrated by curve (3). This phenomenon can be explained by breaking down of particle networks in the suspension. With an increased shear the network will break down and this enables a less viscous flow. Curve (4) and (5) show an ideal and non-ideal Bingham plastic flow. In those types of suspensions a critical stress or yield stress must be exceeded to induce a Newtonian flow and below the critical value the suspension acts as an elastic solid. The critical point is denoted yield stress, $\tau_y$, if it is followed by a Newtonian behavior as in (4). However, it is more usual that a pseudo plastic shear rate region follows the shape of curve (5) and in such a case the (Bingham) yield stress, $\tau_B$, is derived from an extrapolation from the Newtonian region at higher shear rates.

Interpretation of the flow behavior of suspensions may be separated into two categories. The first is to assume minimum particle interaction[59] and the second is to assume large particle interactions typically found in coagulated colloids[60,61,62,63,64,65]. The first category was developed for spherical particles immersed in a liquid with

equal density and particle volume content less than 10 % as described by Einstein. The final expression for viscosity is as follows:

$$\eta = \eta_0(1 + 2.5\phi) \tag{4.2}$$

where $\eta_0$ is the viscosity of the solvent and $\phi$ is particle volume fraction. When the particle volume content rises to values higher than ~10% the equation fails to describe the viscosity. The upper limit can be increased by adding the next term in the series expansion ($6.2\ \phi^2$). However, this can only slightly increase the particle concentration range where the equation is applicable.

### 4.3 Correlation between rheology and ζ-potential

The i.e.p. corresponds to a point where only attractive van der Waals interaction exists and therefore the suspension close to i.e.p. tends to rapidly coagulate and the flow behaves strongly non-Newtonian[60, 66]. A maximum in viscosity or yield stress is commonly found at or close to the i.e.p. when viscosity is plotted as a function of pH[45,61,65,67,68,69,70,71,72,73,74,75,76]. The visco-coulombic effect is strong and it is not unusual that the increase in yield stress/viscosity increases a few orders of magnitude. For many suspensions there is a linear relationship between Bingham yield stress, yield stress or viscosity and $\zeta^2$ at low and moderate ζ-potentials[61,63,65,67,71,72,74,75,76,77,78]. The relationship was first derived and experimentally tested for aqueous kaolin suspensions by Hunter and Nicole[61]. In the equation they assumed that Bingham yield stress is proportional to particle interactions according to DLVO theory. Correlations have since then included yield stress, viscosity and more sophisticated approaches such as creep recovery tests and oscillatory stress[79,80,81]. The equation or similar expressions have been tested for a wide range of different materials that include polystyrene latex (PS), polymethylmethacrylate latex, $ZrO_2$, $TiO_2$, silica, $Al_2O_3$ and laterite aqueous suspensions. A short presentation of the models used in this thesis is given below.

In an impact between two particles a maximum attractive force will occur at an equilibrium minimum distance, $l_0$. The Hunter and Nicole yield stress at this

equilibrium is based on the standard DLVO model multiplied by von Smoluchowski collision frequency per volume[82] as described by eq. 4.3.

$$\frac{\eta(\dot{\gamma})}{\eta_{max}} \approx \frac{\tau_Y}{\tau_{max}} = 1 - \frac{24\pi\varepsilon_0\varepsilon_r\zeta^2 l_0}{H_{212}} ln(1 + e^{-\kappa l_0}) \quad (4.3)$$

Modified to apply for particle interactions and assuming constant surface potential the Bingham yield stress can be expressed as eq. 4.4.

$$\frac{\eta(\dot{\gamma})}{\eta_{max}} \approx \frac{\tau_B}{\tau_{max}} = 1 - \frac{6\varepsilon_0\varepsilon_r\zeta^2 l_0}{H_{212}} ln(1 + e^{-\kappa l_0}) \quad (4.4)$$

In a model developed by Zhou et al. [83] the repulsive potential of the DLVO model was derived by Hogg, Healy and Furstenau[84]. The average distance between coagulated particles, $l_f$, is considered to be located at a slightly longer distance than $l_0$. The force may then be considered to represent the steady-state aggregation process and the expression in eq.4.5 may be derived.

$$\frac{\eta(\dot{\gamma})}{\eta_{max}} \approx \frac{\tau_Y}{\tau_{max}} = 1 - \frac{24\pi\varepsilon_0\varepsilon_r\kappa\zeta^2 l_f^2}{H_{212}\left(1 + e^{\kappa l_f}\right)} \quad (4.5)$$

The $l_0$ and $l_f$ are adjustable parameters in the equations. This value may further be derived as a critical minimum distance, $l_c$, from the Schulze-Hardy approach.

The visco-coulombic effects in organic solvents have been investigated only to a limited extent. Partially it is due to the fact that the charge is less significant or sometimes even insignificant. Nevertheless charging may be of importance particularly in polar organic liquids[85] as revealed in some recent studies concerning both the rheological and surface potential behavior in non-aqueous suspensions[86]. Commonly these studies involve only small amounts of adsorbed organic matter[74,87] and typically the influence of a polymer/polyelectrolyte has been studied[68,69,74,75,87,88,89,90]. In aqueous suspensions Leong et al.[67] studied the influence of anionic additives and simple organic acids. The adsorbate shifted the i.e.p. to lower pH values and decreased the maximum yield stress. They further arranged

anions according to their tendency to induce specific adsorption and received the following sequence: sulfate<lactate<malate<phosphate<citrate. Additionally, the influence of phosphate and citrate on α-alumina aqueous suspensions has recently been investigated by Kay-Sen Khoo et al. [76]. They found a decrease in maximum yield stress to half when citric acid was added to the system. The increase in maximum yield stress in phosphate systems was attributed to hydrogen bonding between phosphate species adsorbed on the interacting particles.

### 4.4 Ionic transport in solutions and suspensions

An approach to study the motion of ions in solutions is by measuring the electrical conductivity. The measured conductance, G, of an electrolyte is the inversed value of the resistance, R.

$$G = \frac{1}{R} \quad [S] \tag{4.6}$$

The conductance is expressed in Siemens, S.

The conductivity, κ is defined as:

$$\kappa = G\frac{l}{A} \qquad \left[\frac{S}{m}\right] \tag{4.7}$$

where l is the length between two plates with a cross-section area, A. The conductivity increases with electrolyte concentration and this further depends on whether the electrolyte is strong or weak. In the nineteenth century Friedrich Kohlrausch demonstrated that molar conductivity of strong electrolytes has a root dependency on the concentration and this was presented in the Kohlrausch's law:

$$\Lambda_m = \Lambda_m^\circ - \mathcal{K}c^{0.5} \qquad \left[\frac{Sm^2}{mol}\right] \tag{4.8}$$

The conductivity at zero electrolyte concentration, $\Lambda_m^\circ$ is called limiting molar conductivity and $\mathcal{K}$ is a coefficient dominantly dependent on the stoichiometry of the electrolyte. Further, Kohlrausch was able to express $\Lambda_m^\circ$ as the sum of the different ion contributions

$$\Lambda_m^\circ = \nu_+\lambda_+ + \nu_-\lambda_- \qquad \left[\frac{Sm^2}{mol}\right] \tag{4.9}$$

where $\lambda_+$ is the molar conductivity contribution from the cations and $\lambda_-$ the contribution of anions, respectively, and $\nu_+$ and $\nu_-$ the number of cations and anions per formula unit of electrolyte[104]. Weak electrolytes are not fully ionized in the solution. In such electrolytes the conductivity is dependent on the degree of ionization, α, which can be expressed as

$$\alpha = \frac{\Lambda_m}{\Lambda_m^0} \tag{4.10}$$

Where the dissociation constant is related to a simple deprotonation equilibrium $HAc \rightleftharpoons H^+ + Ac^-$ by:

$$K_a = \frac{\alpha^2 c}{1-\alpha} \tag{4.11}$$

where c is the electrolyte concentration.

The ionic transport in non-aqueous liquids is less extensive. The solubility is low and weak acids mostly appear in its molecular forms. For instance, the pKa values of oxalic acid in water are 1.3 and 4.3 respectively. However, in ethanol the corresponding values are 4.2 and 8.2[21]. The dissociation of weak acids in mixed alcohol-water solutions are known from extensive studies[21,22,23]. A method to roughly estimate the pKa values of weak acids relates to the Born equation (eq. 4.12) as:

$$pK_{a,solvent} = pK_{a,water} + 121.6\left[\left(\frac{1}{\varepsilon_{solvent}} - \frac{1}{\varepsilon_{water}}\right)\left(\frac{1}{r_{anion}} + \frac{1}{r_{cation}}\right)\right] \tag{4.12}$$

In this equation the ionic radius is presented in Angstroms and ε refers to the relative dielectric constant. However, one limitation with the equation is that it does not consider the non-electrostatic contributions which in water-alcohol mixtures may be of significance[23].

In aqueous solutions the conductivity will be depressed by immersion of metal oxide particles. This is because pre-existing ions in the solution will adsorb at the surface and thus the conductivity will decrease. Recently, conductance measurements of titania in anhydrous or nearly anhydrous n-alcohol suspensions revealed that an increased particle content increases the conductivity in the presence of oxalic and phosphoric acids[91,92]. As mentioned the concentration of ionic species in alcohol solutions are low in contrast to aqueous solutions. This is one factor that will cause a net increase of ionic species in the solution and thus an increased conductivity. The enhancement is due to the strong affinity between the acids and the titania surface. This leads to complexes between the anion of oxalic and phosphoric acids that causes protons at the surface of the particle to solvate into the solution. The effect was called Surface-Induced Electrolytic Dissociation and is opposite to the conductivity behavior of “normal” aqueous suspensions.

# 5. Characterization methods and materials

The following section highlights the principle of the instruments and the material properties used in appended articles. However, details of unique measurement setups are presented in the article section.

## 5.1 Electrophoresis

Particles that posses a surface potential in a suspension and are exposed to an external electrical field will exhibit a motion relative to the liquid in the direction toward the field's electrical pole opposite to particle charge. After a few microseconds of applied electrical voltage a linear relationship between electrophoretic velocity, $\vec{v}_e$, and the applied electrical field, $\vec{E}_\infty$, can be found and this can be expressed by[93]:

$$\vec{v_e} = \mu_e \vec{E_\infty} \tag{5.1}$$

where $\mu_e$ is the electrophoretic mobility[93]. The electrophoretic mobility can be used to derive the ζ-potential. The means of interpreting the ζ-potential are dependent on the suspension. "Ideal" suspensions are represented by relatively simple models in a classical approach while "complex" suspensions require more elaborated models[93]. A well known classical model is the Smoluchowski equation in which the particles are assumed to be non-porous and spherical. The ζ-potential is assumed to be constant and the surface conductance of the electrical double layer is assumed to have a negligible influence on the field-induced potential distribution[93]. Further, the product of the particle radius (a) and reciprocal Debye length are assumed to meet the criteria of $\kappa a \gg 1$. The Debye length represents the thickness of the diffuse ion cloud around the particle and is defined as:

$$\frac{1}{\kappa} = \sqrt{\frac{\varepsilon_0 \varepsilon_r RT}{2F^2 I}} \tag{5.2}$$

where F is Faraday's constant and I ionic strength.

Hence the thickness of the double layer is insignificant compared to the size of the particle. In this case the electric field will provoke a motion of the charge liquid surrounding the particle that will affect the motion of the particle itself[93]. Under these circumstances the Smoluchowski equation can be expressed as

$$\zeta = \frac{\mu_e \eta}{\varepsilon_r \varepsilon_0} \tag{5.3}$$

where η is the bulk viscosity and $\varepsilon_r\varepsilon_0$ is the permittivity. A similar approach but where κa<<1 leads to the Hückel equation:

$$\zeta = \frac{3}{2}\frac{\mu_e \eta}{\varepsilon_r \varepsilon_0} \tag{5.4}$$

In this case the EDL is insignificantly provoked by an external electrical field and this causes almost no liquid motion around the particle. From equations 5.3 and 5.4 it can be seen that Hückel equation will give larger ζ potential values. For κa values within the two extreme the ζ potentials can be calculated using the Henry equation:

$$\zeta = f(\kappa a)\frac{\mu_e \eta}{\varepsilon_r \varepsilon_0} \tag{5.5}$$

The coefficient receives values of $1 \leq f(\kappa a) \leq 1.5$ and thus absolute ζ potential values fall between Smoluchowski and Hückel. However, the latter equation is only valid at ζ<25 mV due to the relaxation effect[94]. The effect can be explained by a force on the particle caused by a distorted EDL and this tug will decrease particle mobility. This distortion is due to the ions in the atmosphere around the particle and the charge particle moves in opposite direction[95]. The effect is treated in advanced models such as O'Brien-White[96] and Dukhin-Derjaguin[97].

Modern electrophoresis is carried out using a laser light source. The technique used in the thesis is called Laser Doppler Micro-electrophoresis. The principle is illustrated in Fig. 5.1.

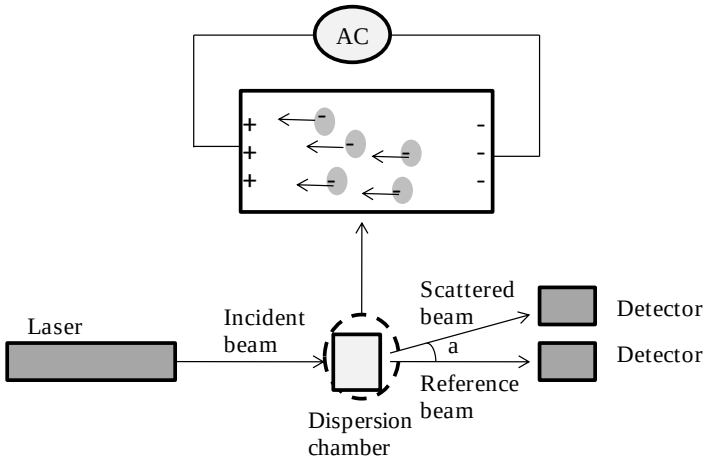


Figure 5.1: Principle for Laser Doppler Velocimetry.

An alternating current causes particles in the dispersion to move with a velocity related to their ζ-potential. Velocity is measured using a technique called Phase Analysis Light Scattering which enables calculations of the electrophoretic mobility. From the velocity the ζ-potential can be calculated. A limitation in the laser technique is its restriction to measurements of high particle content and typically the particle mass concentration is kept below 1‰.

## 5.2 Dynamic light scattering

The particle size in suspensions can be measured by dynamic light scattering (DLS). The instrumental setup is identical to electrophoresis (figure 5.1). The instrument works by analyzing the intensity fluctuations in the detected scattered light. It compares the intensity of the signal at a given time with the intensity at a later time. Any coherence between the first and the second signal will eventually disappear with time. The time frame for this to happen depends on the size of the particles. Larger particles move more slowly and thus need a longer time frame than small particles.

The particle size can then be derived by a correlation diagram. In Malvern ZS instrument a size distribution can be extracted by the use of a software algorithm. This can be presented as an intensity, volume or number distribution. Different methods to derive the distribution may differ with several orders of magnitude. An intensity distribution will favor the larger particle fractions and a number distribution will favor the small particle fractions with the volume distribution in between.

### 5.3 Electroacoustics

There are two approaches to derive an electroacoustic theory. The first was suggested by Enderby and Booth[98,99] about 60 years ago and the second by O'Brien[100] about 20 years ago. In the first approach a sound wave passes throw a suspension and this will provoke the particles (with a density higher than the liquid) to move relative to the liquid. This causes a distortion of the EDL and hence an AC field is induced. The effect is called Colloidal Vibration Potential (CVP) when the open-circuit voltage between the sensing electrodes is the measured output and Colloidal Vibration Current (CVI or CVC) if the short-circuit current is the measured output[101] (DT-1200). The second approach utilizes the reciprocal signal i.e. an acoustic signal is derived from an applied AC field. This effect is called Electrokinetic Sonic Amplitude (ESA) and is the utilized method for the Acoustosizer. The oscillation of the particles by ESA approach is dependent on the particle size and ζ-potential. An ESA measurement cell is illustrated in Fig. 5.2.

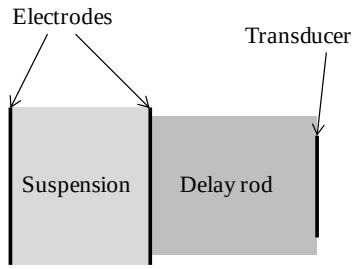


Figure 5.2: ESA measuring unit.

The delay rod is needed to separate the ESA signal from unwanted "cross talk" signal radiated from the high-voltage pulse across the measuring cell[102]. To derive a measuring point the Acoustosizer uses 13 different frequencies in a range of 0.2-20 MHz. The determination of the two quantities is carried out in a two-step process[102]. The first step is to calculate a dynamic mobility spectrum from the ESA signal and the second step is to determine the size and ζ-potential from that spectrum[102]. The dynamic mobility is a complex quantity with both a magnitude and a phase angle[103] and an equation that relates the ESA signal with the dynamic mobility has been derived by O'Brien[100]:

$$ESA = A(\omega)\phi\left(\frac{\Delta\rho}{\rho}\right)\mu_D\left[\frac{Z_s Z_r}{Z_s + Z_r}\right] \tag{5.6}$$

Here ESA is the voltage across the pressure transducer, A(ω) is an instrument constant, $\phi$ is the volume fraction of solids, Δρ is the difference between particle and solvent density, ρ is the density of solvent, $\mu_D$ is the average dynamic mobility of the particle, $Z_s$ is the acoustic impedance for the suspension and $Z_r$ is the acoustic impedance for the rod. In the second step the dynamic mobility can be linked with the particle size and ζ-potential. In case of a spherical particle with a thin double layer it is possible to derive the following expression[102]:

$$\mu_D = \frac{2\epsilon\zeta}{3\eta} G\left(\frac{\omega a^2}{\nu}\right)\left(1 + f(\lambda, \omega')\right) \tag{5.7}$$

where $a$ is the particle radius, ε is the permittivity, η is the viscosity and ν is the kinematic viscosity (η/ρ) of the solvent and ω is the measuring frequency. However, both G and f are complex functions and the exact[102] forms are not explained here. This further includes a modified dynamic mobility formula created by O'Brien and applicable at high solid loads[101]. The Acoustosizer additionally uses a single frequency approach. The Smoluchowski formula is then used and measurements are made at the lowest frequency where it is assumed that the inertial forces are unimportant[102]. In this case the particles are assumed to be in phase with applied AC signal and thus the dynamic mobility equal to the static mobility[48]. The two

approaches can give relatively equal results[48] but this is dependent on the particle size where large particles tend to give a result with underestimated ζ-potentials.

### 5.4 Viscosity measurements

Various techniques are used to measure the viscosity of a fluid such as Oswald viscosity meter and different rotational methods. The Bohlin VOR belongs to the latter category and a setup of the equipment is illustrated in Fig. 5.3.

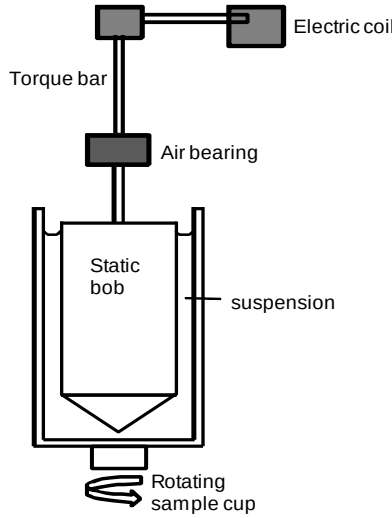


Figure 5.3: Setup of Bohlin VOR.

The suspension is immersed into a temperature controlled cup and during a measurement the cup will rotate with a constant shear rate. Several different shear rates may be used in a shear rate scan to reveal the viscous properties of the suspension. The stress of the dispersion will be transferred from the static sample bob to an electrical coil sensor via an air bearing and torque bar. The sample bob and torque bar (torsion bar) are changeable dependent on dispersion properties.

## 5.5 Conductance measurements

The electrical conductivity is a measure of ion transport in a medium where a high conductivity corresponds to a low flow resistance. A standard technique to measure the conductivity in an electrolyte solution is illustrated in Fig 5.4 were two electrodes are placed in the medium of interest. The conductivity is obtained when $R_1/R_2 = R_3/R_4$ and since it is AC this corresponds to impedance[104]. However, the conductivity cannot directly be taken from the resistance because this will give unreliable results due to complicated current flow. Instead the instrument is calibrated using a standard calibration solvent with known conductivity to derive a cell constant. There are different types of measuring probes available. In this thesis a flow-through probe was used.

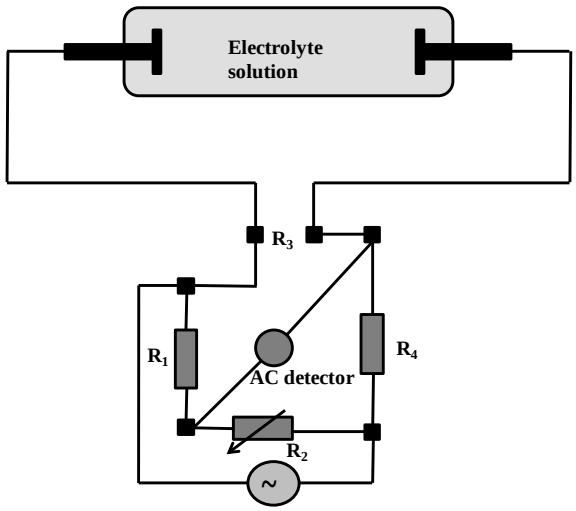


Figure 5.4: Setup for measurement of the conductivity.

## 5.6 FT-IR spectroscopy

Infrared spectroscopy (IR) is a surface sensitive instrumentation that reveals chemical information about the measured sample. In FT-IR the IR frequency is Fourier-transformed and the result is presented as a spectrum. It can reveal

information from both organic and inorganic samples and can identify functional groups since the wavelength for a specified group is characteristic. The method is fast and the sample amount needed is small. In this thesis the sample was immersed in an IR-inert material (KCl) which thereafter was compressed to a tablet. The IR radiation is sent through the tablet and a transmittance spectrum is derived.

### 5.7 Titania and Alumina

Most metals form compounds with oxygen. Oxygen can exist as oxide $O^{2-}$, superoxide $O_2^-$, and peroxide, $O_2^{2-}$. The dominating crystal forms of $TiO_2$ are anatase and rutile. Both rutile and anatase have a high refractive index and chemically stable nature as well as a high whiteness and opacity. This makes them attractive in a broad range of products. Two different anatase particles were used. The particle diameter is about 300 nm and the specific surface area 9 $m^2/g$. The particles were cleaned before use by washing them in aqueous 5 M NaOH and $HNO_3$ followed by rinsing with water. The anatase $TiO_2$ used in paper V-VII was P25 Aeroxide Degussa. It has a particle diameter of ~ 30 nm and a specific surface area of ~ 55 $m^2/g$ and it was used as obtained. Using the derived specific surface area and assuming spherical particles lead to a diameter of ~ 27.7 nm. Thus it was concluded that the particles were single and dense. The alumina was supplied by Sumitomo and is a $\alpha$-alumina of high purity quality. The particle diameter is about 300-400 nm and specific surface area ~ 7 $m^2/g$ and it was used as obtained. However, in potentiometric titrations both $NaOH/HNO_3$ cleaned and non-cleaned alumina was used but no difference in result was seen. The i.e.p./p.z.c. of anatase in aqueous suspensions is commonly at pH of 6-7[26]. In alumina the corresponding pH value is at ~ 9-10[26]. Both metal oxides are considered as hard.

### 5.8 Kaolin and Montmorillonite

Kaolin and Montmorillonite are both clays and belong to the group of phyllosilicates sheet formed silicates. Kaolin mainly consists of kaolinite which is a hydrous

aluminum silicate. Its structural appearance is octahedral alumina and tetrahedral silica sheets stacked alternately[105]. The raw material is white and may be used in different industrial products such as paper coating. However, the usefulness is much broader and it can for instance be found as filler in plastics, rubber and fiberglass[105]. The shapes of the particles are plate-like with high aspect ratio. In addition they are to some extent porous. The charges are not evenly distributed on the surface and some are even located in the bulk. The p.z.c. is found at a low pH value if any[26] and this means that particles mostly posses a negative charge. The clays are known for their cation exchange properties and in addition they tend to selectively dissolve into the solution. Montmorillonite contains hydrated sodium calcium aluminum magnesium silicate. The structure is two tetrahedral sheets with one octahedral sheet in between. The diameter of kaolin particles was 0.1-0.4 μm according to the manufacturer and it was used as obtained. Montmorillonite was fractionated by separating sediment from the stable suspension after 10 minutes since the original product contained coarse grains which are not suitable for the current measurements. Particle size measurements by means of the DT-1200 gave a diameter of 0.2 μm and by means of the Acoustosizer less than 1 μm. The differences in results probably depend on the particle aspect ratio. These results suggest that the ζ-potential is rather uncertain for clays and should be referred to as "apparent". In comparison with alumina and titania kaolin and montmorillonite may be considered as rather soft.

### 5.9 Melamine-formaldehyde

Melamine-formaldehyde (MF) is made by polymerization of melamine and formaldehyde. The material is stiff and strong and can for example be used in tableware or as a material to improve mechanical properties in pulp fiber composites[106]. The MF latex used during the experiments was synthesized in the laboratory. It was synthesized according to a known recipe[107] where melamine is dissolved in aqueous formaldehyde at a temperature of 80°C. Thereafter formic acid was used to induce the polycondensation. There was a slight difference in the synthesis between MF latex used in paper III and IV. In the synthesis of paper III the reaction was terminated 30 s after the turbidity appeared by rapid cooling with

extensive amounts of water. The specific density of MF latex was found to be 1.41 g/cm$^3$ and this is sufficient to receive a signal using the electroacoustic technique. Since the polycondensation was stopped the sizes of the particles were rather heterodispersed. By particle size measurements utilizing three instruments for electrokinetic measurements, diameters were distributed between 0.1-1 μm. The exact size was difficult to find since particle size measurements were rather irreproducible and varied with pH and electrolyte concentration. In paper IV there was no interruption of the polycondensation and the synthesis was stirred for additionally 10 minutes and thereafter left for cooling in room temperature. In figure 5.5 a SEM image of synthesized particles can be seen. The particle diameter was estimated to be 2-7 μm and this was relatively close to hydrodynamic particle sizes measured by dynamic light scattering where the particle diameter where in the range of 2-8 μm.

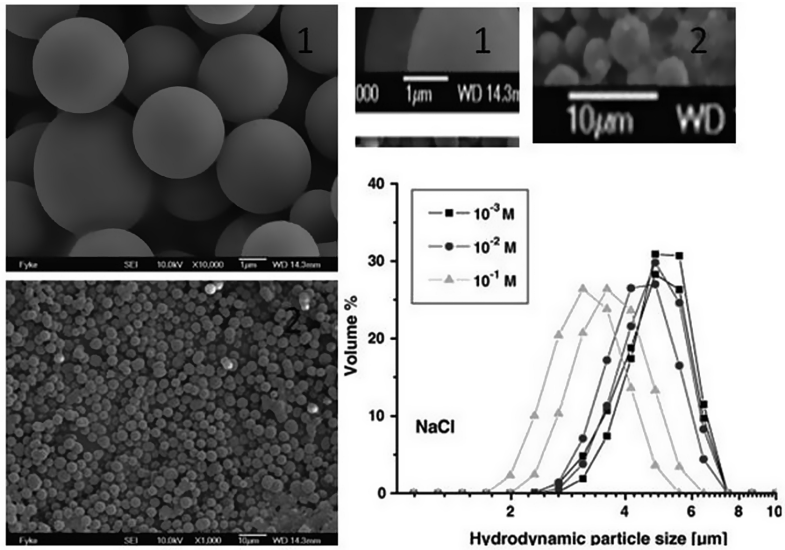


Figure 5.5: Synthesized MF latex particles seen in SEM images and determined by dynamic light scattering particle size measurements.

The hydrodynamic sizes were measured in the presence of NaCl in the range of $10^{-3}$-$10^{-1}$ M and at a pH of about 5. A decrease in size could be found with an increase in

electrolyte concentration. This is a known phenomenon for latexes[108] but the decrease more likely depended on the weak repulsive barrier (low ζ-potential) in 0.1 M electrolyte at pH 5. This caused more scattering and probably less accurate results due to the instability of the suspension. To estimate the structure of the particles the specific surface area was derived by additional methods. By the Langmuir isotherm applied to $N_2$-gas adsorption a specific surface area of 2.1 $m^2/g$ was found. A BET single point and a BET isotherm analysis gave 1.4 and 1.5 $m^2/g$, respectively. The results correspond to spherical particle diameters in the range of 2.1-3.1 μm and an average size of 2.65 μm. From the SEM image it can be deduced that the particles to some extent are porous. Further, the agreement between SEM and the hydrodynamic size indicates that no particle swelling occurs. From a FTIR transmittance spectrum it was deduced that the active groups probably were –NH and $–NH_2$. The MF latex is considered as soft.

# 6. Results and discussions

The colloidal stability of a suspension is strongly dependent on the interactions between the surface (or more precisely its functional sites) and the components in the solution. A schematic diagram is drawn in figure 6.1 which illustrates the influence of the cations and anions on the specific adsorption. Adsorption of anions induces a shift of the i.e.p. toward lower pH and a shift of the p.z.c. toward higher pH. Opposite shifts occur when the nature of the adsorption is cationic[11]. These shifts have strong influence on the suspension. An improved understanding of the affecting parameters will enhance the ability to control the suspension.

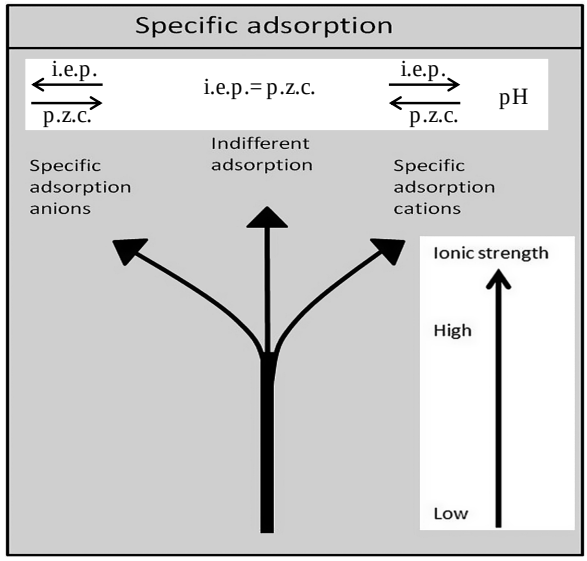


Figure 6.1: The specific adsorption of aqueous suspensions and its dependent parameters.

The first parameter of interest is the ionic strength which may induce specific adsorption especially at higher ionic strength[44]. In articles I-IV the specific adsorption of aquatic electrolytes in suspensions are investigated. Three different parameters related to the surface charging are interlinked in order to describe the ionic interactions at the surface. As presented previously the type of specific

adsorption relates to the selected surface and ion. These two parameters are not mutually exclusive. Furthermore, state of the system also depends on ion-ion and/or ion-surface interactions. A number of 1:1 electrolytes were investigated in order to evaluate how cations and anions can be arranged in ionic series. Except the two qualitative (HSAB and Hofmeister/lyotropic) series, the experimentally determined ion sequences have also been correlated to the thermodynamically defined Born equation (3.4).

In articles V-VIII the ionic interactions in aqueous, mixed and non-aqueous suspensions are investigated. In article V-VII the SIED effect in suspensions of ethanol and methanol solvents was studied. Of primary interest was to see if the effect is only observed for suspensions of weak acids in anhydrous or nearly anhydrous n-alcohols. The acids are related to the specific adsorption of anions. Suspensions of different water content were investigated and this relates to the acid ionic dissociation. Suspensions were primarily investigated by conductivity and ζ-potential measurements. Since the proton dominates over all other ionic species the conductivity will be affected by the ionic dissociation at the surface. The parameters of interest were also pH, $pK_a$, surface affinity and dielectric constant. In the last article (VIII) the viscosity (macroscopic property) of Titania in aqueous and alcoholic suspensions is studied. The study further relates back to the charging properties by evaluating different known models based on the DLVO-theory. The results from the first series of articles will first be discussed individually and thereafter the observations are summarized. This is done because different levels of specificity are revealed in this way. Moreover, the compiled data summarizes the i.e.p. trends.

### 6.1 High ionic strength suspensions - comparison of methods

The nature of the adsorption in a suspension can be characterized if the ζ-potential at more than two different electrolyte concentrations of otherwise similar suspensions is plotted as a function of pH[28]. Then the isoelectric point (i.e.p.) of the suspension of different (1:1) electrolytes will appear at the same pH-value in contrast to

specifically adsorbed ions which will shift the i.e.p. Hence for indifferent electrolytes at a low ionic strength a change in electrolyte concentration will only affect the absolute values of the ζ-potential. If the i.e.p. is shifted toward lower values upon an increase in electrolyte concentration the specific adsorption is anionic and if the shift is toward higher i.e.p. it is cationic. 1:1 electrolytes at low or moderate concentration usually adsorb indifferently to the surface of the particle. In contrast, suspensions containing multivalent ions or if the electrolyte concentration of 1:1 ions is high typically adsorb specifically[109,110]. For example, reports on both cationic[111] and anionic[112] adsorption can be found in the literature and the type of adsorption depends both on the ion and the surface. The relatively high ζ-potentials found at high ionic strength were observed when utilizing the electroacoustic technique about 20 years ago. The technique enabled measurements at high ionic strength which, at the time, was not possible by any electrophoretic technique. The electroacoustic results were surprising since accordingly to the DLVO-theory the ζ-potential would be suppressed to very low absolute values (typically a few millivolts) if the electrolyte concentration was increased to high levels. However, a limitation of the electroacoustic measurements has been the strong background signal caused by the electrolyte at high ionic strength. The signal is subtracted from the result but since the background in very high ionic strength can be of the same magnitude as the signal from the double layer the results are uncertain in absolute values and sign. This has been shown by the partly inconsistent results found utilizing different electroacoustic instruments[111]. In recent times high ionic strength measurements have become available for electrophoretic techniques as well. Physically the suspensions of electrophoretic measurements commonly use a particle content of 0.1wt% or less whereas corresponding electroacoustic measurements use 1-40wt%. Therefore it was considered to be of interest to investigate the ion selectivity of different surface ion interactions by means of electrophoresis. However, firstly a careful evaluation of the methods was needed.

*6.1.1 Alumina suspensions at high ionic strength*

In the first report LiI, $LiNO_3$, NaCl, NaBr, $NaNO_3$, KCl, $KNO_3$ and CsCl salts were added to aqueous Alumina (AKP-30, γ-alumina) suspensions. The electrolyte concentrations extended up to 2 M. Suspensions were analyzed by means of electrophoresis and two different electroacoustic instruments and the data was compared to published results [113]. Additionally the surface charge density for some suspensions was determined. The surface charge density of alumina suspensions for a range of different concentration of $KNO_3$ can be seen in Fig. 6.2. A point of zero charge (p.z.c.) was found at pH 9.4-9.7 and this corresponds well to values for alumina suspensions found in the literature[114]. However, suspensions of an electrolyte concentration of $10^{-3}$ M gave a p.z.c. of 8.8.

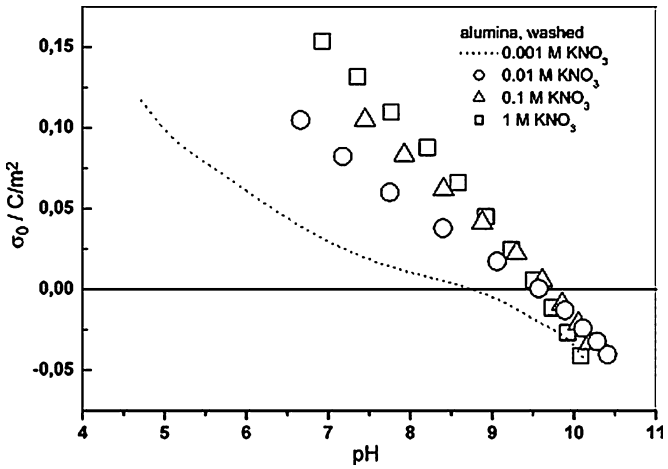


Figure 6.2: Surface charge density of alumina suspensions, at 298 K, plotted as a function of pH.

In order to investigate the reason for this discrepancy alumina suspensions containing $NaNO_3$ were studied as a function of pH. The measurements were made at $10^{-2}$ M and suspensions were titrated from the initial pH up to pH about 10. The suspensions were thereafter titrated in a cycle from high to low and back to high again. This is done to estimate the equilibration time effects.

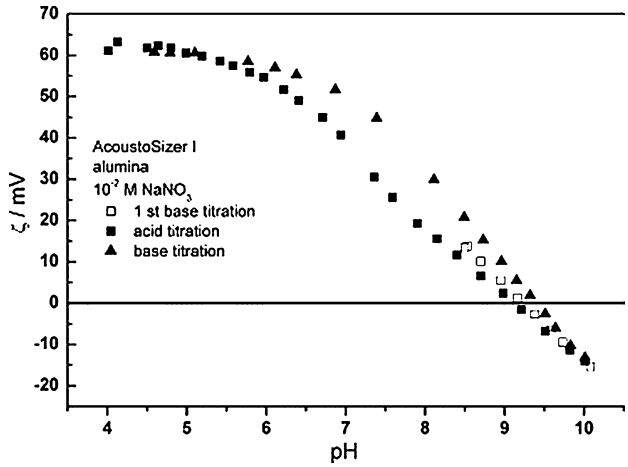


Figure 6.3: Consecutive electroacoustic measurements of Alumina suspensions at 298K in the precence of $NaNO_3$.

The i.e.p. of the slow titration shown in Fig. 6.3 resulted in an i.e.p. at pH=9.2 and the hysteresis were not significant. Hence there was a match between the i.e.p. and p.z.c. and this indicates indifferent behavior at moderate electrolyte concentration. Faster titrations (1 pH unit/hour) increased the hysteresis and an apparent i.e.p. was found at 9.0 (acid titration) and 9.4 (base titration). When electrophoretic measurements were made batch-wise about 10 samples were used for each suspension to cover the pH range. Each sample was aged for at least 4 h prior to the measurement. The pH was measured just before the electrophoretic measurements were done. In Fig. 6.4 the ζ-potential from electrophoretic measurements of two $Na^+$-salt suspensions is plotted as a function of pH. It covers electrolyte concentrations from low ionic strength (LIS) up to 2M (high ionic strength, HIS). A positive and a negative ζ-potential branch could be seen and the absolute value was depressed by the electrolyte. However, relatively high absolute values were obtained even at very high salt content confirming earlier reported results on alumina[113] and metal oxides[110]. Further, absolute ζ-values far from i.e.p. were slightly lower than the ζ-values found from comparable electroacoustic measurements (DT-1200: 65-70 mV and Acoustosizer I: 80 mV[113]). However, the ζ-potentials were calculated by means of Smoluchowski equation despite the fact that the κa values were below 100 which is considered to be the lower limit for the equation[95]. Results were therefore slightly

underestimated and a recalculation of the ζ-potential utilizing O'Brian-White theory which is valid in the region, gave absolute ζ-potentials of about 70 mV. Hence, at LIS all methods were comparable. Further, it should be emphasized that at high ionic strength the Smoluchowski equation was a relatively good approximation.

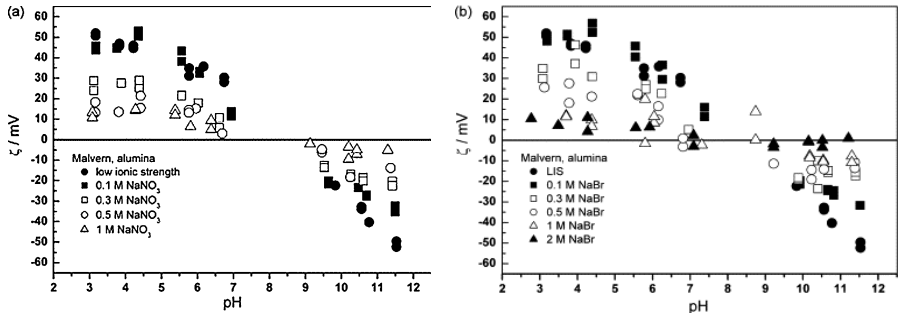


Figure 6.4: ζ-potentials derived by electrophoresis of batch-wise prepared samples at 298K plotted as a function pH in a) $NaNO_3$ and b) NaBr electrolyte. (LIS: low ionic strength).

A disadvantage with the electrophoretic measurements was the more scattered results compared to results derived by electroacoustic technique. Additionally, there was no buffering of the pH in the suspensions due to the very low particle content. This lead to a larger uncertainty and the measurement points derived were less dense. Thus it was not possible to exactly determine the i.e.p. from individual measurements. However, a general trend from several different measurements was found.

The relatively large amount of data made it necessary to confine the results. This was achieved by selecting one pH value from the acidic and one pH value from the basic range. The results from the complete setup of suspensions at pH=11 and 4 can be seen in Table 6.1.a and b respectively. At pH=11 suspensions containing $Li^+$ electrolyte had substantially less negative ζ-potential values than $K^+$ and $Na^+$ electrolytes independent of the method used.

Table 6.1.a: ζ-potential in mV at pH=11 for different electrolytes at various concentrations where M = Malvern (electrophoresis), DT (DT-1200, electroacoustics) and A (Acoustosizer I, electroacoustics[113]).

| | 0.1 M | | | 0.3 M | | | 0.5 M | 1 M | |
|---|---|---|---|---|---|---|---|---|---|
| | M | DT | A | M | DT | A | M | M | A |
| LiI | −20 | | | −10 | | | −5 | −3 | |
| $LiNO_3$ | −19 | −19 | −12 | −9 | −1 | 0 | −5 | +1 | +7 |
| NaCl | −28 | −11 | | −18 | −2 | | −11 | −5 | |
| NaBr | −27 | −12 | | −20 | −2 | | −16 | −9 | |
| $NaNO_3$ | −28 | −13 | −22 | −22 | | −11 | −16 | −6 | −4 |
| KCl | −28 | −17 | −27 | −20 | −6 | −18 | −12 | −10 | −10 |
| $KNO_3$ | −32 | −13 | −28 | −23 | −4 | −19 | −17 | −12 | −10 |
| CsCl | −30 | −11 | | −21 | | | −18 | −10 | |

In addition the difference between the electrophoretic and the electroacoustic measurements was demonstrated. From the latter technique the following sequence for more positive values can be established $Li^+ > Na^+ > K^+ = Cs^+$ at concentrations ≥ 0.1 M. A similar trend utilizing the former technique can only be seen at 1 M concentrations since the differences between the selected salts at lower concentrations were insignificant. However, when the absolute values at pH=11 were related internally, Malvern produced values consistent with Acoustosizer I and the values derived by DT-1200 were substantially lower.

Table 6.1.b: ζ-potential in mV at pH=4 for different electrolytes at various concentrations where M = Malvern (electrophoresis), DT (DT-1200, electroacoustics) and A (Acoustosizer I, electroacoustics[113]).

| | 0.1 M | | | 0.3 M | | | 0.5 M | 1 M | |
|---|---|---|---|---|---|---|---|---|---|
| | M | DT | A | M | DT | A | M | M | A |
| LiI | 40 | | | 22 | | | 18 | 6 | |
| $LiNO_3$ | 40 | 39 | 60 | 25 | 13 | 38 | 15 | 5 | 18 |
| NaCl | 53 | 41 | | 38 | 11 | | 30 | 15 | |
| NaBr | 55 | 49 | | 40 | 18 | | 22 | 12 | |
| $NaNO_3$ | 52 | 44 | 72 | 28 | | 53 | 23 | 16 | 25 |
| KCl | 52 | 42 | 76 | 30 | 17 | 53 | 20 | 13 | 26 |
| $KNO_3$ | 43 | 43 | 69 | 30 | 16 | 49 | 20 | 15 | 22 |
| CsCl | 56 | 46 | | 33 | | | 30 | 20 | |

It is interesting that the only trend within the acidic range was the lower absolute values found for $Li^+$ suspensions. This is surprising since the acidic range is usually

dominated by the nature of the anion and the contribution from nature of the cation is rather small. This insensitivity has, for example, been seen in several potentiometric and electrokinetic studies[114]. Further, from a comparison of the absolute values at pH=4 it was revealed that the absolute values found from different techniques decreases in the order of Acoustosizer > Malvern > DT-1200. From Table 6.1.a and 6.1.b it can be concluded that the results from electrophoretic measurements are consistent with results derived by electroacoustic techniques. The absolute values are relatively high and are substantial even at high electrolyte concentration. Further, the sequence of cations in a series was qualitatively supported by all methods. Additionally, the positive pH branch was found to be independent of cations while the negative branch depended on the nature of the anions.

### *6.1.2 Kaolin and Montmorillonite suspensions at high ionic strength*

In publication II the electrokinetic properties of kaolin and montmorillonite suspensions in 1:1 electrolytes at high ionic strength were investigated. They are, in contrast to metal oxides and silica, not extensively documented in the literature. Similar to alumina suspensions, the ζ-potentials were determined as a function of pH and the ion selectivity was investigated by the shift of i.e.p. and from the absolute ζ-potential values. Both electrophoretic and electroacoustic measurements were performed but the electroacoustic measurements were limited in number of salts and electrolyte concentrations. The study included $LiNO_3$, NaCl, NaBr, KCl, KI, $KNO_3$ and CsCl salts. In Fig. 6.5.a and b the ζ-potentials from the Kaolin suspensions containing $LiNO_3$ and CsCl are plotted as a function of pH, respectively. Electrophoresis produced relatively scattered results which were similar to those of high ionic strength Alumina suspensions. However, ionic sequences could be derived from best-fit second degree polynomials. These can be seen in the figures as lines whereas measured data are indicated by symbols. The absolute values were depressed by an increase in ionic strength and the magnitude of the absolute ζ-potential values was found significant even at high ionic strength. This is illustrated in Fig. 6.5.a where experimental ζ-potential values of 1 M $LiNO_3$ suspensions were

found to between -10 to -20 mV. Similar magnitudes were also found in suspensions of Na salts at 1 M.

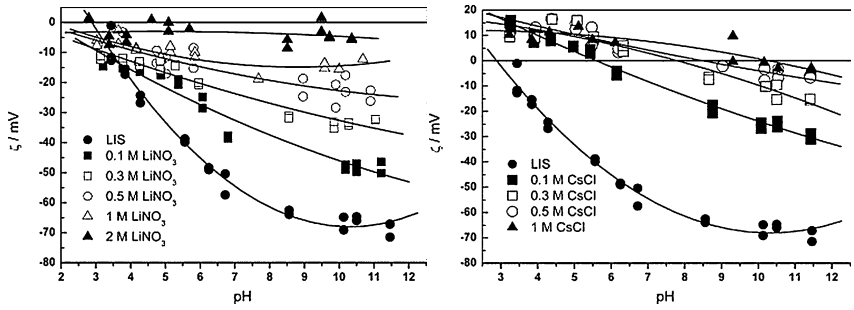


Figure 6.5: ζ-potential as a function of pH at 298K in Kaolin suspensions containing different electrolyte concentration of a) $LiNO_3$ and b) CsCl. The results are determined by electrophoresis. (LIS: low ionic strength).

A comparison between the suspensions of $LiNO_3$ and CsCl salts revealed that there was a shift of the i.e.p. toward higher values by the shift from $LiNO_3$ to CsCl suspensions. The shift of the Cs suspensions was significant even at electrolyte concentrations as low as 0.1 M. A similar shift was also seen in the suspensions containing potassium. Furthermore, Fig. 6.5.b reveals that the shift was dependent on the electrolyte concentration for a given suspension where i.e.p. increased with increased electrolyte concentration. The electroacoustic measurements on the Kaolin suspensions can be found in Fig. 6.6. In general the electroacoustic measurements were in agreement with electrophoretic measurements. At low ionic strength the absolute values from the different methods were within the range of –50 to -70 mV. The differences between the methods were relatively small and in agreement with electrokinetic data for clay found in literature[72,115,116].

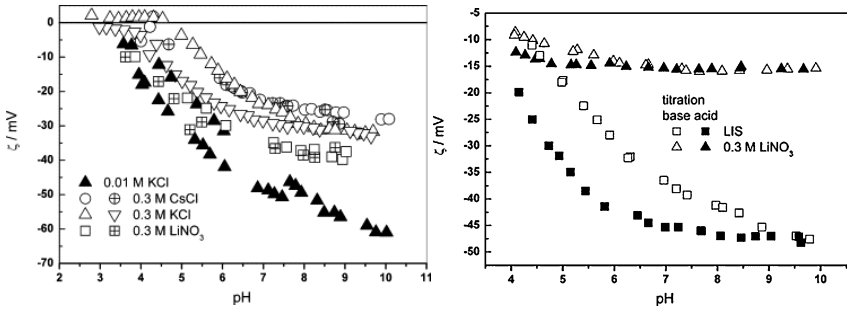


Figure 6.6: The ζ-potentials of Kaolin suspensions as a function of pH at 298K measured by a) Acoustosizer I and b) DT-1200. (LIS: low ionic strength).

The i.e.p. of the suspensions that contained $Cs^+$ or $K^+$ shifted to higher values with increased electrolyte concentration. However, despite very slow titration (<0.5 pH unit/h) a hysteresis was found. It was more pronounced at low or moderate ionic strength and decreased with increased ionic strength. This is likely due to irreversible reactions occurring at high and low pH. The impact will further depend on parameters such as pH range, titration rate and pre-equilibrium. However, the phenomenon was not investigated systematically.

The electrophoretic measurements of the Montmorillonite suspensions that contained $LiNO_3$ and CsCl salts can be seen in Fig. 6.7. Compared to Kaolin the difference between the absolute values at LIS and at HIS was relatively small. In the basic range the magnitude of the ζ-potentials of 1 M electrolyte was about half of LIS. Further, the influence of the selected salt was insignificant except for the CsCl suspensions. Those suspensions produced an i.e.p. which was shifted to higher values with increased electrolyte concentration.

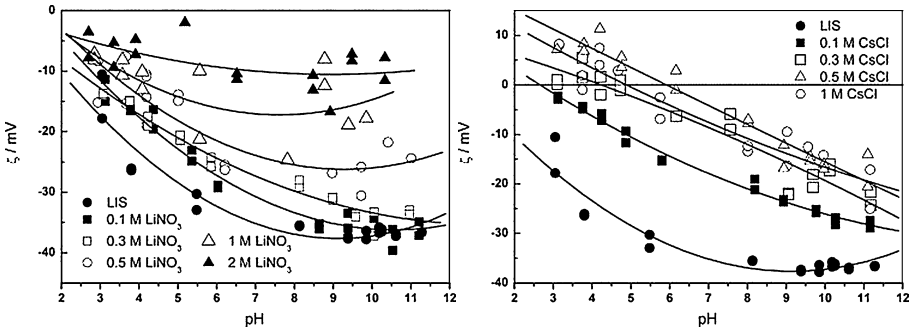


Figure 6.7: ζ-potential as a function of pH in Montmorillonite suspensions containing different electrolyte concentration at 298K of a) $LiNO_3$ and b) CsCl. The results are derived by electrophoresis and lines represent best fit 2nd degree polynomials of each series, respectively. (LIS: low ionic strength).

The Montmorillonite suspensions were further analyzed by the two electroacoustic techniques. The ζ-potentials derived by Electroacoustics were inconsistent with earlier findings[81,117] and the DLVO theory. The main concerns were that absolute values were unrealistically low at low and moderate ionic strength and increased with increased electrolyte concentration. Thus the measurements were concluded to be unsuccessful and could not be used for further analysis. A plausible explanation for its unsuccessfulness was the influence of impurities.

The results were thereafter interpreted by relating findings from the clay suspensions to results from different analyzed materials found in the literature[110]. If clays are compared to hard metal oxides such as $TiO_2$ and $Al_2O_3$ they could be referred to as soft. This is because clays have a relatively low dielectric constant and the preferential order for alkali metal cation adsorption is Cs > Rb > K > Na > Li compared to a reversed order for metal oxides. Additionally the i.e.p. is located at a low pH (if one exists) at moderate ionic strength (MIS). The properties are similar to the properties of silica which also can be categorized as soft. This is not surprising, since montmorillonite has a complicated kaolin like layer structure ($Al_2SiO_4O_{10}(OH)_2$) with dominating silica layer. In this sense the materials follow the HSAB principle (Table 3.1) where soft acids preferentially react with soft bases and the opposite, hard acids preferentially react with hard bases. In Table 6.2 a general categorization of the surfaces is made together with their surface potential

behavior in suspensions. The table is only qualitative. Nevertheless, it describes the electrokinetic potential of the suspensions better at HIS compared to the DLVO theory. It should be emphasized that the table attributes the ionic specificity to the ion-pair as well as the ion-surface interactions. Moreover, it is limited to HIS since in MIS and LIS the distribution of the ions close to the surface is dominantly determined by electrostatic forces and thus only the DLVO theory can describe that region.

Table 6.2: The absolute values of ζ-potential and induced shifts in i.e.p. by hard-soft principle by the surface and ions of 1:1 electrolyte (II).

| Surface | Anion | Cation | Below i.e.p. | Above i.e.p. | i.e.p. Shift | Example |
|---|---|---|---|---|---|---|
| Hard | Soft | Hard | High ζ | Low \|ζ\| | Up | $TiO_2$-NaI* |
| Hard | Hard | Soft | Low ζ | High \|ζ\| | Down | $Al_2O_3$-$LiNO_3$* |
| Soft | Soft | Hard | Low ζ | High \|ζ\| | Down | Kaolin-$LiNO_3$ |
| Soft | Hard | Soft | High ζ | Low \|ζ\| | Up | Kaolin-CsCl |

*ref. [110]

The table is only qualitative and there is no absolute scale for the categorization in terms of hard-soft character. The predominant attractive (hard-hard or soft-soft) interactions between counterions and surface determines the change in i.e.p.. Coions are repelled from the surface and produce only secondary effects. Hence the principles summarized in Table 6.2 only suggest that certain effects may occur.

### *6.1.3 Melamine-formaldehyde lattices at high ionic strength*

In paper III the electrokinetic potential of MF latex was investigated at HIS. The concept was similar to the previous studies and suspensions were analyzed by electroacoustics and electrophoresis. In particular it was of interest to see if the relatively high ζ-potentials found for other materials at HIS could also be seen for soft latexes and thus generalize the phenomenon. The influence of ionic strength on latices has been investigated previously. A commonly appearing phenomenon is a maximum in ζ-potential found at an electrolyte concentration about $10^{-2}$-$10^{-3}$ M

using a 1:1 electrolyte[108,118,119]. This anomalous behavior can be assigned to a "hairy" layer on the surface of the latex[120]. In most cases this maximum will disappear if the conduction inside the shear plane is properly considered for[121]. As for other materials, the ionic behavior in LIS and MIS is well investigated but studies at HIS are rare. MF latex may be categorized as a "soft" material according to the HSAB principle. The relatively high density compared to other latexes such as polystyrene makes them suitable to use in electroacoustic measurements were a substantial difference between the density of the media and the particle is needed to produce a signal. The result from electroacoustic measurements can be seen in Fig. 6.8. Measurements were performed by both electroacoustic techniques and covered electrolyte concentrations from LIS up to 0.3 M. The LIS contained no added electrolyte and thus the only electrolyte in the suspensions was added during titration of both acid and base. Both electroacoustic techniques gave an i.e.p. at pH of about 11. This was consistent with the results from electrophoretic measurements seen in Fig. 6.9. However, there was a relatively large difference between the methods when it came to absolute values. This was partly compensated by recalculation of the "Smoluchowski" ζ-potentials that underestimated the absolute values, by a model valid in given suspension conditions. For example, a recalculation by means of O'Brian-White theory produced ζ-potentials of 60 mV at pH 6 calculated from an electrolyte concentration of $10^{-3}$ M and a particle size of 0.1 μm.

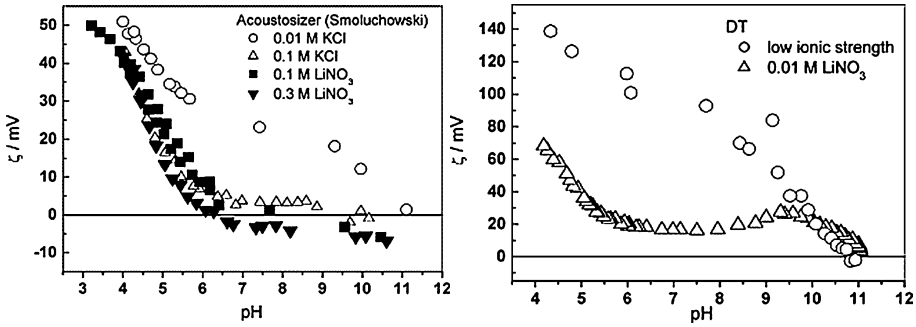


Figure 6.8: M-F latexes; ζ-potentials as a function of pH measured at 298K by means of a) Acoustosizer b) DT-1200 electroacoustic techniques.

At an electrolyte concentration of 0.01 M the ζ-potentials were depressed within the pH-range of about 5-9. Both electroacoustic methods were relatively consistent and at electrolyte concentration of 0.1 M the depression was even more significant and only ζ-potential values below 10 mV were found in the region. At 0.3 M electrolyte concentration there was a shift of the sign of the ζ-potential to negative values at a pH close to 6. However, this did not affect the absolute values which remained relatively low.

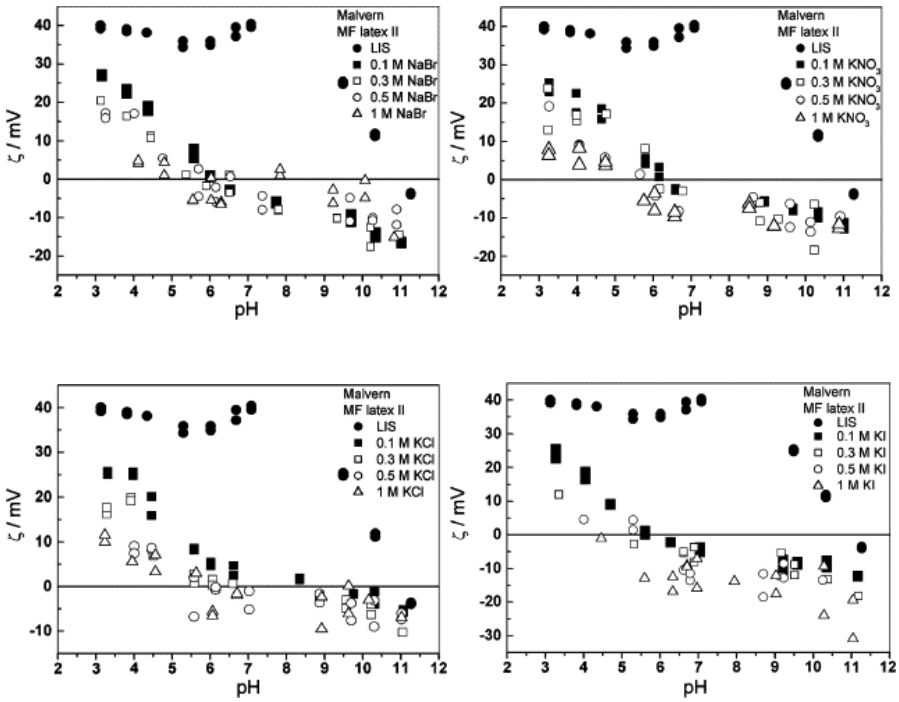


Figure 6.9: M-F latex; ζ-potential as a function of pH measured at 298K by electrophoresis in presence of a) NaBr b) $KNO_3$ c) KCl and d) KI at various electrolyte concentrations. (LIS: low ionic strength).

The influence of different salts was evaluated by electrophoresis and the results are collected in Fig. 6.9. The measured points were relatively scattered and an exact i.e.p. was not possible to determine. To derive a value a best-fit polynomial trend curve was used. This resulted in an arrangement of the anions in the sequence of I > $NO_3$ = Br > Cl. From suspension measurements of different chlorine (KCl, NaCl, and

CsCl), nitrate ($LiNO_3$, $KNO_3$) and iodide (LiI, KI) salts it could be deducted that the influence of the cations was rather insignificant. As mentioned earlier the MF latex can be classified as soft and thus will show greater affinity toward soft acids and bases. As seen the affinity toward $I^-$ (soft anion) was indeed stronger than to $Cl^-$ (hard anion). The absolute ζ-potential values found at HIS were significant in magnitude up to 1M. For example, in the case of 1 M KI electrolyte (6.9.d) the ζ-value was in excess of -20 mV. This value is in the same range as values found for metal oxides and supports the findings that the ζ-potential does not follow the DLVO theory at HIS.

## 6.2 Moderate ionic strength suspensions

The electrokinetic properties at moderate ionic strength has for most suspensions been thoroughly investigated. However, there are still some materials that have not been fully investigated and among those materials is MF latex. Thus it is of interest to evaluate the ionic strength and selectivity in a broader range for MF latexes.

### *6.2.1 Melamine-formaldehyde latex at moderate ionic strength*

In paper IV the electrokinetic properties of MF latex were investigated in the MIS range ($10^{-3}$-$10^{-1}$ M). The aim was to investigate if an ion selectivity trend could be seen at MIS due to the relatively strong effect of electrolyte concentration seen at HIS. The study included electrophoretic and electroacoustic measurements on MF latex suspensions and the salts included were NaCl, NaBr, $NaNO_3$, $NaClO_4$, KBr, KI and $KNO_3$. The influence of particle content on electroacoustic measurements can be seen in Fig. 6.10. Suspensions contained $10^{-3}$-$10^{-1}$ M of NaBr were titrated as a function of pH. Measurements were made in multi-frequency mode since "Smoluchowski" single frequency mode tends to underestimate the ζ-potentials of large particles. Some "Smoluchowski" mode measurements confirmed the suspicion. The multi-frequency mode was not able to produce all experimental points thus some of the points are missing in the two-way titration. However, it was fully possible to

derive ζ-potential trends despite this shortcoming. Two different particle contents in the range of 3.1-7.3 vol% were used for each electrolyte concentration but the ζ-potentials were not affected by the change. A small hysteresis could be seen in the titrations and this may be attributed to slow equilibration where the particle porosity distorted the result. The ζ-potential was decreased by an increase in electrolyte concentration. They were further depressed in the region of 5<pH<10 and this corresponds well with the depression found in paper III at HIS. At electrolyte concentrations of $10^{-3}$ and $10^{-2}$ M no charge reversal was found but at $10^{-1}$ M it was observed and the i.e.p. was found at a pH ~5.5. This value is slightly lower compared to MF latex at corresponding electrolyte concentration reported in paper III (Fig.6.8). However, the small difference might be due to some difference in measurement setup and synthesis of MF latex.

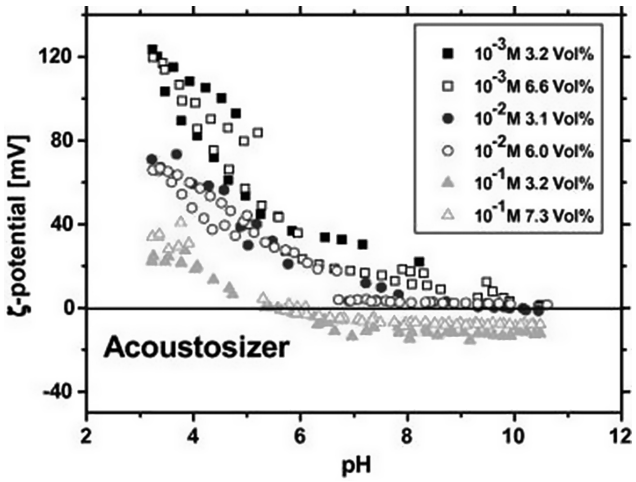


Figure 6.10: Electroacoustic measurements of MF latex suspensions at 298K where the ζ-potentials are plotted as a function of pH at varying NaBr concentrations and particle contents.

The corresponding electrophoretic measurements of NaBr suspensions can be seen in Fig. 6.11. The ζ-potentials were derived using the Smoluchowski equation. The lines demonstrate a second-order polynomial fit that was applied to derive i.e.p. values. The measurements were less scattered compared to measurements made at HIS and

the lines followed the measurements well. Additionally, the results were relatively close to the result found by electroacoustic measurements. In a comparison of the absolute ζ-potential values at a pH ~ 3 the electroacoustic measurements gave about 120, 70 and 40 mV and corresponding values in electrophoretic measurements were 90, 70 and 40 mV. This difference was not larger than differences seen for other suspensions. To ensure the correctness of measurements a control calculation of the electrophoretic measurements using the Dukhin-Semenikhin equation[122] was made but it did not influence the result more than 3mV at $10^{-3}$ M and even less at higher concentrations. However, the agreement was less accurate at higher pH and charge reversals were found for both $10^{-2}$ and $10^{-3}$ M at a pH < 10.

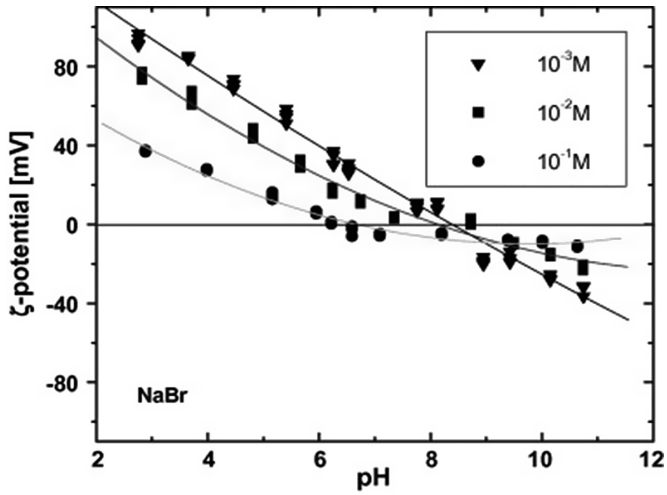


Figure 6.11: Electrophoretic measurements of MF latex suspensions at 298K where the ζ-potentials are plotted as a function of pH at varying electrolyte concentration of NaBr.

Corresponding electrophoretic measurements were made for six other salts. The i.e.p. values were collected for each salt and concentration. It was found that the shift in i.e.p. was mainly dependent on the ionic strength and cation or anion trends could not be distinguished being either small or insignificant.

### 6.3 Ion specificity trends

In paper IV the influence of selected electrolytes was evaluated accordingly to Fig. 6.12 where the i.e.p. is plotted against the negative logarithm of the ionic strength (pI). The error bars are related to extrapolations from the positive and negative ζ-potential branch, respectively.

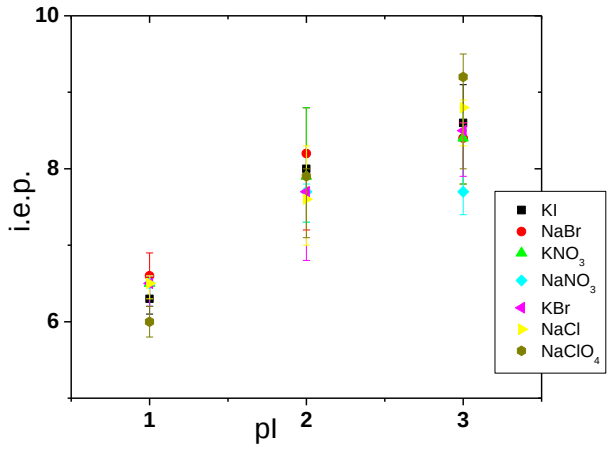


Figure 6.12: MF latex suspensions of seven different salts. The i.e.p. is plotted as a function of the negative logarithm of the ionic strength.

Fig. 6.12 clearly illustrates the influence of the ionic strength but not the influence of selected electrolyte. Thus this was further evaluated by ionic series. The significance of the anion effect was evaluated by correlation with two phenomenological series, HSAB and a Hofmeister (lyotropic) series. Additionally, anions were correlated with the Born scale representing the work of (dis)charging an ion and being proportional to $z^2/r$ (eq. 3.4). The purpose of using three different scales was to relate the results broadly to different ionic series found in the literature.

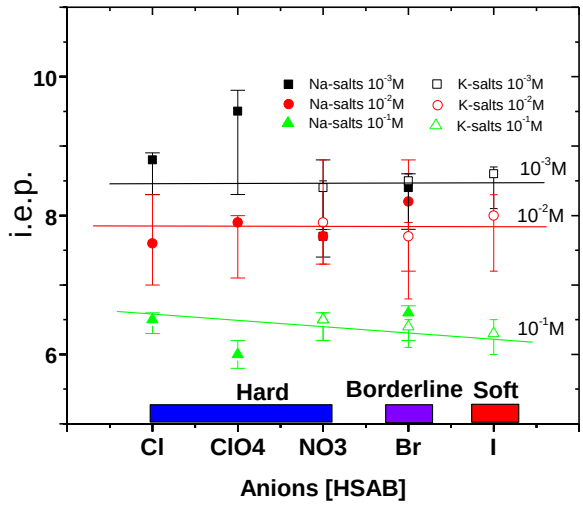


Figure 6.13: Correlation of the anions in MF latex suspensions according to the HSAB principle.

The correlation of the anions according to the HSAB principle can be seen in Fig. 6.13. There is no difference between hard and soft anions and thus the order among these anions could be rearranged. The MF latex could be categorized as soft, as discussed earlier. This means that soft anions should show greater affinity toward the MF latex than hard anions in order to comply with the principle. A greater affinity is indicated by a decrease in i.e.p. The influence of the increasing electrolyte concentration can clearly be seen as a decrease in i.e.p. However, the influence of the anion was insignificant (the $10^{-3}$ and $10^{-2}$M suspensions) or very weak ($10^{-1}$ M), if any. Thus the HSAB principle cannot give an unequivocal interpretation of MF latex at moderate electrolyte concentration. In Fig. 6.14 the anions are arranged in a typical Hofmeister series[123] ($Cl^- > Br^- > NO_3^- > I^- > ClO_4^-$ based on the ability to stabilize proteins). It should be emphasized that the arrangement in a Hofmeister series is dependent on several assumptions and therefore the order may vary. At $10^{-2}$ M the general trends for ion selectivity are insignificant as observed by the HSAB correlation. In case of the suspensions of $10^{-3}$ M a trend toward decreased surface affinity for more stabilizing ions can be seen. However, it should be noticed that the

trend is within the error margins and it is therefore only apparent. At $10^{-1}$ M there is an opposite trend where less stabilizing ions show grater affinity toward the MF latex. The trend is consistent and does not exclude any ion. The trend is relatively weak and is only qualitative.

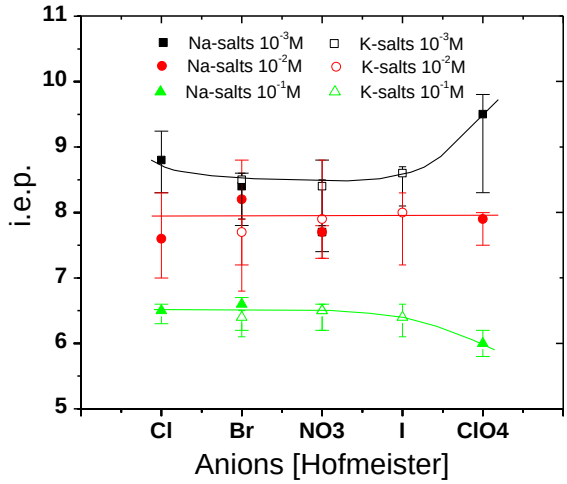


Figure 6.14: Correlation of the anions in MF latex suspensions according to a typical Hofmeister series.

In the last approach the i.e.p. was correlated by a thermodynamic property. This has its advantages compared to the two phenomenological series since there is a large amount of relevant data available. In the equation the work of (dis)charging an ion is proportional to $z_i^2/r_i$ and this is further equal to the charge potential ($z_i/r_i$) since it concerns 1:1 electrolytes. The correlation can be seen in Fig. 6.15 where i.e.p. is plotted against $z_i^2/r_i$.

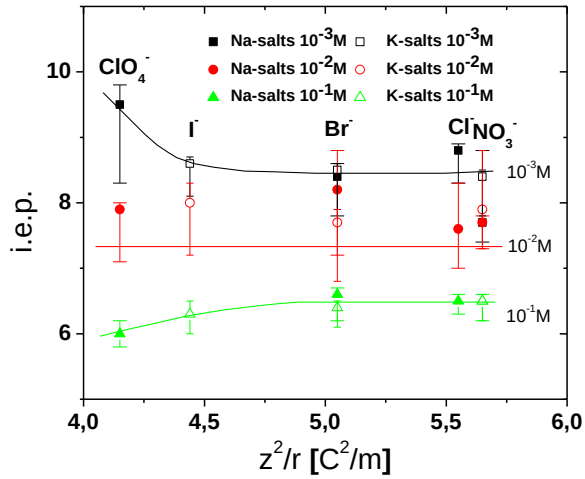


Figure 6.15: Correlation of the anions in M-F latex suspensions according to Born's scale representing the work to (dis)charge an ion.

There is a slight rearrangement in the series compared to Hofmeister series where $NO_3^-$ is moved from the middle. Despite the change there is no significant change in the appearance of the correlation. That is, at $10^{-3}$ M an increased i.e.p. can be seen with a decreased $z_i^2/r_i$ but the trend is within the error margins. At $10^{-2}$ M there is no visible trend. A small significant trend can be seen for $10^{-1}$ M suspensions where an increased surface affinity (decreased i.e.p.) is found with a decreased $z_i^2/r_i$. As can be seen in the Figures 6.13-15 there are relatively small difference in anionic sequences between series. The general trends tend to be similar except from $ClO_4^-$ in the HSAB correlation. It appears that even if different approaches are used to derive ionic series there is no large deviation in the outcome. However, there is a clear advantage in using the thermodynamic scale since it offers a semi-quantitative solution to the correlation. Thus it is recommended to use this approach.

This approach can also be applied to other measured suspensions which will enable a comparison of the results. In Figures 6.16-18 the i.e.p. as a function of pI was plotted for alumina, kaolin and MF latex suspensions. The latter figure is an extension of Fig. 6.12 where suspensions of high ionic strength are included. In general, there is a large uncertainty in electrophoretic measurements at high ionic strength[27]. This can

be seen as large deviations in the error bars from individual titrations of suspensions. In Fig. 6.16 alumina suspensions are presented. The i.e.p. at MIS was about 1 pH unit below i.e.p. values found for LIS. This was likely to be not a real decrease but a result of the extrapolation of the i.e.p. caused by the lack of experimental points in the critical pH range. From this it can be concluded that the selection of ions in the alumina suspensions only affected the absolute ζ-potential values as seen in section 6.1.1.

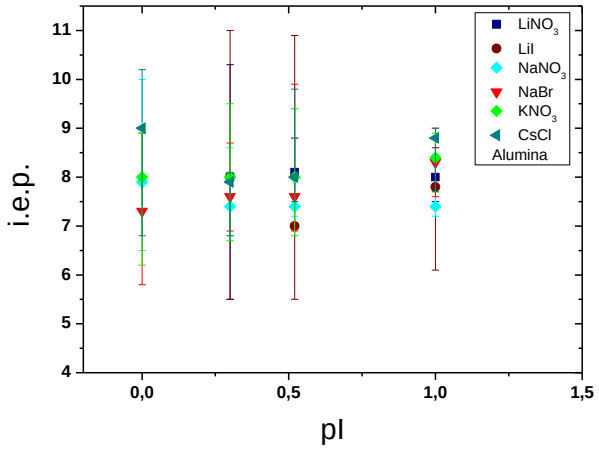


Figure 6.16: i.e.p. as a function of the negative logarithm of the ionic strength of alumina suspensions.

The i.e.p. values for the kaolin suspensions (Fig. 6.17) were increased with increased ionic strength (lower pI). Relatively large differences were seen between different salts where the use of CsCl salt gave much higher i.e.p. values. Further, the study included suspensions of $LiNO_3$, NaCl and NaBr salts. No i.e.p. values were found for those suspensions and thus if a value exists it must be found at a pH lower than 2.5. Further it could be seen that the influence of CsCl electrolytes even exceeds the influence of the ionic strength. The montmorillonite suspensions studied at identical electrolytes gave i.e.p. values only for the CsCl suspensions. This concurs with the results for the kaolin suspensions in terms of the highest i.e.p. for a given salt but it can be only poorly illustrated in a figure and is thus left out here.

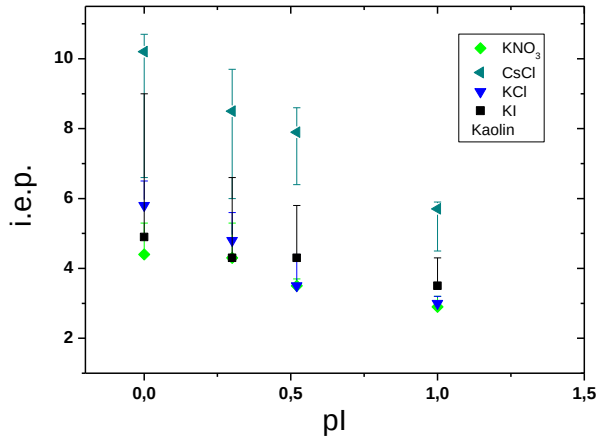


Figure 6.17: i.e.p. as a function of the negative logarithm of the ionic strength of Kaolin suspensions.

In Fig. 6.18 the extended trend for the MF latex suspensions can be seen. The figure is based on the results reported in papers III and IV. The i.e.p. is constantly rising from relatively low salt concentrations to 1 M. One exception could be found at 0.1 M where the suspension of KCl salt gave a very high value. However, a large uncertainty was found in the value when the positive ζ-potential branch was extrapolated. Based on the general trend from a large number of suspensions of different salts it is unlikely that this particular KCl value illustrates a real effect.

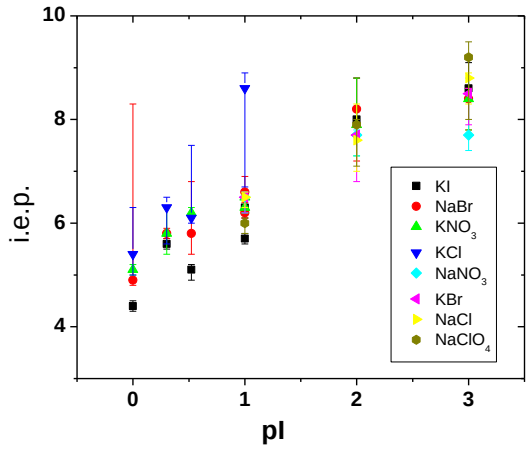


Figure 6.18: i.e.p. as a function of the extended negative logarithm of the ionic strength of MF latex suspensions.

Three methods to evaluate the ion selectivity were presented in paper IV. One of them was based on the thermodynamic Born equation (3.4). Due to its thermodynamic foundation this correlation is chosen for the suspensions of clays, alumina and MF latex at high ionic strength. Moreover, it was possible to evaluate both the anions and cations in a similar manner. Six paths where tested which included cationic and anionic correlation of alumina, MF latex and kaolin suspensions. From those correlations only anionic correlation of MF latex and cationic correlation of kaolin suspensions gave consistent trends. In Fig. 6.19 the anion correlation of MF latex suspensions can be seen. The influence of the ionic strength was significant over the entire concentration range. At electrolyte concentrations ≥ 0.1 M a lower $z^2/r$ value gave a significantly lower i.e.p.. Further, it can be seen that the results from measurements at high ionic strength coincide with the measurements at moderate electrolyte concentration (Fig. 6.15) where a decrease in i.e.p. can be seen with reduced $z^2/r$ for 0.1 M electrolyte concentration. However, the influence was relatively small and at 1.0 M the influence of the electrolyte concentration was larger. At 0.5 and 1.0 M the trends were not fully consistent since at the highest $z^2/r$, values do not relate to highest i.e.p.

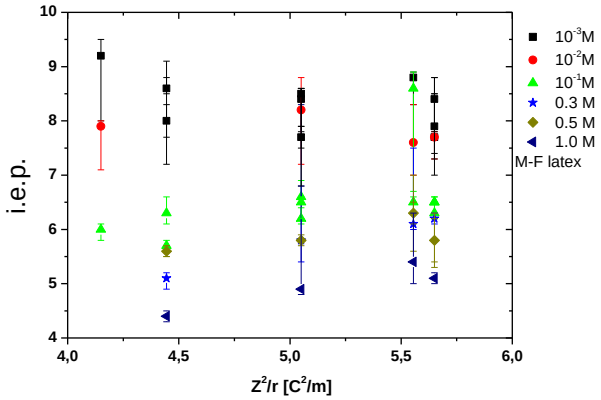


Figure 6.19: Anionic correlation of i.e.p. of MF latex suspensions by the $z^2/r$.

The cation correlation of the kaolin suspensions can be seen in Fig. 6.20. The study involved four cations which were combined with four different anions. For suspensions that contained $Na^+$ and $Li^+$ ions no i.e.p. were found and therefore only two $z^2/r$ values could be displayed. The result is not surprising since lower i.e.p. values were expected for higher $z^2/r$ values in accordance with the results. The $z^2/r$ position (not i.e.p.) where the $Na^+$ and $Li^+$ suspensions would be found, if any existed, is indicated in the figure as well as the lowest pH at which an i.e.p. could be found (the line). The trend was found to be similar for montmorillonite suspensions. The only difference is that the i.e.p. values where generally lower which lead to i.e.p. values only in presence of CsCl. Moreover, the non-consistent trend in the anionic correlations (Fig. 6.20) suggests that the cationic trend is plausible despite the limited range. The influence of the selected ions was relatively strong and exceeds the ionic selectivity found for MF latex suspensions and even the influence of the CsCl electrolyte.

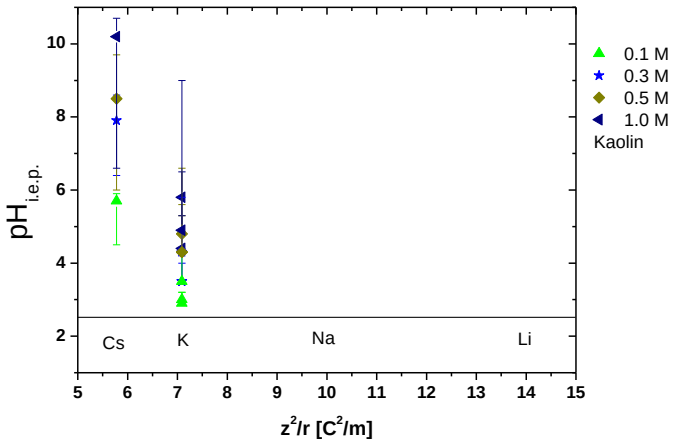


Figure 6.20: Cation correlation of i.e.p. of Kaolin suspensions by the $z^2/r$.

The lack of a trend for other suspensions indicates that the influence of the cations and anions is insignificant. An example of non-consistent correlation is presented in Fig. 6.21 where anions are correlated for Kaolin suspensions.

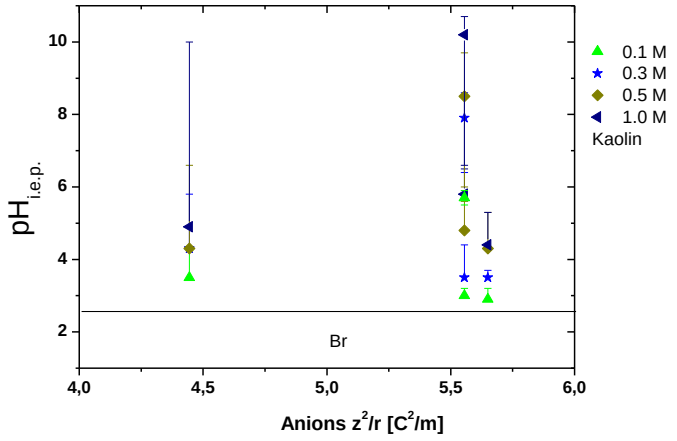


Figure 6.21: Anion correlation of i.e.p. of Kaolin suspensions by the $z^2/r$.

If the results from the MF latex and kaolin suspensions are arranged according to the HSAB principle some interesting trends are revealed. In paper IV it was shown that in general a soft ion will give a low $z^2/r$ value and the opposite will be the case for hard ions. Since the MF latex is classified as soft the preferential adsorption of ions should be toward soft ions and thus low $z^2/r$ values. In Fig. 6.19 it can be seen that this is clearly the case. In the case of the kaolin suspensions the result is somewhat different. Firstly, since kaolin is classified as soft and therefore the ionic adsorption should be preferential toward low $z^2/r$ values. In Fig. 6.20 the cations with lower $z^2/r$ values also show greater affinity toward soft kaolin. But if the complete electrolyte is considered, kaolin does not show greater affinity toward the anions than to the cations. The opposite trends clearly demonstrate that the result is not only dependent on the individual properties of the ions. This means that the surface-ion interaction is important but the driving force for the adsorption is linked to the ion-ion interactions as well. The phenomena have earlier been found at high ionic strength and this supports the suggestion in paper II which is summarized in Table 6.2. Interestingly, it is still possible to extract the ionic contributions from the cationic and anionic branch, respectively.

## 6.4 Surface-Induced Electrolytic Dissociation of weak acids in metal oxide suspensions of mixed alcohol-water solvents

This part (papers V-VIII) reports on the adsorption of species onto alumina and titania particles in aqueous, alcoholic and mixed alcohol/water medium. The effect of ions in the solution was investigated by conductivity measurements. The Surface-Induced Electrolytic Dissociation (SIED) is related to the adsorption and dissociation of acids. In addition, an evaluation of the consistency of a previously suggested adsorption model to quantitatively interpret the results[124] was carried out.

### *6.4.1 The SIED effect in metal oxide suspensions of mixed alcohol/water solvents*

As mentioned earlier the SIED effect has recently been observed in anhydrous or nearly anhydrous n-alcohol suspensions of metal oxides (alumina, titania and

hematite)[91,92]. The aim of paper V was to investigate the SIED phenomenon for titania and alumina in alcohol and mixed alcohol-water suspensions in order to test if the phenomenon occurs more generally. The SIED phenomenon will occur provided that the anionic affinity toward the surface is strong enough and the acid is weak enough in the solution. In Table 6.3 the first $pK_a$ values for oxalic acid in ethanol and phosphoric acid in methanol is presented. From this table it can be seen that the dissociation in alcohol-rich solvents differs only slightly from anhydrous solutions. The change from high to low $pK_a$ values is gradual and it was considered interesting to see if this is the case for the SIED phenomenon as well.

Table 6.3: The first dissociation constant and relative permittivity of a) oxalic acid in water and ethanol-water mixtures (interpolated from [21]) and b) the first dissociation constant and permittivity of phosphoric acid in pure methanol, ethanol, water and mixed methanol-water solutions ([23] interpolated from [22]).

| Solvent | ε | $pK_{a1}$ | Solvent | ε | $pK_{a1}$ |
|---|---|---|---|---|---|
| Water | 78.5 | 1.27 | Water | 78.5 | 2.11 |
| 20% Ethanol | 67.0 | 1.67 | 20% Methanol | 70.0 | 2.71 |
| 40% Ethanol | 55.0 | 2.00 | 40% Methanol | 60.9 | 3.09 |
| 50% Ethanol | 49.2 | 2.30 | 50% Methanol | 56.4 | 3.35 |
| 60% Ethanol | 43.2 | 2.62 | 60% Methanol | 51.7 | 3.67 |
| 70% Ethanol | 38.3 | 2.93 | 70% Methanol | 47.4 | 4.02 |
| 80% Ethanol | 32.8 | 3.24 | 80% Methanol | 42.6 | 4.40 |
| 90% Ethanol | 28.8 | 3.61 | 90% Methanol | 37.9 | 5.07 |
| 94% Ethanol | 26.5 | 3.81 | Methanol | 32.6 | 5.15 |
| | | | Ethanol | 24.3 | 6.15 |

Fig. 6.22 presents the conductivity of titania suspensions as a function of sulfuric acid concentration at high alcohol content. As expected the conductivity is depressed by $TiO_2$ corresponding to a “normal” aquatic behavior. The conductivity in the presence of oxalic acid is shown in Fig. 6.23. The result is opposite as the conductivity was enhanced by the particle load demonstrating the SIED effect. Since sulfuric acid is much stronger ($pK_{a\,1} \approx -3$ in water) than oxalic acid ($pK_{a\,1} \approx 1.25$ in water) the number of pre-existing ions is higher which eventually will cause ionic species in the solution to adsorb at the titania surface. This does not exclude

dissociation of ionic species from the surface but it cannot fully compensate the adsorption.

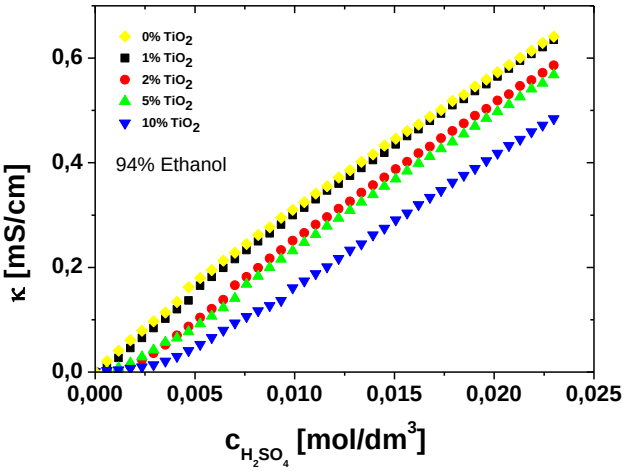


Figure 6.22: The conductivity of high ethanol content titania suspensions as a function of sulfuric acid.

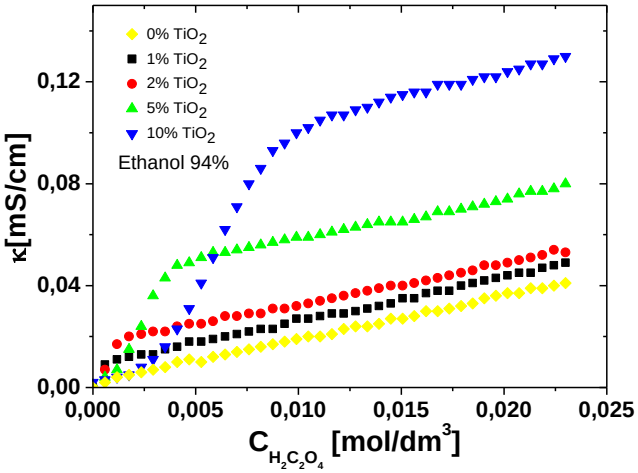


Figure 6.23: The conductivity of high ethanol content titania suspensions as a function of oxalic acid.

The titania suspensions of oxalic and phosphoric acid ($pK_{a\,1} \approx 2.16$ in water) changed gradually to a "normal" behavior with higher amounts of water. Thus there is no critical solvent composition from which a dramatic change from SIED to "normal" behavior occurs. In Fig. 6.24 the conductivity of titania suspensions of oxalic acid in 50wt% ethanol shows an aquatic (normal) behavior. At 60-70wt% ethanol the conductivity was almost independent of the amount of titania. In suspensions of phosphoric acid the shift to "normal" behavior was found first at 20wt% ethanol. Methanol has a higher dielectric constant and the corresponding turnover point for titania suspensions of oxalic acid is found at 70wt% methanol. The corresponding shifts for phosphoric acid was not reached at the lowest investigated methanol content (MeOH= 60wt%).

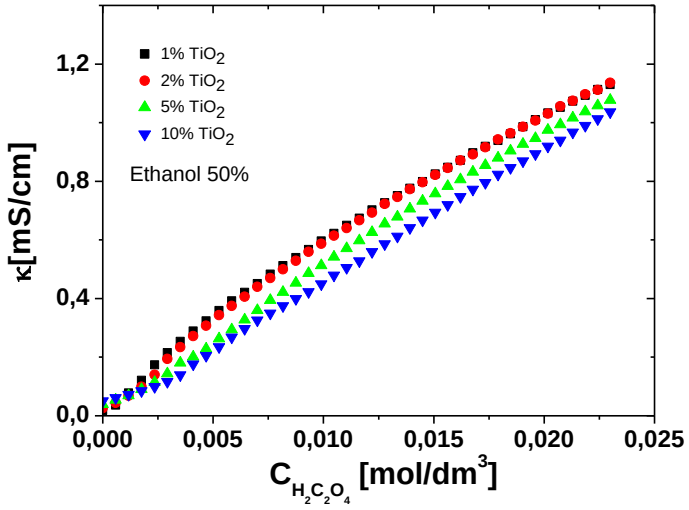


Figure 6.24: The conductivity of 50wt% ethanol content titania suspensions as a function of oxalic acid.

In previous investigations[92] it was demonstrated that the SIED effect was found in alumina suspensions as well. However, the suspensions still showed a "normal" behavior for alumina at favorable SIED conditions. At high ethanol or anhydrous methanol, high alumina content and high oxalic acid concentration, the difference between those and the titania particles in the present study, was that the specific

surface area was much lower. It may be therefore assumed that the "normal" behavior was due to the lower specific surface area which was smaller by a factor 7 relative to titania. This may lead to a lower number of protons produced in a reaction between alumina and oxalic acid and it will not compensate the uptake of pre-existing ions form the solution. However, it should be emphasized that the specific surface area is not proportional to surface site density as the number of sites per unit area may vary between different crystal lattices at the surfaces. The site density has been studied in detail for aqueous suspensions[125] but this does not correspond to mixed solvents in which substantially lower site densities can be found[126].

An interpretation of the rather extensive results in a more compact way is presented for the oxalate adsorption in the following. The initial step is to omit the influence of particle content. This is done by normalization (division) of the acid concentration ($\Gamma = n_{H2C2O4}/A_{TiO2}$) and the conductivity ($\Omega = \kappa/A_{TiO2}$) by the total particle surface area and the result can be seen in Fig. 6.25.a. The influence of the particle content is insignificant and linearity is restored after an initial increase caused by the SIED. The first part shows the enhancement effect caused by proton dissociation from the surface. When saturation between the surface and the solvent is reached an increase of the amount of ionic species in the solvent is controlled by the acid ($pK_a$) constant. The equilibrium is revealed as a linear increase of $\Omega$ when plotted as a function of increased acid concentration. A linear extrapolation of the second part of the curve will give the limiting normalized concentration $\Gamma_0$, the limiting normalized conductivity $\Omega_0$ and the slope ($\upsilon_k$). In Fig. 6.25.b an illustration on how to derive those values is presented from an enlargement of Fig. 6.25.a including the negative $\Gamma$ values needed for a control of consistency. However, those values will not have a physical significance. The limiting values and the slope are related to the linear equation (eq. 6.1).

$$\Omega = \Omega_0 + \upsilon_k \Gamma \qquad (6.1)$$

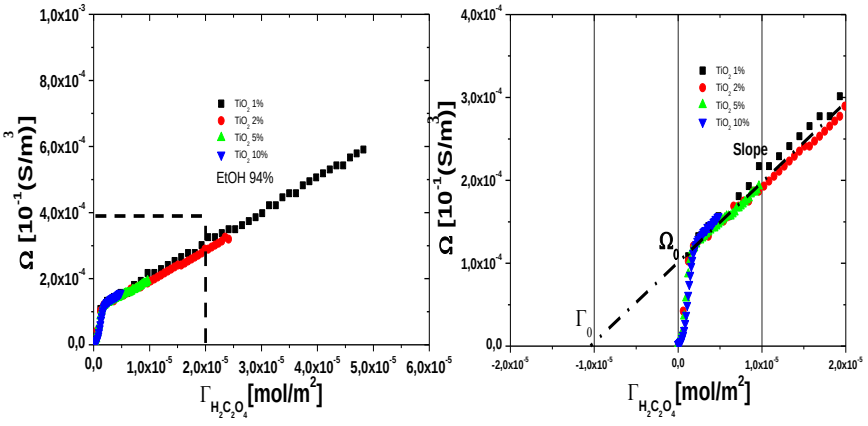


Figure 6.25: a) The conductivity normalized by surface area (Ω) and concentration normalized by surface area (Γ) in 94wt% EtOH titania suspensions of oxalic acid; b) enlargement (dotted window) includes extrapolated negative Γ values.

The first (non-linear) part of the curve seen in Fig. 6.25.a is the only part affected by the particles. The SIED effect is shown by the increased limiting normalized conductivity ($\Omega_0$). In "normal" suspensions ionic species will adsorb at the surface and this will be seen as negative $\Omega_0$. However, as shown in Fig. 6.27.a and b the limiting values are exceedingly small in comparison with the other (SIED) systems. In the presence of the SIED effect $\Gamma_0$ will be negative and $\Omega_0$ will be positive as long as the initial conductivity is relatively small. The opposite will occur for suspensions of "normal" behavior. The limiting $\Gamma_0$ and $\Omega_0$ values are relatively independent of particle content and acid concentration. The slope will correspond to the degree of dissociation of ionic species in solution. These values are plotted for all measured titania systems (e.g. anhydrous and mixed alcohol suspensions including pure water in presence of $H_2SO_4$, $H_2C_2O_4$ and $H_3PO_4$) as a function of water content in Fig. 6.26. The points are equipped with error bars related to the standard deviation from the particle concentrations. The strong increase in dissociation of ionic species by adding water can be seen. The suspensions of $H_2SO_4$ are significantly more dissolved even at high ethanol content relative to other suspensions and this represents the "normal" behavior. As the water content is increased the ionic dissociation is enhanced in other suspensions as well. The degree of dissociation in solution can

qualitatively be arranged in a series $H_2SO_4 > H_2C_2O_4 > H_3PO_4$ in agreement with the $pK_a$ values. Furthermore, a slightly higher dissociation in methanol-rich solution relative to ethanol-rich solutions can also be seen for oxalic acid suspensions. The corresponding difference cannot be observed in the case of phosphoric acid.

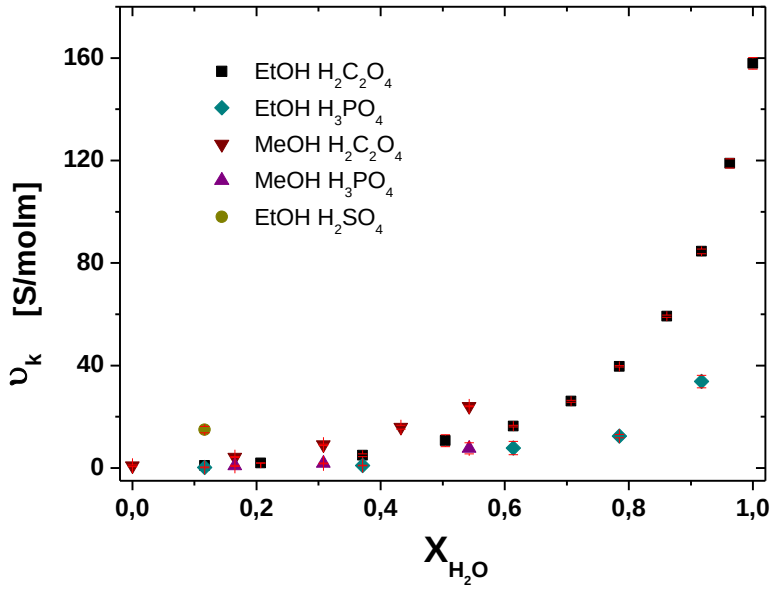


Figure 6.26: The slope ($\upsilon_k$) of the surface area normalized conductivity and normalized concentration as a function of water content for the tested systems.

Fig. 6.27.a presents the $\Gamma_0$ values of all suspensions. Negative values were observed for suspensions of phosphoric and oxalic acid and a value close to zero in case of sulfuric acid at higher alcoholic contents. The negative $\Gamma_0$ represents the hypothetical normalized concentration needed to bring the extension of the high concentration (linear) part of the $\Omega$-$\Gamma$ curves (Fig 6.25) to zero in absence of the SIED effect. In Fig. 6.27.a a horizontal line is drawn in order to separate SIED from "normal" suspensions. In suspensions of oxalic acid a shift to "normal" behavior occurs at about 0.4 mole fraction of water. The corresponding shift in suspensions of phosphoric acid was found at about 0.6 mole fraction of water. Hence the acids can

be arranged in a series of $H_2SO_4 > H_2C_2O_4 > H_3PO_4$ by the occurrence of "normal" behavior which is identical to the level of dissociation and further correlates to the strength of the acid ($pK_a$).

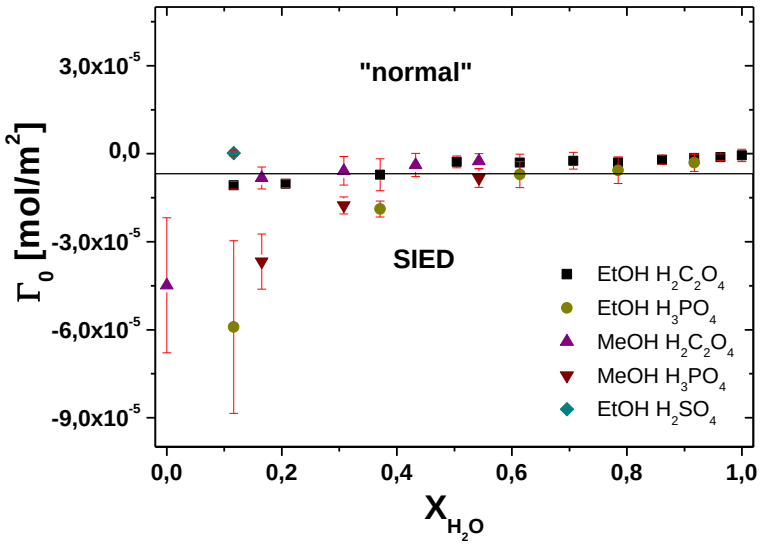


Figure 6.27.a: The limiting normalized concentration ($\Gamma_0$) value as a function of water content taken from the linear regressions of suspensions from the surface area normalized conductivity as a function of acid concentration. The solid line separates "normal" suspensions from those involving the SIED effect.

In Fig. 6.27.b $\Omega_0$ is plotted as a function of mole fraction. The SIED effect cannot be distinguished from the normal behavior. The reason is that the increase in initial conductivity with increased water content will shield the SIED effect. Moreover there is an increased scatter as a function of the water content, showing the successive collapse of the normalization procedure (Fig. 6.25).

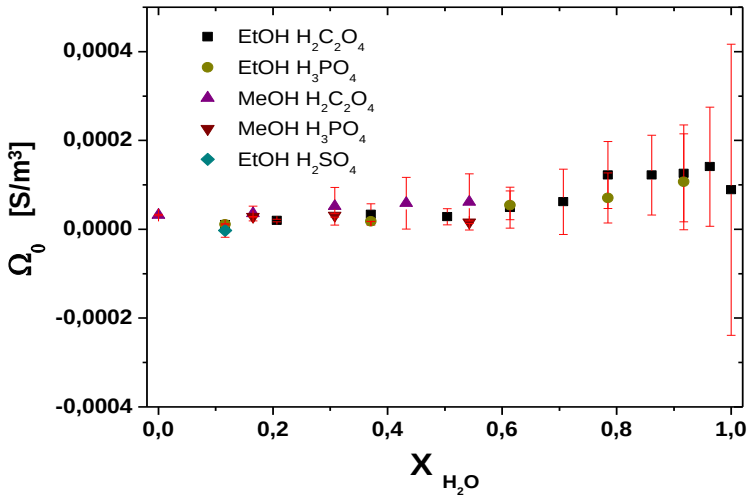


Figure 6.27.b: The limiting normalize conductivity ($\Omega_0$) value as a function of water content taken from the linear regressions of suspensions from the surface area normalized conductivity as a function of acid concentration.

*6.4.2 Adsorption of acids in (aqueous) alcoholic titania suspensions*

No adsorption model that describes the adsorption of neutral and anionic acid species to the particle surface in alcohol-rich suspensions has been developed. Despite extended efforts, no adsorption model requiring only few adjustable parameters or a single site model was found to describe the observations. However, a multi-site adsorption model that considers the SIED effect in alcoholic suspensions has recently been published[124]. Therefore, a qualitative evaluation of the existing model will be given.

As mentioned earlier the dissociation of acid in alcoholic or alcoholic-rich solutions of phosphoric and oxalic acid may be assumed to be limited to the single de-protonated acid and the pure molecular form and thus the system may be described by three internally connected equilibria defined in Fig. 6.28.

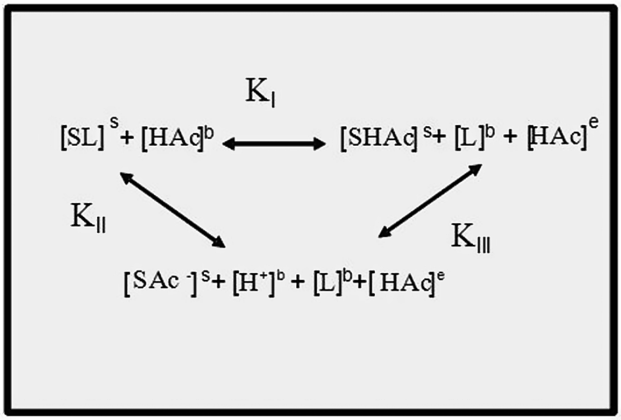


Figure 6.28: The equilibria of the acid in the suspensions.

Here S represents the solid and L the liquid on the solid surface (s). In equilibrium I the acid molecule adsorbs in its non-dissociated form to the surface and the liquid is released from the surface to the bulk (b) solution. The first equilibrium has earlier been investigated[127] but this approach is only possible if the amount of acid depleted from the solution is determined ($[SHAc]^s = [HAc]^b - [HAc]^e$, where e = equilibrium) . The SIED effect is here represented by equilibrium II which involves both adsorption of the anionic acid and proton release from the surface. The adsorption process from the first two equilibria occurs simultaneously and thus there must be a proton release from the surface which is represented by equilibrium III. The three interconnected equilibria may therefore be written as:

$$K_I = \frac{[SHAc]^s[L]^b[HAc]^e}{[SL]^s[HAc]^b} \tag{6.2}$$

$$K_{II} = \frac{[SAc^-]^s[H^+]^b[L]^b[HAc]^e}{[SL]^s[HAc]^b} \tag{6.3}$$

$$K_{III} = \frac{K_{II}}{K_I} = \frac{[SAc^-]^s[H^+]^b}{[SHAc]^s} \tag{6.4}$$

The contribution of the surface potential (the Boltzmann distribution) to the proton release is disregarded in the system. It can be assumed that the dissociation in the

solution is independent of the presence of particles. Thus the surface proton concentration $[H^+]^s$ may be derived by subtracting the proton concentration in a particle free solution $[H^+]^b$ from the proton concentration in dispersion $[H^+]^e$. However, none of these quantities are easy to obtain in non-aqueous suspensions and the previously mentioned model was based on conductance measurements and interpolated values of $K_I$ and $K_{II}$[24]. The reactions were assumed to occur at different surface sites and both surface site densities and equilibrium constants are adjustable parameters. The model further requires the dissociation constants of the solvent of interest. The data are adjusted by the conductivity at various particle contents. In this adjustment it is assumed that neither $K_{II}$ nor $K_I$ are proportional to the titania content. The extracted equilibrium constants indicate a strong affinity toward the surface. Since there are too many adjustable parameters and similar result may be achieved with another setup of constants the molar conductivities found from measurements were not compared with literature data[22,23]. The challenge is to find a consistent model that applies for a wide range of solvents and different solvent mixtures. However, a $\Lambda_m^0$-plot as a function of water content will roughly give a value which can be compared with the assumed $\Lambda_m^0$ values[124].

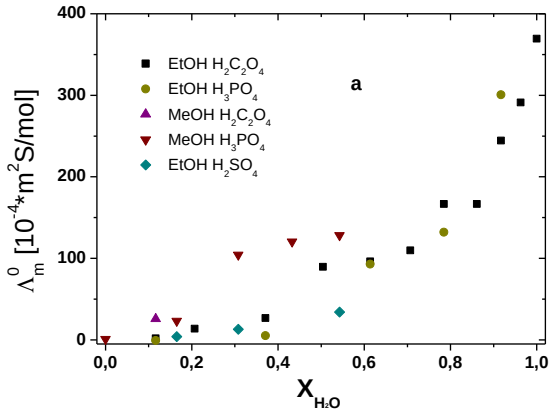

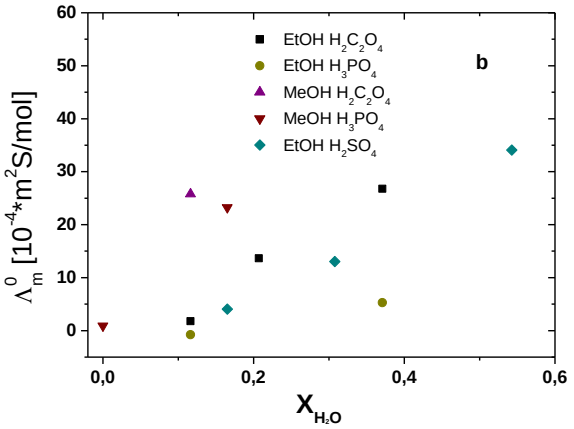


Figure 6.29.a) The limiting molar conductivity ($\Lambda_m^0$) as a function of water content for particle free water/alcohol solutions, b) an enlargement of the "critical" high alcohol content region.

As can be seen in Fig. 6.29.b all $\Lambda_m^0$ values at low water content are lower than those assumed in the model ($\Lambda_m^0$($H_2O$ in 94wt% EtOH) = 40.2*$10^{-4}$ [$m^2$S/mol] and $\Lambda_m^0$($H_2O$ in100wt% MeOH) = 49*$10^{-4}$ [$m^2$S/mol]. In addition, the value used in the model for pure water ($\Lambda_m$ ($H_2O$) =349.65*$10^{-4}$ [$m^2$S/mol]) corresponds rather well with the values found $\Lambda_m$ ($H_2O$) = 370*$10^{-4}$ [$m^2$S/mol] for water. In Fig. 6.30-31 the normalized conductivity and acid concentration are plotted against the mol fraction of water. The dramatic increase in conductivity with water content will successively conceal the conductivity emerging from the SIED effect regardless of the system used. Nevertheless, the "normal" effect is revealed since it disrupts the constant increase in conductivity as seen for the water and water-rich suspensions in Fig. 6.30.

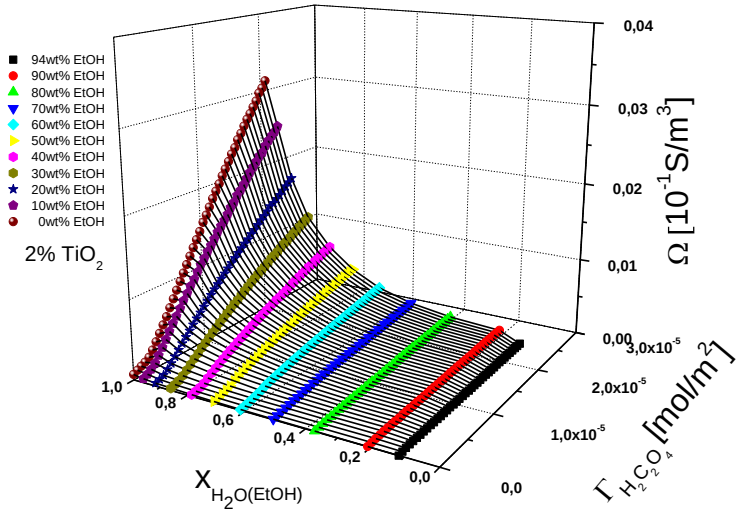


Figure 6.30: The normalized conductivity and oxalic acid concentration plotted against mol fraction of water.

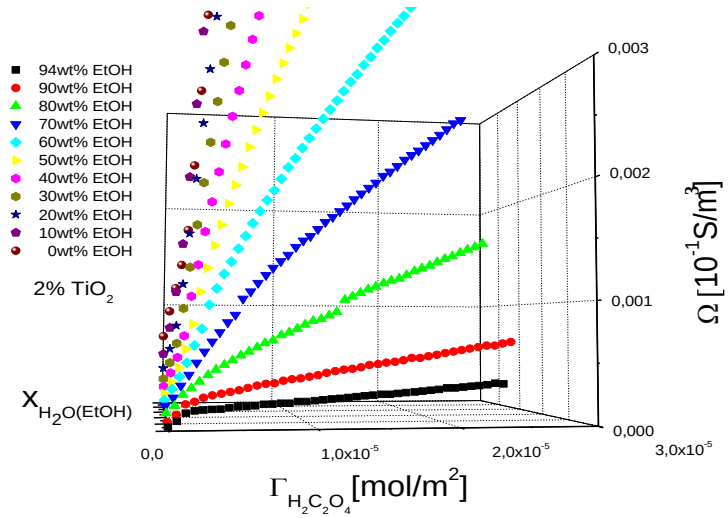


Figure 6.31: An enlargement of Fig. 6.30 emphasizing the conductivity emerging from the SIED effect.

Hopefully there will be improvements made to the adsorption models relying e.g. on the use of different methods such as a surface sensitive method[128]. All methods will, to some extent, be limited and thus the optimal approach may be found by combination of different methods and instruments. The SIED effect was only recently discovered and therefore it was of interest to study the adsorption process more thoroughly.

### *6.4.3. Surface charging in (aqueous) alcoholic titania suspensions*

The conductivity follows the ionic concentration in the solution but this does not correspond to the effective surface. However, by subtracting the conductivity of the pure solution ($\kappa_{sol}$) from the conductivity of the suspension ($\kappa_{dis}$) conductivity representing the particle effect will be derived ($\kappa_{red}$). In Fig. 6.32.a the reduced relative conductivity ($\Omega_{red}$) is plotted as a function of normalized concentration. By and large the conductivity is not influenced by the particle content. An initial drop in the conductivity is seen for suspensions of higher particle content. This is not seen at low particle content likely due to the low acid concentration in which the effect is seen. The result indicates simultaneous reactions since $\Omega_{red}$ obtains both negative and positive values. In Fig. 6.32.b the suspensions of phosphoric acid experienced a similar plateau. When figures a and b are compared it can be seen that the plateau is higher for suspensions in phosphoric acid. Qualitatively this means that the SIED effect is stronger for phosphoric acid. Furthermore, there is no initial drop in the suspensions of phosphoric acid. It is possible that this depends on the less extensive affinity towards the particle in the initial stage of added acid (Fig. 6.32.b). As mentioned $\Omega_{red}$ appear with both positive and negative values and this illustrates the $K_I$ and $K_{II}$ reactions. However, the $K_{III}$ is not traceable but it must be at equilibrium when the plateau is reached.

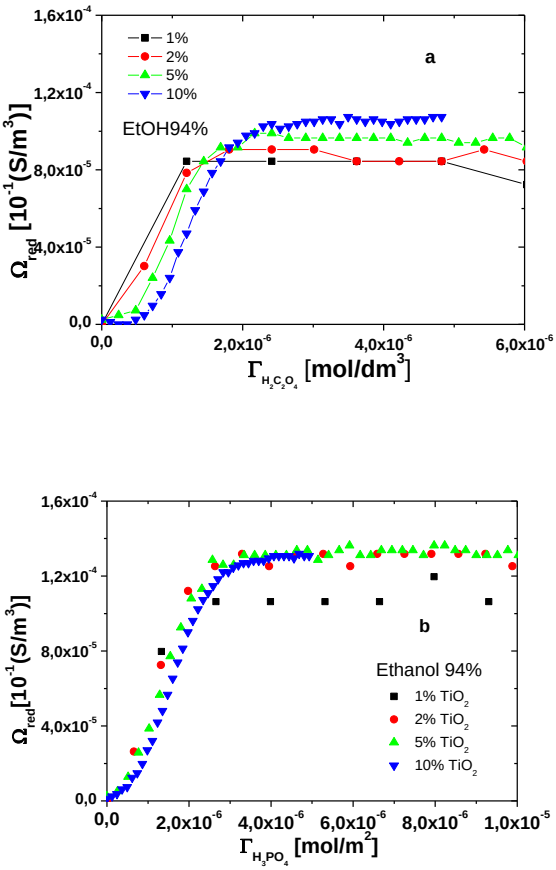


Figure 6.32: The reduced conductivity of ethanol titania suspensions as a function of normalized concentration of a) oxalic acid b) phosphoric acid.

Due to the more extensive data the focus will be placed on evaluation of the oxalic acid systems. It is possible to evaluate the proton concentration in the solution by measuring pH. Due care has to be taken when measuring pH in non-aqueous liquids and mixed solutions of reduced water content. However, for oxalate in methanol and ethanol solutions an investigation for IUPAC found the pH values measured potentiometrically to be sound[129]. Moreover, the dissociation in alcohol rich solvents follows pH of the mixture over a wide composition range (paper VII). Hence it was considered safe to convert the measured pH values to equilibrium proton concentration in solution. This was done according to eq. 6.5:

$$\Gamma_H^d = \left(\frac{V}{A}\right)\left(c_H^f - c_H^i\right) \quad \left[\frac{\text{mol}}{\text{m}^2}\right] \tag{6.5}$$

where $\Gamma_H{}^d$ is the normalized change in concentration for H in the dispersion, index f represents final, and index i stands for initial. The result is presented in Fig. 6.33 where the normalized change in proton concentration is plotted as a function of normalized concentration of oxalic acid. The particle concentrations only slightly affect the suspensions until the plateau is reached. However, the plateau is reached at enhanced $\Gamma_H{}^d$ values for decreased particle concentrations. For suspensions of 5 and 10wt-% $TiO_2$ a slight decline in limiting normalized change in proton concentration could be seen.

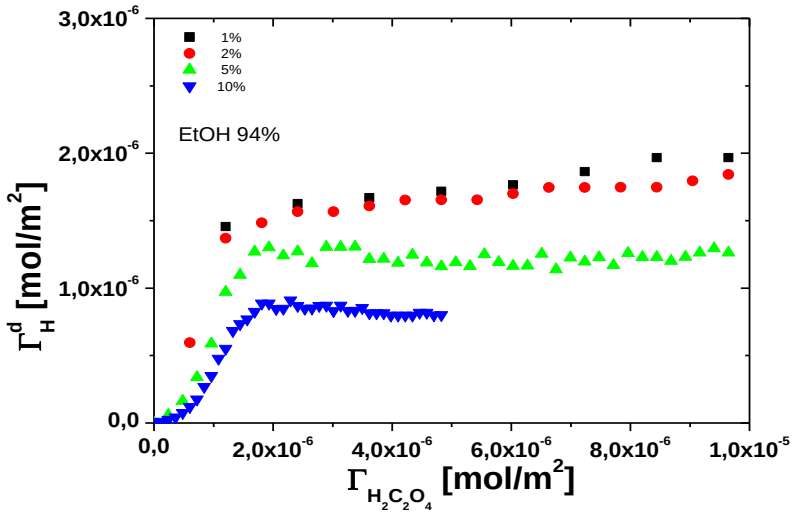


Figure 6.33: The normalized change in proton concentration as a function of normalized oxalic acid concentration.

In Fig. 6.34 the reduced conductivity is plotted as a function of the change in proton concentration. A considerable dependency exists in the range of the SIED effect (rising $\Omega_{red}$). However, at the plateau the suspensions are almost independent but all particle fractions were found at different levels.

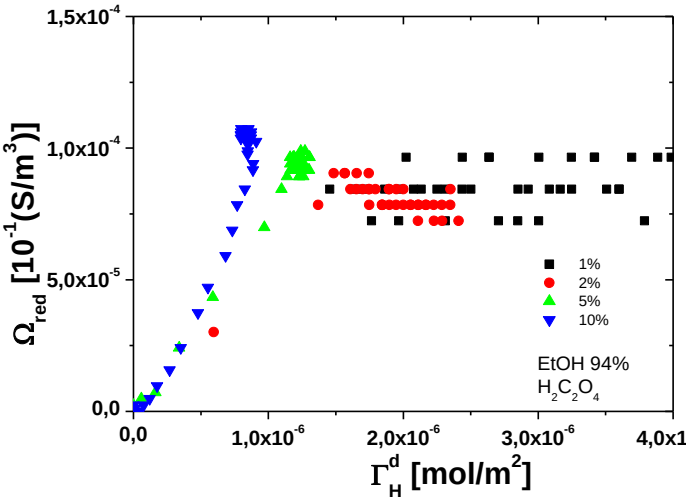


Figure 6.34: The normalized reduced conductivity as a function of normalized change in proton concentration.

Obviously, only for the 5 and 10wt% particle suspensions is a roughly linear correlation between the reduced normalized conductivity and normalized proton concentration in suspension found. For 1 and 2 wt% suspensions the reduced normalized conductivity is almost independent on the normalized proton concentration. From Fig. 6.33-34 it may be concluded that none of the normalizations produced a master curve. In general the curves fit rather well at the initial increase which represents the SIED effect. The influence of the particle fraction is rather significant when the proton concentration is plotted as a function of normalized concentration. When the reduced conductivity is plotted as a function of change in proton concentration the difference is less significant. Thus the latter method (Fig. 6.34) is more successful in producing an overall master curve but still a significant dependency on particle fraction is visible.

The ion interactions at the surface of the particle are reflected by surface charge density and ζ-potential. It is thus of interest to reveal how the ζ-potential is related to the normalized conductivity and the surface charge density. In Fig 6.35.a the ζ-potential of ethanol titania suspensions in presence of oxalic acid is plotted as a function of acid concentration normalized with the particle surface area. It can be seen that the ζ-potential is independent of particle content. A charge reversal can be

seen at about $2*10^{-6}$ mol/m$^2$ and a stabilization of the ζ-potential at about $5*10^{-6}$ mol/m$^2$. The change in ζ-potential from positive to negative corresponds to $K_{II}$ in Fig. 6.28. Thus the ζ-potential indicates stable equilibria at acid concentration higher than $5*10^{-6}$ mol/m$^2$. In Fig. 6.35.b the corresponding ζ-potential in presence of phosphoric acid is shown. The plateau is reached at about the same amount of acid. However, the drop in ζ-potential occurs in two stages suggesting a slight difference in chemical mechanism.

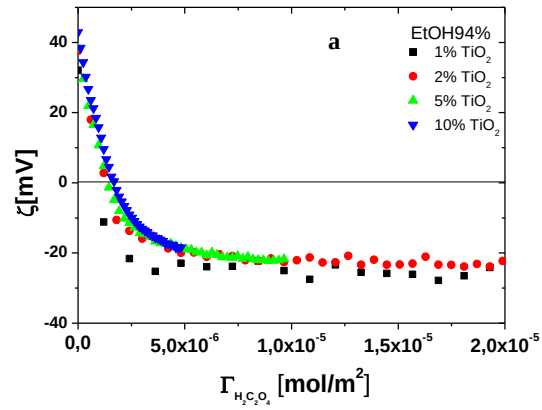


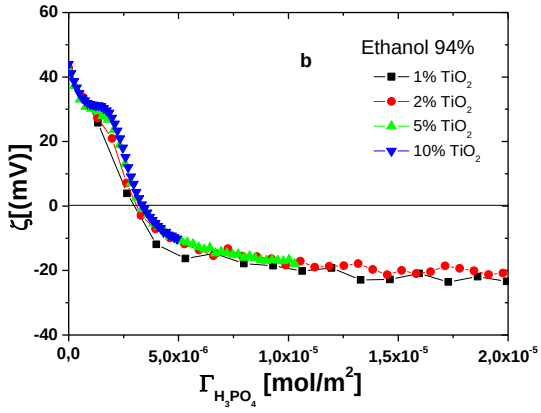


Figure 6.35.a;b: The ζ-potential of ethanol titania suspensions as a function of normalized concentration of a)oxalic acid and b) phosphoric acid.

The normalized conductivity ($\Omega_{red}$) was considered to represent the amount of released protons. It is therefore of interest to investigate if it provides a good measure of the effective charging (ζ-potential) of the particle. In Fig. 6.36 the ζ-potential is plotted as a function of the normalized reduced conductivity. All curves produce a sigmoid shape and they effectively merge to a master curve. The $\Omega_{i.e.p.}$ does, however, not fully agree with the break points when the reduced normalized conductivity is plotted as a function of the normalized concentration (Fig. 6.32) or the normalized change in proton concentration (Fig. 6.34). Three ranges can be distinguished in the figure. The first range represents anion and acid adsorption and is found at low reduced normalized conductivity and high ζ-potential values. The second range represents the SIED effect (in the middle) and the third range is found at high normalized reduced conductivity and negative ζ-potential values. It is obvious that the dependency of ζ-potential and reduced normalized conductivity is related but they differ substantially from each other. This is particularly pronounced at low and high oxalic acid and proton concentrations.

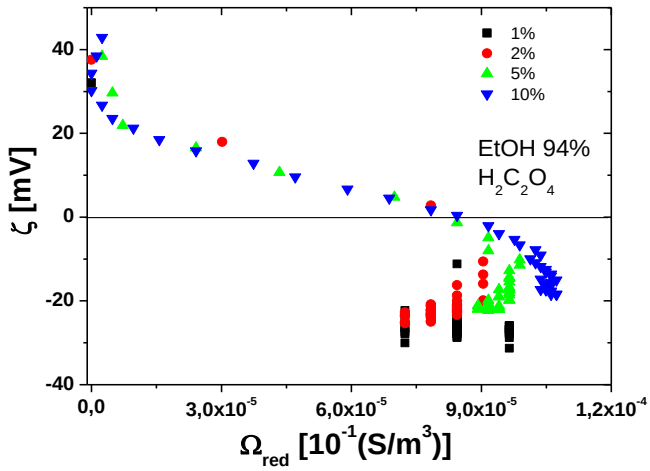


Figure 6.36: The ζ-potential as a function of normalized reduced conductivity in suspensions of oxalic acid.

Of particular interest was to correlate the effective surface potential (ζ-potential) to the relative surface charge density ($\sigma_0$) since both characterize the charging of the particles. Such correlation can be seen in Fig. 6.37 where the ζ-potential is plotted as

a function of the surface charge density. The normal method to derive the surface charge is to separate the particles from the suspension before the titration as a function of pH. Since only protons are considered and their solution equilibrium may be assumed to be rather independent on the presence of particles the surface charge density was calculated relative to oxalic acid free suspension accordingly to eq. 6.6.

$$\sigma_0 = F\left(\frac{V}{A}\right)\left[\left(c_H^f - c_H^i\right)_{dis} - \left(c_H^f - c_H^i\right)_{sol}\right] \qquad \left[\frac{C}{m^2}\right] \tag{6.6}$$

Fig. 6.37 reveals the same sigmoid shape as found in Fig. 6.36 and all three ranges can be found. For suspensions up to 5 wt-% $TiO_2$ the curves are nearly superimposed. For the 10 wt-% $TiO_2$ suspension show less dependency and the curve is shifted to the left. The sigmoid shape reveals that the ζ-potential responds to the suspension charging and surface charging with different mechanisms. The reduction of the surface charge density is rather extensive at negative ζ-potentials and the $\sigma_0$-reversal is induced after the charge reversal.

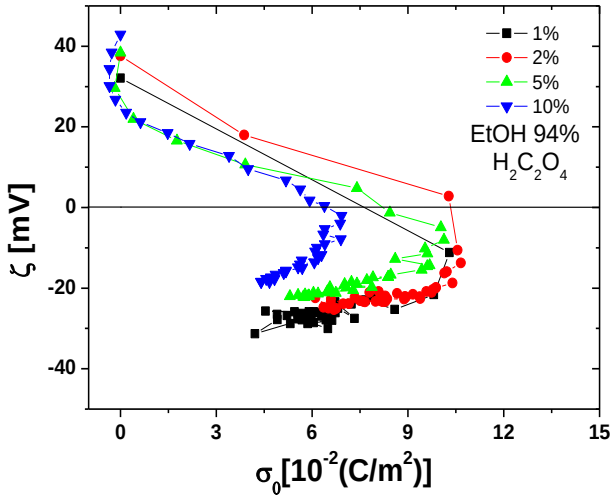


Figure 6.37: The ζ-potential as a function of change in surface charge density.

To summarize the results the dependency of ζ-potential on the selected equilibrium ($\Gamma_H^d$) and transport properties ($\Omega_{red}$) of the suspension medium suggest that at least three equilibria are involved and each of them can be distinguished experimentally.

Three different equilibria ranges are also revealed when the ζ-potential is plotted as a function of surface charge density but different dependencies on solution and surface charging are clearly discerned.

## 6.5 Visco-coulombic characterization of alcoholic suspensions that exhibit the SIED effect

In the last paper (VIII) the visco-coulombic properties of different alcoholic and alcohol-rich suspensions of titania were studied. Since they exhibit the SIED effect it was of interest to relate the phenomenon to the surface potential and the colloidal properties of the suspensions. By the visco-coulombic approach a macroscopic property of the suspension will additionally be revealed. This was done by applying different models related to the DLVO-theory, mostly derived for aqueous suspensions in order to evaluate their applicability in non-aqueous suspensions. Additionally the aim was to find predominant causes for the observed suspension behavior. The study involved measurements of the dynamic viscosity by means of a Bohlin VOR. A range of shear rates were scanned in a loop (Fig. 6.38) for different acid concentrations. From these the intrinsic shear rates at 0.581, 5.81 and 58.1 $s^{-1}$ were selected for comparison of the viscosity with the ζ-potentials. To interpret the surface potential an Acoustosizer II was used. The dynamic mobility from a single frequency mode was used to calculate the ζ-potentials.

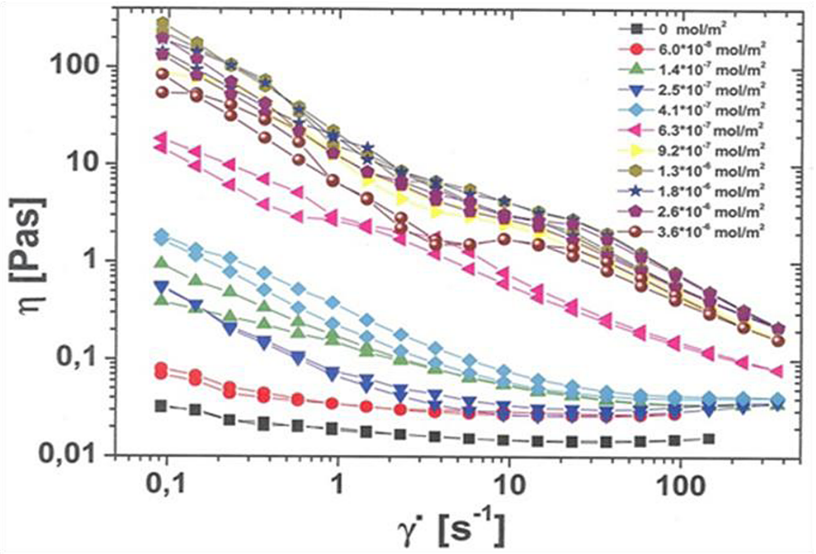


Figure 6.38: The dynamic viscosity of alcohol-rich titania suspensions at 293K with and without the presence of oxalic acid.

The charge reversal of an ethanol-rich titania suspension upon an increase of oxalic acid is shown in Fig. 6.39. As shown this effect was seen in all measured suspensions, that is, methanol, ethanol and water in presence of oxalic and phosphoric acid, respectively. Thus the charge reversal of the alcoholic suspensions coincides with the SIED effect. Additionally, $\zeta^2$ values are shown since those are predicted to show a linear relationship with the viscosity in models for viscosity presented below.

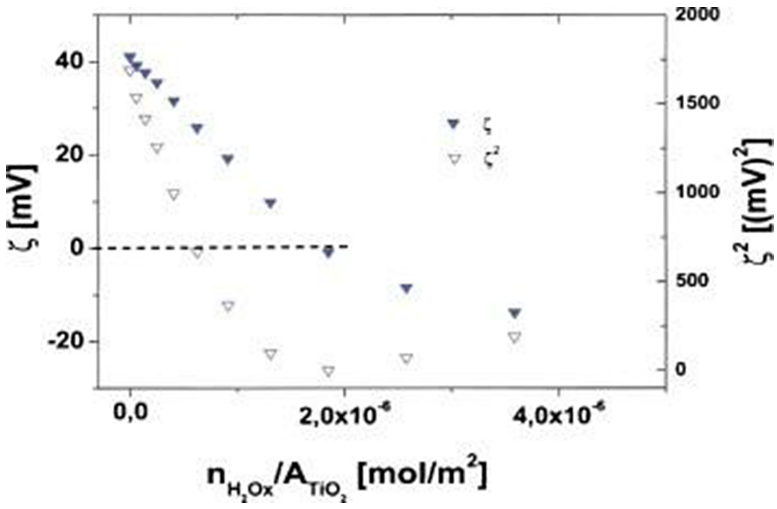


Figure 6.39: The ζ-potential (filled triangles) and $\zeta^2$ (open triangles) of 94wt% ethanol suspensions as a function of oxalic acid concentration.

In this investigation the point where ζ=0 is denoted the isoelectric concentration (i.e.c.). The i.e.c. concentration is also represented by the minimum of $\zeta^2$ ($c_{min}$) plotted as a function $n_{Acid}/A_{TiO2}$ . There are some alternative approaches to extract the critical values of the suspensions and those are presented in Table 6.2-3. A maximum in yield stress is often found close to the i.e.p. of the suspension[73] and it has been shown that the viscosity equally well illustrates this effect[71]. In Fig. 6.40 the viscosity (shear rate = 5.81 $s^{-1}$) is plotted as a function of normalized particle surface area with oxalic and phosphoric acid concentration, respectively. The figure illustrates the extrapolated maximum ($c_{max1}$) of the different suspensions which coincides with i.e.c.. The viscosity branch after the maximum did not fully return to the initial low viscosity. This was generally the case for all suspensions. The critical concentration can also be derived from measured ($c_{max2}$) maximum viscosity at given shear rates.

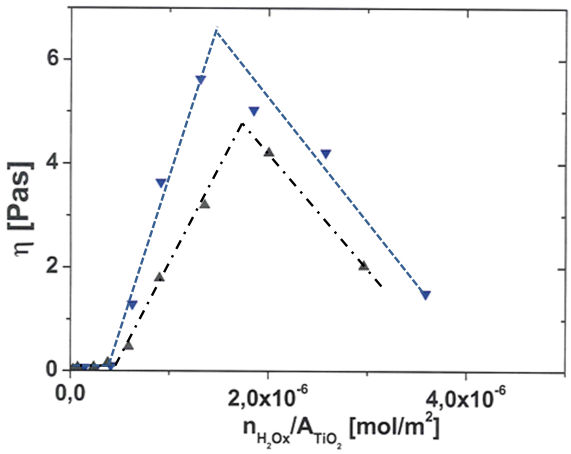


Figure 6.40: The viscosity (shear rate 5.81$s^{-1}$) of ethanol (94wt%) titania suspension as a function of surface area normalized oxalic (inverted triangles) and phosphoric (upright triangles) acid. The lines illustrate the viscosity trends.

Table 6.2: $c_{min}$ and $c_{i.e.c.}$ are the extrapolated minimum value of $\zeta^2$ and i.e.c. respectively. $c_{max1}$ and $c_{max2}$ refer to the extrapolated and measured maximum viscosity for shear rates of 0.581, 5.81 and 58.1 $s^{-1}$, respectively. Values are given as $10^{-6}$ [$mol/m^2$].

| shear rate | | | 0.58 $s^{-1}$ | | 5.81 $s^{-1}$ | | 58.1 $s^{-1}$ | |
|---|---|---|---|---|---|---|---|---|
| | $c_{min}$ | $c_{iec}$ | $c_{max1}$ | $c_{max2}$ | $c_{max1}$ | $c_{max2}$ | $c_{max1}$ | $c_{max2}$ |
| System | | | | | | | | |
| H2O–OxA | 1,35 | 1,64 | 1,20 | 1,81 | 1,48 | 1,81 | 1,47 | 1,81 |
| MeOH–OxA | 1,54 | 2,11 | 2,69 | 2,69 | 1,94 | 1,75 | 2,07 | 2,07 |
| EtOH–OxA | 1,11 | 1,80 | 1,24 | 1,80 | 1,35 | 1,23 | 1,48 | 1,28 |
| EtOH–POA | 1,55 | 1,97 | 1,50 | 1,37 | 1,75 | 2,00 | 1,63 | 2,00 |

In Fig. 6.41 the viscosity at a shear rate of 5.81 $s^{-1}$ is plotted against $\zeta^2$ in 94wt% ethanol suspensions containing oxalic and phosphoric acid, respectively. A linear relationship was, as expected, found and this enables the extrapolation to the viscosity maximum at $\zeta^2 = 0$. Moreover, the ζ-potential value at $\eta = 0$ can further be used to determine equilibrium distance between particles or the Hamaker constant (eq. 4.3-4.5). Only values from the positive ζ-potential branch are plotted in Fig 6.41 because of asymmetric viscosity behavior at negative ζ-potentials. However, this was

expected since a reversed linear relationship after charge reversal assumes an indifferent suspension behavior which is not the condition here.

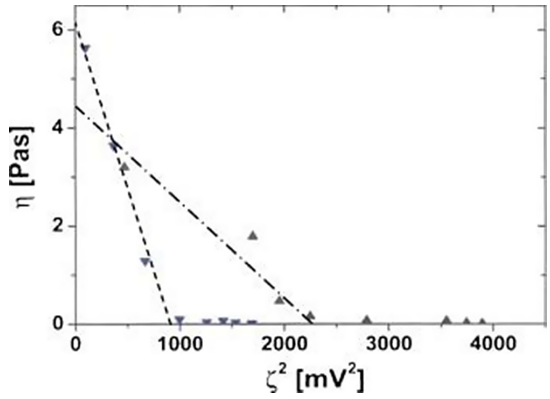


Figure 6.41: The viscosity as a function of $\zeta^2$ for titania suspensions in ethanol (94wt%) containing oxalic (inverted triangles) and phosphoric (upright triangles) acid.

The general trend of the different critical concentrations (Table 6.2) is that the $c_{min}$ values are slightly lower than the $c_{i.e.c.}$ values. The $c_{max1}$ and $c_{max2}$ values shift from measurement to measurement. However, the $c_{max2}$ value is dependent on the chosen sample composition and the distance from $c_{i.e.c.}$ vary between different systems. Thus the values will to some extent be accidental. Compared to the $c_{i.e.c.}$ and $c_{min}$ values $c_{max1}$ and $c_{max2}$ generally fall roughly in between. In Table 6.3 it can be seen that the maximum viscosity values ($c_{max1}$ and $c_{max2}$) roughly agree with the critical concentrations. The trend is not significantly affected by a change in shear rate. However, seemingly the extrapolated viscosity values ($\eta_{max1}$) are more reliable than the measured values ($\eta_{max2}$). This may be due to the instability of the suspensions close to the i.e.c. caused by aggregation.

Table 6.3: The extrapolated ($\eta_{max1}$) and the measured ($\eta_{max2}$) viscosity for three different shear rates at 20°C and given in [Pas]. Extrapolated $\eta_\zeta$ and $\zeta_\eta$ fro the positive $\zeta$-potential branch from $\eta$ against $\zeta^2$ plots ($\zeta$-potentials in mV).

| Shear rate | 0,58 $s^{-1}$ | | 5,81 $s^{-1}$ | | 58,1 $s^{-1}$ | | 0,58 $s^{-1}$ | 5,81 $s^{-1}$ | 58,1 $s^{-1}$ | 0,58 $s^{-1}$ | 5,81 $s^{-1}$ | 58,1 $s^{-1}$ |
|---|---|---|---|---|---|---|---|---|---|---|---|---|
| | $\eta_{max1}$ | $\eta_{max2}$ | $\eta_{max1}$ | $\eta_{max2}$ | $\eta_{max1}$ | $\eta_{max2}$ | $\eta_\zeta$ | $\eta_\zeta$ | $\eta_\zeta$ | $\zeta_\eta$ | $\zeta_\eta$ | $\zeta_\eta$ |
| System | | | | | | | | | | | | |
| H2O–OxA | 1,75 | 1,75 | 0,56 | 0,51 | 0,07 | 0,07 | 2,42 | 0,5 | 0,07 | 49,6 | 49,6 | 50,3 |
| MeOH–OxA | 18,4 | 18,4 | 2,00 | 1,73 | 1,06 | 0,86 | 19,0 | 2,42 | 1,07 | 26,9 | 29,4 | 29,4 |
| EtOH–OxA | 42,9 | 36,5 | 6,27 | 5,70 | 1,62 | 1,26 | 42,0 | 6,24 | 1,44 | 26,8 | 28,5 | 27,6 |
| EtOH–POA | 28,0 | 24,1 | 4,65 | 4,23 | 0,82 | 0,78 | 28,6 | 4,17 | 0,71 | 47,0 | 48,2 | 48,4 |

### *6.5.1 Visco-coulombic modeling of alcoholic suspensions*

The measurements were related to six different models originating from the DLVO-theory designed for aqueous suspensions. This enables an estimation of the applicability of the models in non-aqueous systems considered. Each model is based on different assumptions which are extensively discussed in paper VIII. Thus only the main conditions, final expressions and results will be presented here.

Two different approaches are based on the Schulze-Hardy model for suspensions[130] that predicts the critical coagulation concentration ($c_c$). At $c_c$ indifferent electrolytes erase the repulsive charge barrier. The model is strongly dependent on the valency of the ions and only weakly on the character of the ion. The dependency on the valency is reduced at low potentials. Thus it provides a test for the influence of valency or dissociation degree of acids on the viscosity enhancement. In the first approach the expression for the electrostatic repulsion between two equal spheres derived by Reerink and Overbeek[131] is combined with the contribution from the attraction[132]. In the second approach, derived by Hogg et al.[84] (HHF), for the electrostatic repulsion for equal spheres the assumption was made that $\psi_d \approx \zeta$. However, the final expressions (eq. 3. 2) were at the end very similar and only the constant representing aqueous suspensions at T=25°C changed slightly where k (eq. 3.2) was found to be $7.116*10^{-41}$ in the first and $6.991*10^{-41}$ in the second approach (VIII) .Thus it was assumed that the equations were based on the same constrains. The model was tested

by comparing the critical concentrations in Table 6.2 with the derived $c_c$ values calculated with Hamaker values from the literature[133]. The results can be seen in Table 6.4. The aqueous suspensions were found to be in a typical range found for monovalent salts in hydrophobic sols[130]. Thus the $c_c$ values are considered relevant.

Table 6.4: $c_c$ for aqueous and alcoholic titania suspensions calculated from eq. 6.4 using derived constant from each approach. ζ-potentials from Table 6.3, dielectric constants from [134]. Hamaker constant for the liquid $H_{11}$[133] and the pure particles $H_{22}$ [135]and suspensions $H_{212}$ are shown respectively.

| System | ζ | $\varepsilon_r$ | $H_{11}$ | $H_{212}$ | $c_c$(app. 1) | $c_c$(app. 2) | $c_c$(app. 1) | $c_c$(app. 2) | $c_c$(app. 1) | $c_c$(app. 2) |
|---|---|---|---|---|---|---|---|---|---|---|
| H2O–OxA | 49,8 | 80,1 | 37,3 | 43,1 | 0,121 | 0.119 | $1,96\times10^{-5}$ | $1,92\times10^{-5}$ | $1,99\times10^{-5}$ | $1,96\times10^{-5}$ |
| MeOH–OxA | 29,2 | 33,0 | 35,0 | 45,7 | 8,90×10-4 | $8,75\times10^{-4}$ | $1,82\times10^{-7}$ | $1,78\times10^{-7}$ | $0,74\times10^{-7}$ | $0,73\times10^{-7}$ |
| EtOH–OxA | 27,6 | 38,0 | 42,4 | 38,0 | 4,63×10-4 | $4,55\times10^{-4}$ | $0,94\times10^{-7}$ | $0,93\times10^{-7}$ | $0,39\times10^{-7}$ | $0,38\times10^{-7}$ |
| EtOH–POA | 47,9 | 38,0 | 42,4 | 38,0 | 4,20×10-3 | $4,13\times10^{-3}$ | $8,61\times10^{-7}$ | $8,46\times10^{-7}$ | $3,50\times10^{-7}$ | $3,44\times10^{-7}$ |

The Morrison stability ratio model (eq. 3.3) encounters the DLVO-theory differently. It assumes insulating spheres, that the ionic strength is negligible and that only the electrostatic repulsive contribution needs to be considered (the attractive contribution is neglected). The expression is built upon the stability ratio and if $10^5$ is assumed to be the minimum ratio of stability it can be predicted by eq. 3.3. The model has been proved successful in predicting the stability of non-aqueous suspensions[136]. Hence the limit for stability would be found close to 1 for the model to be successful. It was shown (Fig. 6.41) that the model was able to predict the stability in ethanol (94wt %) and methanol suspensions of oxalic acid rather well. However, in aqueous suspensions containing oxalic acid and ethanol suspensions of phosphoric acid it was not fully accurate. It seems that a criterion for the model to be predictable is that the suspension is sufficiently non-charged with a low degree of acid dissociation. Otherwise the model showed an extended range of the linear rise and a maximum characteristic for destabilized suspensions close to the isoelectric concentration.

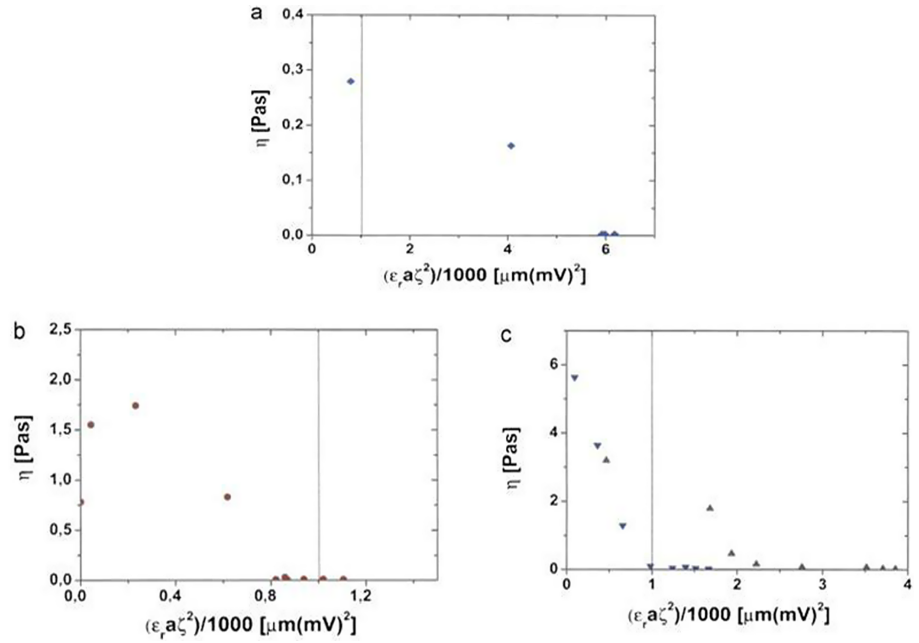


Figure 6.41: a) The viscosity of water-oxalic acid, b) methanol-oxalic acid and c) ethanol-oxalic acid (inversed triangles) and ethanol-phosphoric acid (upright triangles) titania suspensions as a function of the stability ratio ($(\varepsilon_r a\zeta^2)/1000$) at 293K. The lines at unity represent the limit for stable suspensions.

Three different models predicting the viscosity of suspensions have been tested. Several models are available but for consistency two models based on the standard attractive potential[132] and one based on the HHF repulsive potential[84] were selected. The current models are presented in theory section (4.4). The fits to experimental points have been found to be sensitive to the characteristic length between particles. In the models represented by equations (4.3-4.5) the critical distance was obtained from the fit to the experimental points.

The critical distance ($l_c$) between particles when coagulated is induced was derived from the Schulze-Hardy approach as the inverted Debye length for aqueous suspensions as:

$$l_c = \frac{1}{\kappa_c} \approx 4.072 \left(\frac{H_{212}}{\varepsilon_r \zeta^2}\right) nm \qquad (6.7)$$

The critical distance values are collected in Table 6.5.

Table 6.5: The equilibrium and steady-state distance of single particles and dense coagulates.

| length | H2O-OxA | MeOH-OxA | EtOH-OxA | EtOH-POA |
|---|---|---|---|---|
| $l_c$ | 0.88 nm | 6.6 nm | 8.0 nm | 2.7 nm |
| $l_0$ (eq. 4.3) | 0.45 nm | 2.7 nm | 1.1 nm | 0.72 nm |
| $l_0$ (eq. 4.4) | 5.8 nm | 34 nm | 14 nm | 9.1 nm |
| $l_f$ (eq. 4.5) | 5.8 nm | 19 nm | 18 nm | 12 nm |

All values are of reasonable magnitude. The attractive interaction forces are expected to extend only to about 1 nm from the particle. It was found that $l_f$ and $l_0$ from equations 4.4 and 4.5 are larger and $l_0$ from equation 4.3 is smaller than $l_c$. However, the larger values found for $l_f$ was expected since those are of equilibrium distance and consider coagulated aggregates but not single particles. Since the values found in equation 4.4 are very similar it may be assumed that those values also consider coagulates.

In Fig. 6.42 the fitting of the different systems utilizing the models can be seen. All models were able to predict the aqueous suspensions of oxalic acid rather well. This was also the case in alcoholic suspensions at ζ-potential values higher than 0. However the models were not as consistent in predicting the values at negative ζ-potentials. Overall, the Zhou model was found to be superior in predicting the enhancement of the viscosity and additionally better in predicting the decrease after the charge reversal. The model is in contrast to the other two models based upon interaction forces while the other methods consider interaction energies. In current alcoholic suspensions it may therefore be suggested that this approach is more favorable in describing the process.

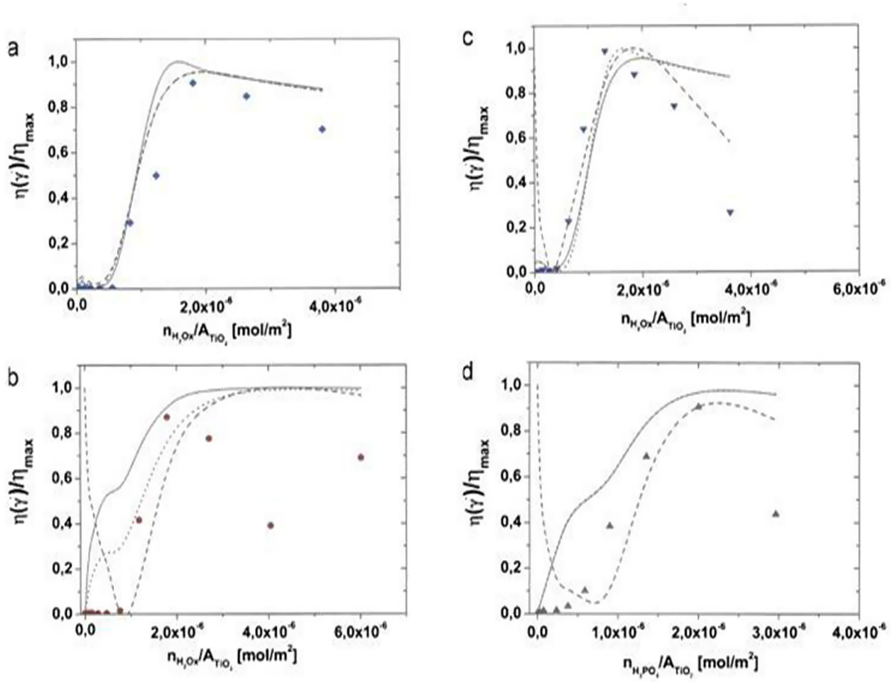


Figure 6.42: Model fitting to viscosity ratio's from measured values using eq. 4.3 (dotted lines), eq. 4.4 (full lines) and eq. 4.5 (dashed lines). The current systems are in suspensions of a) water-oxalic acid, b) methanol-oxalic acid, c) 94 wt% ethanol-oxalic acid and d) 94wt% ethanol-phosphoric acid. The shear rate was 5.81 $s^{-1}$.

# 7. Summary

The influence of the interactions between solutes and the particle surface on the charging behavior of suspensions has been studied. Initially the ionic strength and selectivity in aqueous 1:1 electrolytes suspensions of titania, alumina, clays and melamine-formaldehyde were investigated. The aim was to enhance the understanding on what parameters control the ionic adsorption. In particular the effective surface potential at high ionic strength was of interest.

Electrophoretic and electroacoustic techniques were compared and despite the high ionic strength the surprisingly high absolute ζ-potential values were found to be rather consistent. Parameters that affected the ionic adsorption were pH, ionic strength and ionic selectivity.

At high ionic strength, the type of adsorption, that is, specific cat- or anionic or indifferent was seemingly dependent on both ion-surface as well as on ion-ion interactions. It was possible to derive the characteristic ionic contributions which mainly followed ionic phenomenological series found in literature and moreover the thermodynamically defined Born model.

Different levels of specific adsorption could be distinguished. In a weakly influenced system, such as the alumina suspensions in Paper I, only the magnitude of the absolute ζ-potential value decreased. Additionally a shift in the i.e.p. could additionally be seen. At moderate electrolytic concentrations the type of adsorption of ions was mainly indifferent. A qualitative path depending on the selected particles and electrolyte could be seen and this offers an opportunity to control the colloidal properties.

Phosphoric and oxalic acids are weak in non-aqueous solutions and show strong affinity toward the particle surface. The influence of the surrounding medium was investigated for alcoholic, mixed alcohol-water and water. In alcoholic system the ionic dissociation is much less pronounced than in water and thus the acid chiefly appear in its molecular form and in a smaller amount in the monovalent anionic

form. In alcohol-rich suspensions the anionic acid adsorbed on the surface as shown by the charge reversal of the ζ-potential from a positive to a negative value. Additionally this led to proton dissolution resulting in enhanced conductivity of the suspensions. This enhancement is opposite to the conductance behavior of aqueous suspensions which was recently discovered and called Surface-Induced Electrolytic Dissociation (SIED). By conductance measurements it was shown that this effect gradually changed to an aqueous behavior by increased water content without any critical concentration. However, the effect only appeared if the acid was weak enough in the alcohol solution and the acids had a strong enough affinity toward the surface. Thus the use of sulfuric acid in alcoholic or alcoholic-rich suspensions did not lead to the SIED effect. Additionally, the SIED effect was relatively small compared to the conductivity at higher water content.

The SIED effect was not seen in alumina suspensions in contrast to previous investigations. The difference as compared to titania suspensions was that the specific surface area was almost an order of magnitude smaller. Hence the amount of protons able to release from the surface was not sufficient to compensate for dissociation in the solvent. In suspensions of phosphoric acid the aqueous “normal” behavior was only seen at 20wt% ethanol content or less. Thus it was of interest to further investigate the effect since it may offer a path to control the colloidal properties of the suspension.

In a thorough investigation of (aqueous) alcoholic suspensions of oxalic acid the charging properties of the suspensions were linked both to the conductivity and to the potentiometrically determined proton concentration. Both the normalized reduced conductivity and the normalized change in proton concentration in dispersion were plotted as a function of normalized acid concentration. Next they were related to each other and finally the ζ-potential was plotted against both of them. In the latter case the normalized change in proton concentration was expressed as changed surface charge density. The normalized conductivity was rather independent of the particle fraction and the SIED effect was seen as an increase in normalized reduced conductivity. At high normalized concentration a plateau was found. The normalized change in proton concentration a similar increase was found in the SIED range.

However, at high normalized concentration the plateaus were dependent on the particle fraction. A sigmoid curve was found when the ζ-potential was plotted as a function of normalized conductivity and surface charge density. The curves were mostly independent of particle fraction. Three different ranges could be distinguished. The first range anion and acid adsorption was found at low normalized concentration and high ζ-potential. The second range represented the SIED effect which was characterized by a linearly reduced ζ-potential. The third range was represented by negative ζ-potentials and high normalized reduced conductivity or high surface charge density. The result revealed that an accurate model require a third equilibrium.

The alcoholic, alcoholic-rich and aqueous suspensions were related to the viscosity properties. This was done by means of electroacoustic ζ-potential and dynamic viscosity measurements. The acid concentration required for charge reversal (i.e.c.) was found to be close to maximum viscosity for the suspension. This illustrated that the colloidal properties of the suspensions were controlled by the SIED effect. Different models originating from the DLVO-theory were tested for applicability in alcoholic suspensions. The purpose was to determine what parameters are controlling the visco-coulombic effects. Generally the aquatic models were applicable in alcoholic suspensions but there were exceptions. It was found that the viscosity enhancement close to the i.e.c. was most successfully described by a model based on interaction forces rather than the models derived from equilibrium interaction energies.

# 8. Acknowledgement

First of all, I want to thank Professor Jarl Björn Rosenholm for supervision and support. Additionally I want to thank for getting the opportunity to be a part of the department of Physical Chemistry (FyKe).

I also would like to thank Professor Mika Lindén and Professor Jouko Peltonen for support and supervision. Further I would like to thank Professor Marek Kosmulski for support and I´m thankful for the intense periods in the laboratory.

I thank all personnel at FyKe for creating a fantastic atmosphere to work and develop in. Especially I would like to thank Cristina Luojola for help with the practical problems at FyKe and the co-authors for the professional work.

I thank my wife and family for understanding. I cannot put down in words what you mean to me but you are the most precious I have. I thank my parents for being there and supporting me during all my life.

The national Technology Agency of Finland and the Academy of Finland are acknowledged for financial support.

# 9. References

[1] B. Deryaguin, L. D. Landau, Acta Physicochim. USSR, 14, 1941, 633.

[2] E. W. Verwey, J. Th. G. Overbeek, "Theory of Stability of Lyophobic Colloids", Elsevier, 1948, Amsterdam, The Netherlands.

[3] H. Sculze, J. Prakt. Chem., 2, 1882, 27, 1883, 320.

[4] W. B. Hardy, Proc. Roy. Soc., 66, 1900, 110.

[5] P. Debye, Phys. Zeit., 21, 1920, 178.

[6] W. H. Keesom. Phys. Zeit., 22, 1921, 643.

[7] H. B. G. Casimir, D. Polder, Phys. Rev. Vol. 73, 4, 1948, 360.

[8] T. F. Tadros, Colloid Stability, The Role of Surface Forces –Part 1, Chap. 1, Wiley-VCH, 2007, Weinheim, Germany.

[9] H.C Hamaker, Physica, 4, 1937, 1058.

[10] E. M. Lifshitz, Soviet Physics JETP 2, 1956, 73.

[11] J. Lyklema, "Fundamentals of Interface and Colloid Science Vol. II: Solid-Liquid Interfaces" ,Chap. 3, Academic Press Ltd, London, 1995.

[12] G. D. Parfitt," Dispersion of Powders in Liquids, With Special Reference to Pigments", 3rd ed., Elsevier Applied Science Publisher, 1981, Chap. 1.

[13] P. C. Hiemenz, R. Rajagopalan, "Principle of Colloid and Surface Chemistry" 3rd ed., Chap. 11, Marcel Dekker Inc., New York, US, 1997.

[14] R. J. Hunter, "Introduction to Modern Colloid Science", Chap. 9, Oxford University Press, Oxford, UK, 1993.

[15] J. S. Shaw, "Colloid and Surface Chemistry" 4th ed. Chap. 8, Butterworth-Heinemann, 1992 , Bodmin, Cornwall, UK.

[16] E. J. Verwej, J. Phys. Chem., 51, 3, 1947, 631.

[17] I. D. Morrison, Langmuir, 7, 1991, 1920.

[18] J-P. Jolivet, "Metal Oxide Chemistry and Synthesis, From solution to Solid state", Chap. 1, John Wiley & Sons Ldt, West Sussex, England, 2000.

[19] A. Ringbom, "Complexation in Analytic Chemistry", Wiley-Interscience, New York, 1963.

[20] J-P. Jolivet, "Metal Oxide Chemistry and Synthesis, From solution to Solid state", Appendix to part 1, John Wiley & Sons Ldt, West Sussex, England, 2000.

[21] S. K. Gumtya, S. C. Lahiri, S. Z. Aditya, Z. Phys. Chem., 216, 2002, 971.

[22] A. Bhattacharrya, A.K. Maandal, S. C. Lahiri, Electrochim. Acta, 25, 1980, 559.

[23] G. Bandyopadhyay, S. C. Lahiri, Z. Phys. Chem., 216, 2002, 729.

[24] J-P. Jolivet, "Metal Oxide Chemistry and Synthesis, From solution to Solid state", Chap. 9, John Wiley & Sons Ldt, West Sussex, England, 2000.

[25] J-P. Jolivet, "Metal Oxide Chemistry and Synthesis, From solution to Solid state", Chap. 6, John Wiley & Sons Ldt, West Sussex, England, 2000.

[26] M. Kosmulski, "Surface Charging and Points of Zero Charge", Surfactant Science Series, Vol.145, Chap. 3, CRC Press, Boca Raton, FLA, USA, 2009.

[27] J. Lyklema, " Fundamentals of Interface and Colloid Science, Vol. I, Chap. 4, Academic Press Ltd., London, 1993.

[28] M. Kosmulski, "Surface Charging and Points of Zero Charge", Surfactant Science Series, Vol.145, Chap. 1, CRC Press, Boca Raton, FLA, USA, 2009.

[29] A. V. Delgado, F. González-Caballero, R. J. Hunter, L. K. Koopal, J. Lyklema, Pure Appl. Chem. , Vol. 77, No. 10, 2005, 1753.

[30] F. Hofmeister, Arch. Exp. Path. Pharm., 24, 1888, 247.

[31] R. L. Baldwin, Biophysical Journal, Vol. 71, 1996, 2056.

[32] M. R. Das, J. M. Borah, W. Kunz, B. W. Ninham, S. Mahiuddin, J. of Col. Interface Sci., 344, 2010, 482.

[33] P. L. Nostro, L. Fratoni, B. W. Ninham, P. Baglioni, Biomacromolecules, 3, 2002, 1217.

[34] R. Zangi, M. Hagen, B. J. Berne, J. Am. Chem. Soc., 129, 2007, 4678.

[35] Y. Zhang, S. Furyk, D. E. Bergbreiter, P. S. Cremer, J. Am. Chem. Soc., 127, 2005, 14505.

[36] K. D. Collins, Methods, 34, 2004, 300.

[37] K. D. Collins, Biophysical J., Vol. 72, 1997, 65.

[38] J. O'M. Bockris, A.K.N. Reddy, "Modern Electrochemistry", Vol. 1, Chap. 2, Plenum Press, New York, 1970.

[39] K. D. Collins, G. W. Neilson, J. E. Enderby, Biophysical Chemistry, 128, 2007, 95.

[40] R. G. Pearson, J. Am. Chem. Soc. 85, 1963, 3533.

[41] R. G. Parr, R. G. Pearson, J. Am. Chem. Soc., 105, 1983, 7512.

[42] R. G. Pearson, J. Am. Chem. Soc., 110, 1988, 7684.

[43] D. F. Shriver, P. W. Atkins, C. H. Langford, "Inorganic Chemistry", 2nd ed., Chap. 5, Oxford University Press, 1994.

[44] M. Kosmulski, J. B. Rosenholm, J. Phys. Chem., 100, 1996, 11681.

[45] M. Kosmulski, J. Gustavsson, J. B. Rosenholm, Colloid Polym Sci., 277, 1999, 550.

[46] S. B. Scales, P. J. Scales, T. W. Healy, Langmuir, 15, 1999, 2836.

[47] M. Kosmulski, Langmuir, 18, 2002, 785.

[48] G. V. Franks, J. Int. Sci., 249, 2002, 44.

[49] M. R. Das, J. M. Borah, W. Kunz, B. W. Ninham, S. Mahiuddin, J. Col. Interface Sci., 344, 2010, 482.

[50] M. Boström, E. R. A. Lima, F. W. Tavares, B. W. Ninham, J. Chem. Phys., 128, 2008, 135104.

[51] B. W. Ninham, V. Yaminsky, Langmuir, 13, 1997, 2097.

[52] J-P. Jolivet, "Metal Oxide Chemistry and Synthesis, From solution to Solid state", Chap. 7, John Wiley & Sons Ldt, West Sussex, England, 2000.

[53] J. Langmuir, J. Am. Chem. Soc., 38, 1916, 2221.

[54] H. B. Brandl, J. Col. Interface Sci., 277, 2004, 1.

[55] J. B. Peri, J. Phys. Chem., Vol. 69, 1, 1965, 220.

[56] L. K. Koopal, Electrochimica Acta, Vol. 41, 14, 1996, 2293.

[57] T. Hiemstra, W. H. van Riemsdijk, G. H. Bolt, J. Col. Interface Sci., 133, No. 1, 1989, 91.

[58] T. Hiemstra, J. C. M. de Wit, W. H. van Riemsdijk, , J. Col. Interface Sci., 133, No. 1, 1989, 105.

[59] I. M. Krieger, Adv. Col. Interface Sci., 3, 1972, 111.

[60] R. J. Hunter, Adv. Col. Interface Sci. 17, 1982, 197.

[61] R. J. Hunter, S. K. Nicol, J. Col. Interface Sci., 28, No. 2, 1968, 250.

[62] B. A Firth, R. J. Hunter, J. Col. Interface Sci., 57, No. 2, 1976, 248.

[63] B. A. Firth, J. Colloid Interface Sci., 57, No. 2, 1976, 257.

[64] B. A Firth, R. J. Hunter, J. Col. Interface Sci., 57, No. 2, 1976, 266.

[65] J. P. Friend, R. J. Hunter, J. Col. Interface Sci, 37, No. 3, 1971, 548.

[66] G. E. Morris, W. A. Skinner, P. G. Self, R. St. C. Smart, Colloids Surf. A, 155, 1999, 27.

[67] Y. K. Leong, P. J. Scales, T. W. Healy, D. V. Boger, J. Chem. Soc. Faraday Trans., 89, 1993, 2473.

[68] Y. K. Leong, P. J. Scales, T. W. Healy, D. V. Boger, Colloids Surf. :A, 95, 1995, 43.

[69] R. Greenwood, L. Bergström, J. Euro. Ceramic Soc., 17, 1997, 537.

[70] P. J. Scales, S. B. Johnson, T. W. Healy, P. C. Kapur, AIChE J., 44, No. 3, 1998, 538.

[71] M. Kosmulski, J. Gustafsson, J. B. Rosenholm, J. Col. Interface Sci., 209, 1999, 200.

[72] S. B. Johnson, A. S. Russell, P. J. Scales, Colloids Surf. A, 141, 1998, 119.

[73] Y. K. Leong, B. C. Ong, Powder Tech., 134, 2003, 249.

[74] P. J. Harbour, D. R. Dixon, P. J. Scales, Colloids Surf. A, 295, 2007, 38.

[75] B. C. Ong, Y. K. Leong, S. B. Chen, Powder Tech., 186, 2008, 176.

[76] K-S. Khoo, E- J. Teh, Y-K. Leong, B. C. Ong, Langmuir, 25, 2009, 3418.

[77] K. S. Avramidis, R. M. Turian, J. Colloid Interface Sci., 143, No. 1, 1991, 54.

[78] J. Gustafsson, P. Mikkola, M. Jokinen, J. B. Rosenholm, Colloids Surf. A., 175, 2000, 349.

[79] J. de Vicente, J. D. G. Durán, A. V. Delgado, Colloids Surf. A, 195, 2001, 181.

[80] M. del Mar Ramos-Tejada, A. Ontiveros, R. Del Carmen Plaza, A. V. Delgado, J. D. G. Durán, Rheol. Acta, 42, 2003, 148.

[81] J. D. G. Durán, M. M. Ramos-Tejada, F. J. Arroyo, F. González-Caballero, J. Col. Interface Surf., 229, 2000, 107.

[82] M. von Smoluchowski, Phys. Z., 17, 557, 1916, 548.

[83] Z. Zhou, P. J. Scales, D. V. Boger, Chem. Eng. Sci., 37, 2001, 2901.

[84] R. Hogg, T. W. Healy, D. W. Furstennau, Trans. Faraday Soc., 62, 1966, 1638.

[85] J. E. Gordon, " The Organic Chemistry of Electrolyte Solutions", Chap. 2, 1975, John Wiley & Sons, NY, USA.

[86] F. Boschini, A. Rulmont, R. Cloots, R. Moreno, Ceramics International, 35, 2009, 1007.

[87] P. J. Harbour, D. R. Dixon, P. J. Scales, Colloids Surf. A, 295, 2007, 67.

[88] T. F. Tadros, P. Taylor, G. Bognolo, Langmuir, 11, 1995, 4678.

[89] J. Wang, L. Gao, Ceramics International, 26, 2000, 187.

[90] M. C. Blanco López, B. Rand, F. L. Riley, J. Euro. Cer. Soc., 20, 2000, 1579.

[91] M. Kosmulski, P. Próchniak, J. B. Rosenholm, Langmuir, 26, 3, 2010, 1904.

[92] M. Kosmulski, P. Prócniak, E. Mączka, J. B. Rosenholm, J. Phys. Chem. C, 114, 2010, 17734.

[93] Á. V. Delgado, "Interfacial Electrokinetics and Electrophoresis", Chap. 1, 2002, Marcel & Decker Inc.,, NY, USA.

[94] P. H. Wiersema, A. L. Loeb, J. TH. G. Overbeek, J. Col. Interface Sci., 22, 1966, 78.

[95] P. C. Hiemenz, R. Rajagopalan, "Principle of Colloid and Surface Chemistry" 3rd ed. Chap. 12, Marcel Dekker Inc., New York, US, 1997.

[96] R. W. O'Brien, L. R. White, J. Chem. Soc. Faraday Trans 2, 74, 1978, 1607.

[97] S.S. Dukhin, B. V.Deryaguin, edit. E. Matijević, Surface and Colloid Science, Vol. 7, John Wiley, NY, USA, 1974.

[98] J. A. Enderby,Proc. R. Soc., London, A 207, 1951, 329.

[99] F. Booth, J. A. Enderby, Proc. Am. Phys. Soc., A 208, 1952, 32.

[100] R. W. O'Brien, J. Fluid Mech., 190, 1990, 71.

[101] R. W. O´Brien, A. Jones, W. N. Rowlands, Colloids Surf. A, 218, 2003, 89.

[102] R. W. O'Brien, D. W. Cannon, W. N. Rowlands, J. Col. Interface Sci., 173, 1995, 406.

[103] R. J. Hunter, R. W. O'Brian, Colloids Surf. A, 126, 1997, 123.

[104] P. W. Atkins, "Physical Chemistry", 5th ed., chap 24, Oxford University Press, Oxford, UK, 1994.

[105] M. S. Prasad, K. J. Reid, H. H. Murray, App. Clay Sci., 6, 1991, 87.

[106] W. Gindl, G. Jeronimidis, J. Mat. Sci., 39, 2004, 3245.

[107] P. Wojtaszcyk, P. Schaaf, B. Senger, M. Zembala, J. C. Voegel, J. Chem. Phys., 99, 1993, 7198.

[108] M. R. Gittings, D. A. Saville, Colloids Surfaces A, 141, 1998, 111.

[109] M. Kosmulski, A. S. Dukhin, T. Priester, J. B. Rosenholm, J. Col. Interface Sci., 263, 2003, 152.

[110] M. Kosmulski, J. B. Rosenholm, Colloids Surf. A, 248, 2004, 121.

[111] M. Kosmulski, J. B. Rosenholm, Adv. Colloid Interface Sci. 112, 2004, 93.

[112] G. V. Franks, S. B. Johnson, P. J. Scales, D. V. Boger, T. W. Healy, Langmur 15, 1999, 4411.

[113] W. N. Rowlands, R. W. O'Brian, R. J. Hunter, V. Patrick, J. Colloid Interface Sci., 188, 1997, 325.

[114] M. Kosmulski, "Chemical Properties of Material Surfaces", Surfactant Science Series, Vol. 102, Chap. 3, Marcel Dekker, New York, 2001.

[115] M. Alkan, O. Demirbas, M. Dogân, Microporous Mesoporous Mater., 83, 2005, 51.

[116] I. Sondi, J. Biščan, V. Pravdić, J. Colloid Interface Sci., 178, 1996, 514.

[117] M. J. Avena, C. P. De Pauli, J. Colloid Interface Sci., 202, 1998, 195.

[118] O. El-Gholabzouri, M. Á. Cabrerizo-Vílchez R. Hidalgo-Álvarez, J. Col. Interface Sci., 261, 2003, 386.

[119] R. Folkersma, A. J. G. van Diemen H. N. Stein, 14, 1998, 5973.

[120] M. Kosmulski, "Chemical properties of material surfaces", Chap. 6, 2001, Marcel Dekker Inc., NY, US.

[121] R. J. Hunter, Adv. Col. Interface Sci., 100-102, 2003, 153.

[122] S.S. Dukhin, N.M. Semenikhin, KolL. Zhur., 32, 1970, 366.

[123] Y. Zhang, P. S. Cremer, Cur. Opin. Chem. Bio., 10, 2006, 658.

[124] M. Kosmulski, Adsorption, 16, 2010, 343.

[125] M. Kosmulski, "Chemical properties of material surfaces", Chap. 4, 2001, Marcel Dekker Inc., NY, US.

[126] J. Szczypa, L. Wasowska, M. Kosmulski, J. Colloid Interface Sci., 126, 1988, 592.

[127] J. B. Rosenholm, H. Rahiala, J. Puputti, V. Stathopoulos, P. Pomonis, I. Beurroies, K. Backfors, Colloids Surf. A, 250, 2004, 289.

[128] P. A. Connor, A. J. McQuillan, Langmuir, 15, 1999, 2916.

[129] T. Mussini, A.K. Covington, P. Longhi, S. Rondinini, Pure & Appl. Chem. 57, 1985, 865.

[130] J. S. Shaw, "Colloid and Surface Chemistry" 4th ed. Chap. 3, Butterworth-Heinemann, 1992 , Bodmin, Cornwall, UK.

[131] H. Reerink, J. Th. G. Overbeek, Discuss. Faraday Soc., 18, 1954, 74.

[132] J. Israelachvili, "Intermolecular and Surface Forces" 2th ed. Cap. 2, Academic Press, 1994, London, UK.

[133] I. Larson, C. J. Drummond, D. Y. C. Chan, F. Grieser, j. Am. Chem. Soc., 115, 1993, 11885.

[134] D. R. Lide (Ed.), "CRC Handbook of Chemistry and Physics" 87th ed., CRC Press, 2006, Boca Raton, FL, US.

[135] J. B. Rosenholm, Adv. Colloid Interface Sci., 156, 2010, 14.

[136] J. B. Rosenholm, Colloids Surf. A, 354, 2010, 197.

Per Dahlsten

# Specific Surface Charging of Latex, Clay and Mineral Oxide Particles in Aqueous, Non-Aqueous and Mixed Solvent Systems

## A study of particle interactions in suspensions

The findings of this thesis may be used to control suspensions in industrial processes and to improve products such as coated paper and pigment based paints. The influence of electrolytes on the interactions between different particles in suspensions is highlighted. Metal oxide particles, Clays and Melamine-Formaldehyde lattices were investigated. The ionic specificity effects were studied at low and at high electrolyte concentrations in aqueous suspensions. The influence of electrolytes were arranged according to three different ionic series. Additionally, non-aqueous and mixed solvent titania and alumina suspensions with phosphoric, oxalic and sulfuric acids were investigated. The focus was directed on the influence of the acids on charging in titania suspensions. The zeta-potential is related to conductivity, proton concentration and surface charge density. Finally, the stability of the suspensions were monitored by viscosity and correlated to the zeta-potential.


Åbo Akademi University Press | ISBN 978-952-12-2818-6